



**UNIVERSITÀ DEGLI STUDI DI NAPOLI FEDERICO II**

**Dottorato di Ricerca in Biologia Applicata XXII Ciclo**

**Curriculum in Fisiologia**

**Effects of polyunsaturated fatty acid metabolism on  
the eco-physiology of marine planktonic diatoms**

**Tutore**

**Prof. Sergio Esposito**

**Dr. Angelo Fontana**

**Dottorando**

**Nadia Lamari**

**Napoli, Novembre 2009**

*Ai miei genitori*

## Table of Contents

Abstract.....	7
<b>Chapter I: State of the art and thesis objectives</b>	
I. 1. General introduction.....	9
I. 2. Ecological function of microalgal secondary metabolites.....	11
I. 3. Diatom chemistry.....	13
I. 4. Aims of the thesis.....	16
<b>Chapter II: A new method for the oxylipin detection and determination in marine diatoms</b>	
II. 1. <b>Introduction</b> .....	17
II. 2. <b>Materials and Methods</b> .....	18
II. 2. 1. Reagents and equipment.....	18
II. 2. 2. Synthetic oxylipin analogues .....	18
II. 2. 3. Cell culture samples .....	19
II. 2. 4. Marine phytoplankton samples.....	19
II. 2. 5. Extraction procedure.....	20
II. 2. 6. LC-MS analysis of non-volatile oxylipins.....	20
II. 2. 7. GC-MS analysis of non-volatile oxylipins.....	21
II. 2. 8. Oxylipin quantification.....	22
II. 3. <b>Results</b> .....	22
II. 3. 1. Oxylipin signature of <i>Thalassiosira rotula</i> .....	22
II. 3. 2. UV data for structural elucidation.....	24
II. 3. 3. LC-MS/MS analysis of epoxyde fatty acid derivatives.....	25
II. 3. 4. LC-MS/MS analysis of keto fatty acid derivatives.....	27
II. 3. 5. GC-MS analysis of silyl-derivatives.....	28
II. 3. 6. Reproducibility and sensitivity in LC-MS.....	30
II. 3. 7. Analysis of marine phytoplankton.....	31

II. 4. <b>Discussion</b> .....	33
--------------------------------	----

**Chapter III: Effects of diatom metabolites on the reproduction of zooplankton grazers**

III. 1. <b>Introduction</b> .....	36
III. 2. <b>Materials and Methods</b> .....	37
III. 2. 1. Cell culture samples.....	37
III. 2. 2. Marine zooplankton samples.....	38
III. 2. 3. Feeding experiments.....	39
III. 2. 4. Statistical analysis.....	39
III. 2. 5. Fluorescence labelling and confocal microscopy of copepods fed with diatoms.....	40
III. 2. 6. Chemical analysis.....	41
III. 2. 7. Oxylin preparation.....	41
III. 2. 8. LOX assay.....	42
III. 2. 9. hROS detection.....	42
III. 3. <b>Results</b> .....	43
III. 3. 1. Effects of diatom diets on copepod reproduction.....	43
III. 3. 2. Effects of non-PUA producing diatoms on copepod reproduction.....	45
III. 3. 3. Chemical analysis of lipoxygenase products.....	46
III. 3. 4. Phyco-oxylin profiling.....	48
III. 3. 5. Lipoxygenase activity.....	50
III. 3. 6. Teratogenic and apoptotic activity of diatom products.....	50
III. 3. 7. Measurement of highly reactive oxygen species levels.....	52
III. 4. <b>Discussion</b> .....	54

**Chapter IV: Oxylin production in the pennate diatom *Pseudo-nitzschia delicatissima***

IV. 1. <b>Introduction</b> .....	59
IV. 2. <b>Materials and Methods</b> .....	60
IV. 2. 1. Microalgal culturing.....	60

IV. 2. 2. Extraction of lipoxygenase products.....	61
IV. 2. 3. Lipoxygenase assays.....	61
IV. 3. <b>Results</b> .....	62
IV. 3. 1. Phyco-oxylin signature of <i>Pseudo-nitzschia delicatissima</i> .....	62
IV. 3. 2. Lipoxygenase products along the growth curve.....	65
IV. 4. <b>Discussion</b> .....	68

**Chapter V:** Characterization of phyco-oxylin as chemical markers for taxonomy of cryptic diatoms

V. 1. <b>Introduction</b> .....	70
V. 2. <b>Materials and Methods</b> .....	72
V. 2. 1. Microalgal isolation and culturing.....	72
V. 2. 2. Molecular analysis.....	73
V. 2. 3. Chemical analysis.....	73
V. 3. <b>Results</b> .....	75
V. 3. 1. Morphological diversity.....	75
V. 3. 2. Genetic diversity.....	76
V. 3. 3. Chemical diversity.....	76
V. 3. 4. LC-MS/MS analysis of epoxy alcohols.....	78
V. 4. <b>Discussion</b> .....	81

**Chapter VI:** Identification and preliminary purification of a galactolipid-hydrolyzing enzyme from *Thalassiosira rotula*

VI. 1. <b>Introduction</b> .....	85
VI. 2. <b>Materials and Methods</b> .....	86
VI. 2. 1. Reagents and equipment.....	86
VI. 2. 2. Cell culture samples.....	87
VI. 2. 3. Extraction and isolation of the glycolipids from <i>Posidonia oceanica</i> ....	87
VI. 2. 4. Fractionation of crude enzymatic extract.....	88
VI. 2. 5. Protein quantification.....	89
VI. 2. 6. Assay for galactolipid-hydrolyzing activity.....	90

VI. 2. 7. GC-MS analysis of free fatty acids.....	90
VI. 2. 8. SDS polyacrylamide gel electrophoresis (SDS-PAGE).....	91
VI. 2. 9. Trypsin digestion of SDS-PAGE separated proteins.....	91
VI. 2. 10. MALDI-ToF analysis, peptide mass fingerprinting, nESI-MS/M and protein identification.....	93
VI. 3. <b>Results</b> .....	94
VI. 3. 1. First purification of galactolipid-hydrolyzing enzyme.....	94
VI. 3. 2. Second purification of galactolipid-hydrolyzing enzyme.....	99
VI. 3. 3. Third purification of galactolipid-hydrolyzing enzyme.....	105
VI. 3. 4. Solubilisation of galactolipid-hydrolyzing enzyme from cell membranes.....	110
VI. 3. 5. Substrate specificity of galactolipid-hydrolyzing enzyme.....	112
VI. 4. <b>Discussion</b> .....	113
 <b>Chapter VII: Conclusions</b> .....	 115
 <b>Abbreviations</b> .....	 120
 <b>Appendix</b> .....	 124
 <b>References</b> .....	 142

## Abstract

Le diatomee, organismi unicellulari fotosintetici, costituiscono il principale gruppo di microalghe del fitoplancton marino e svolgono un ruolo principale nel ciclo globale della fissazione del carbonio. Considerate da sempre una buona ed innocua fonte di cibo per i microscopici erbivori (come ad esempio, i copepodi) che costituiscono lo zooplancton, le diatomee a partire dalla fine degli anni 90 sono state oggetto di numerosi studi per la capacità di sintetizzare composti antimitotici, come alcune aldeidi polinsature e altri derivati di ossidazione enzimatica di acidi grassi poliinsaturi, che bloccano l'embriogenesi ed inducono teratogenesi nei copepodi.

Durante la tesi dottorale è stato sviluppato un semplice approccio analitico per lo studio di questi composti. La metodologia, che utilizza tecniche di spettrometria di massa/massa, (LC-MS/MS e GC-MS/MS), ha consentito la caratterizzazione di un ampio numero di molecole, genericamente chiamate ossilipine, termine che identifica un'eterogenea famiglia di prodotti derivati dall'ossidazione di acidi grassi ad opera di pathway ossigenasici. La tecnica permette di risalire alle attività enzimatiche coinvolte nel processo biosintetico e, quando è stata applicata a diverse specie dei generi *Thalassiosira*, *Choetoceros*, *Skeletonema* e *Pseudo-nitzschia*, ha messo in evidenza che la sintesi di queste molecole nelle diatomee è specie-specifica. Inoltre, le variazioni dei profili ossilipinici all'interno di una stessa specie sono state anche utilizzate con successo come marker tassonomici per l'identificazione di clade criptici o pseudo-criptici.

La valutazione delle proprietà ecologiche delle ossilipine ha dimostrato che esiste una chiara correlazione tra l'ossidazione enzimatica degli acidi grassi e l'effetto teratogenico causato nei copepodi dall'ingestione di diatomee. In particolare, i risultati suggeriscono che l'impatto negativo di queste microalghe sulla riproduzione dei copepodi è associabile alla sintesi di specie chimiche instabili e reattive, come gli idroperossidi, che promuovono la formazione di radicali, per esempio i ROS, che sono in grado di aggredire il DNA, determinando, in tal modo, gli effetti teratogenici e apoptotici riportati in letteratura. La tossicità delle diatomee sui copepodi non è quindi dovuta ad una singola classe di molecole, come si è creduto fino ad oggi, ma piuttosto

alla produzione di una complessa miscela di molecole di cui, probabilmente, solo una parte è stata identificata.

L'effetto delle ossilipine sullo zooplancton è comunque uno dei possibili ruoli biologici che queste molecole sembrano assolvere. In effetti, in analogia con quanto accade in altri organismi, come ad esempio piante ed animali, queste molecole sembrano avere più di una funzione. In condizioni fisiologiche, la loro sintesi varia durante le fasi del ciclo di crescita delle diatomee in maniera dipendente dalla densità di popolazione. In particolare, gli studi condotti durante questo dottorato di ricerca hanno dimostrato che la concentrazione massima di tali metaboliti coincide con le fasi terminali della curva di crescita, suggerendo perciò che tali composti possano svolgere un ruolo di segnale chimico di fine bloom.

# Chapter I

## State of the art and thesis objectives

### I. 1. *General introduction*

Plankton is defined as the living part of material, which passively floats in the sea or freshwater. Phytoplankton is the portion of plankton that generally grows autotrophically using CO<sub>2</sub> as its sole carbon source and light as its energy source.

In the contemporary ocean, marine phytoplankton is comprised of photoautotrophic organisms from 12 taxonomic divisions spanning three Kingdoms (Falkowski et al., 1998). It includes photosynthetic bacteria, such as prochlorophytes (e.g. *Prochlorococcus*) and cyanobacteria (e.g. *Synechococcus*) (Giovannoni & Rappè, 2000), and eukaryotic microalgae, such as chromophytes (brown algae), rhodophytes (red algae), and chlorophytes (green algae) (Van Den Hoek et al., 1997). The marine phytoplankton represents the major contributor of marine carbon fixation. These organisms can fix approximately the same amount of carbon, a few grams per square meter per day, as a terrestrial forest (Smetacek, 2001). Since today the world's oceans cover two-thirds of the Earth's surface, they contribute approximately 50% of the total primary productivity of our planet (Figure I.1).

Diatoms are unicellular chromophyte algae that colonize the oceans down to depths to which photosynthetically available radiation can penetrate. They are the most important group of marine phytoplankton as they are responsible for close to 40% of marine primary productivity (Falkowski & Raven, 2007). Diatom abundance is generally highest at the beginning of spring and in the autumn, when light intensity and day length are optimal for their photosynthesis. In some regions of the oceans, the annual production of fixed carbon can be up to 2 kg m<sup>-2</sup> equivalent to a cereal or corn crop (Field et al., 1998).

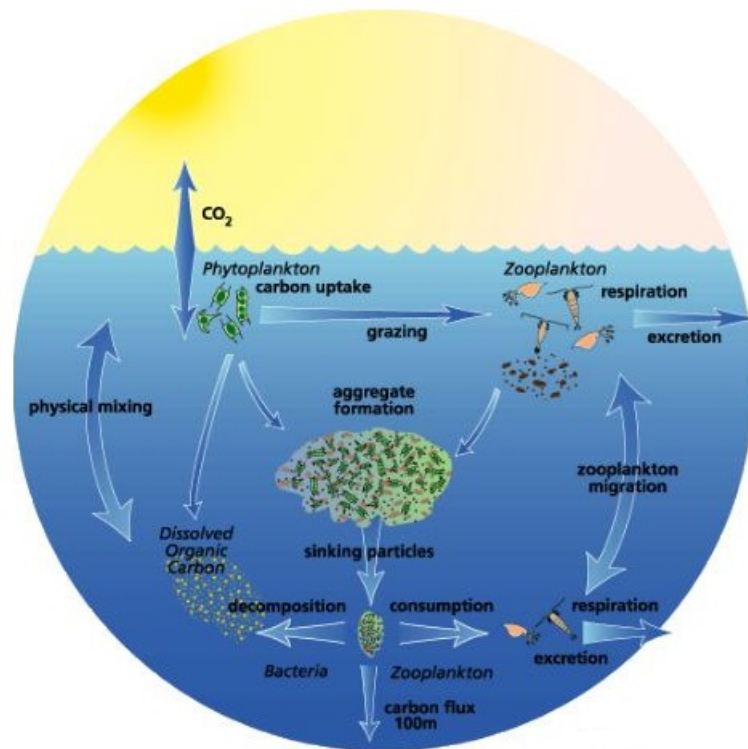
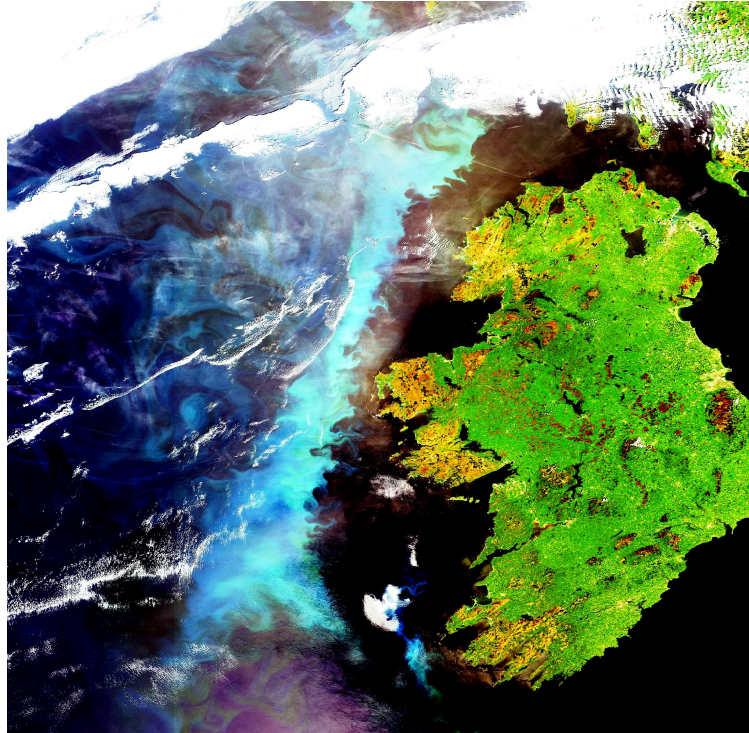


Figure I.1. The carbon cycle in the ocean.

When the population of these organisms increases to a concentration of hundreds to thousands of cells per milliliter, the water is coloured green-blue, yellow-brown or red. This phenomenon is known as “algal bloom” (Figure I.2). Sometimes these events involve toxic phytoplankton such as dinoflagellates of the genera *Alexandrium* and *Karenia* or diatoms of the genus *Pseudo-nitzschia*. These blooms then referred to as “harmful algae blooms”. Of the over 5000 known species of marine phytoplankton, about 300 species can under certain circumstances proliferate in exponential numbers and only about 2% of these species have the capacity to produce potent toxins, which can negatively affect the local ecosystem as well as fishing and aquaculture activities (Landsberg, 2002).



**Figure I.2.** A flash of blue and green lits the sea off Ireland as a phytoplankton bloom grows in the North Atlantic Ocean.

### I. 2. *Ecological function of microalgal secondary metabolites*

Many microalgae produce a variety of different, often unique, molecules which are released into the environment (Hay, 1996). These chemicals are referred to as secondary metabolites. They are not directly involved in building up the machinery of life and constitute a very small fraction of the total biomass of an organism. In marine ecosystems, much attention has focused on chemical ecological interactions within and among invertebrate species, such as sponges, molluscs, echinoderms and polychaetes, particularly in benthic tropical ecosystems, where species diversity and resource competition are expected to be high (Hay & Fenical, 1996). Although the function of microalgal secondary metabolites has remained mostly uninvestigated, evidences that they may play an important role for algal bloom development, dynamics, and fate are increasing (Landsberg, 2002; Paffenhöfer et al., 2005).

Chemically-mediated interactions of phytoplankton are poorly understood due to the lack of information on the chemical nature and biosynthetic pathways of the involved allelochemicals. For example, the production of saxitoxin by the dinoflagellate *Alexandrium* increased in the exponential growth phase and under phosphor limitation,

while it decreased under nitrogen limitation (Anderson et al., 1990). Domoic acid is produced in higher quantities by several diatoms of the genus *Pseudo-nitzschia* during the stationary growth phase and under silica and phosphorus limitation, but production ceases under nitrogen limitation (Pan et al., 1998). In such situations, like at the end of a bloom, the competitive balance will turn toward allelopathic species, which will have an enhanced advantage. Pratt (1966) observed that the phytoplankton community in the Narragansett bay was alternatively dominated by blooms of the diatom *Skeletonema costatum* and the dinoflagellate *Olisthodiscus luteus*. *In vitro* and *in situ* experiments showed that *O. luteus* achieved dominance by producing a tannin-like substance that had an inhibitory effect on *S. costatum* at high concentrations, but stimulated the growth of this diatom at lower concentrations. Pratt suggested that this may explain the alternating dominance of these two species. Another example is the occurrence of the monospecific bloom of the domoic acid-producing diatom *Pseudo-nitzschia pungens* in Cardigan Bay simultaneously with another diatom *Rhizosolenia alata* in Hillsborough River estuary (Subba Rao et al., 1995). The authors reported that the growth *R. alata* and *P. pungens* were coincidentally suppressed (*R. alata* by domoic acid, and *P. pungens* by *R. alata* cell-free extracts) and hypothesized that allelopathy may therefore play a role in algal succession.

A recent line of research is highlighting the role of secondary metabolites as information-conveying molecules in cell-to-cell signalling, so called infochemicals (Vos et al., 2006). There is clear evidence in terrestrial ecosystems that when attacked by grazers plants can produce secondary metabolites that attract the carnivores of these grazers (Agrawal, 2000). Several authors have suggested that similar interactions may also occur in aquatic ecosystems (Wolfe, 2000). Steinke et al. (2002) suggest that the volatile dimethylsulfide that is released during grazing by microzooplankton can be exploited by mesozooplankton copepods, thus enabling them to more efficiently graze on microzooplankton. In addition, some pelagic sea birds can sense dimethylsulfide (Nevitt et al., 1995) which may enable them to locate and exploit zooplankton-rich areas that could decrease the grazing pressure on phytoplankton. Attraction of copepods to dimethylsulfide is suggested, but not shown in Steinke et al. (2002) and it

is not confirmed whether the resulting multitrophic food web interactions actually protect the algae from grazing.

In addition to the above-mentioned studies, it has been also shown that secondary metabolites produced by phytoplankton can also have adverse effects on the zooplankton grazers. The negative impact of toxins on their predators provides a strategy for an indirect process of chemical defence. When the dinoflagellate *Gymnodinium breve* is fed to copepods, a paralyzing effect and elevated heart rate is observed in most adult copepods and a loss of the neuromuscular control in the nauplii. Ianora et al. (1999) report reduced sperm quality in copepods fed certain dinoflagellate diets, but it remains unclear whether this is due to nutrient deficiency or related to toxin production. It has been suggested that the dinoflagellate *Gyrodinium aureolum* greatly reduces egg production in copepods due to nutritional deficiency rather than toxin production (Irigoien et al., 2000).

Another defensive strategy against grazers, well-known in higher plants, is an activated enzyme-cleavage mechanism of defence. The general pattern involves the activation of one or more inactive precursor compounds stored in the cells. Upon wounding or stress by grazing, these inactive molecules are enzymatically converted to the toxic compound. An example of such a mechanism of defence in phytoplankton has been reported for the bloom-forming coccolithophorid *Emiliana huxleyi*. This alga produces the gas dimethylsulfide and the feeding deterrent acrylate via the cleavage of dimethylsulfoniopropionate that occurs immediately after cell injury by grazers (Wolfe et al., 1997).

### I. 3. *Diatom chemistry*

Diatoms are often major components of algal blooms and have long been considered as principal components of planktonic copepods diets (Kleppel, 1993). In the last decade the diatom-copepod interaction accepted in biological and fishery oceanography has become a paradox (Ban et al., 1997) based on the growing evidence that diatoms may use a chemical defence system, which can potentially be harmful for predators and competitors (Pohnert, 2004). Miralto et al. (1999) were the first to identify the diatom

compounds responsible for inhibitory effects during copepod embryogenesis as 2-*trans*-4-*cis*-7-*cis*-decatrienal, 2-*trans*-4-*trans*-7-*cis*-decatrienal, and 2-*trans*-4-*trans*-decadienal. When testing the anti-cell-growth activity of the diatom aldehydes on animal models the results suggested that these aldehydes were the probable agents of copepod reproductive failure when diatoms were the major source of food. On the other hand, Wichard et al. (2005b) indicated that the formation of reactive aldehydes was not a universal property of all diatoms, but is highly variable among species and strains. For example, while *Thalassiosira rotula*, isolated from the Gulf of Naples, produced high amounts of 2-*trans*-4-*cis*-7-*cis*-decatrienal and significant amounts of 2-*trans*-4-*cis*-heptadienal, 2-*trans*-4-*cis*-octadienal and 2-*trans*-4-*cis*-7-*cis*-octatrienal (d'Ippolito et al., 2002b) a strain, isolated off the coast of California, completely lacked these compounds, even though the two strains are genetically closely related and morphologically nearly identical (Pohnert et al., 2002).

Recently, a new class of oxygenated fatty acid metabolites, previously intensely studied in mammals and higher plants, was reported from marine microalgae (d'Ippolito et al., 2005). The term used for this class of compounds is oxylipins. Gerwick defined "oxylipin" as an encompassing term for oxidized compounds formed from fatty acids by a reaction involving at least one step of mono- or dioxygenase-dependent oxidation (Gerwick et al., 1991). The presence of a series of these products with 16 carbon atoms and oxidation at C-9, such as 9-keto-7*E*-hexadecenoic acid (9-KHME), 9-hydroxy-7*E*-hexadecenoic acid (9-HHME), 9-hydroxy-hexadeca-6*Z*,10*E*,12*Z*-trienoic acid (9*S*-HHTrE) and 9-hydroxy-hexadeca-6*Z*,10*E*,12*Z*,15-tetraenoic acid (9*S*-HHTE) was revealed in the analysed diatom *T. rotula*. Also C<sub>16</sub> derivatives with an oxidation at C-6 were reported, such as 6-keto-hexadeca-7*E*,9*Z*,12*Z*,15-tetraenoic acid (6-KHTE) and 6-hydroxy-hexadeca-7*E*,9*Z*,12*Z*,15-tetraenoic acid (6-HHTE) together with the 6-keto-hexadeca-7*E*,9*Z*,12*Z*-trienoic acid (6-KHTrE) and the corresponding alcohol 6-hydroxy-hexadeca-7*E*,9*Z*,12*Z*,15-trienoic acid (6-HHTrE) (d'Ippolito et al., 2005). Furthermore, a single C<sub>20</sub> derivative, 11-hydroxy-eicosa-5*Z*,8*Z*,12*E*,14*Z*,17*Z*-pentaenoic acid (11-HEPE), was identified as a product of this microalgae.

Given the presence of oxylipins in higher plants and mammals, there was increased interest in their biosynthetic origin in diatoms. The first biosynthetic study in marine

diatoms was in 2000, when Pohnert demonstrated the production of aldehydes may derive from the breakdown of C<sub>20</sub> polyunsaturated fatty acids by lipoxygenase/hydroperoxide lyase. Afterwards d'Ippolito and co-workers (2003) described by experiments with labelled hexadeca-6Z,9Z,12Z-trienoic acid (HTrA) that the formation of octadienal and octatrienal in *S. costatum* involved lipoxygenase-mediated oxidation of C<sub>16</sub> fatty acids. But the first direct proof of a mechanism involving lipoxygenases was obtained with the characterization of the intermediate 9-hydroperoxy-hexadeca-6Z,10E,12Z-trienoic acid in *T. rotula* (d'Ippolito et al., 2006). In plants, animals and fungi the sequence of lipoxygenase pathway leading to the oxylipin formation shows striking similarities and evidence on their role in the pathological and physiological processes in these organisms was accumulated in the last decades. Thus the presence of the complex network of oxygenated products in marine diatoms opens intriguing questions about the role of fatty acid derivatives for example in the regulation of phytoplankton communities.

#### I. 4. *Aims of the thesis*

Starting from the detection of non-aldehydic oxylipins in diatoms in 2005 by d'Ippolito et al. the objectives of this PhD thesis were:

- to clarify the role of the enzymatically oxidized fatty acid products in the negative effects of marine diatom diets on copepod reproduction, especially in respect to the question if one or more sets of compounds are the causative agent of these effects;
- to analyse the regulation of the oxygenase pathways along the growth curve by qualitative and quantitative monitoring of their end products;
- to investigate the species-specificity of oxylipin profiles and assess their potential and applicability as chemical markers for identification of cryptic diatoms in cultures and field samples in comparison to standard techniques like genetically and morphologically markers ;
- to identify a galactolipid-hydrolyzing enzyme involved in the release of fatty acids from complex lipids in order to illuminate the up-stream enzymatic machinery that feeds the lipoxygenases with the substrates for oxylipin production.

## Chapter II

### **A new method for the oxylipin detection and determination in marine diatoms**

#### **II. 1. Introduction**

Oxylipins, lipoxygenase-derived oxygenated fatty acids, have been recognized as important chemical mediators in ecological and physiological processes of marine and freshwater diatoms. In their natural habitat, the wounding of the diatom cell by grazers is suggested to trigger an enzymatic cascade leading to the production of a great diversity of these reactive oxygenate species, like hydroperoxy-, hydroxy-, keto-, oxo-, epoxy alcohols and aldehydes (Wendel & Jüttner, 1996; Pohnert & Boland, 2002; Wichard et al., 2005a; d'Ippolito et al., 2005). Because conventional extraction procedures of diatom cells do not allow oxylipin detection in the laboratory, the cell damage needs to be induced artificially by mechanical devices in order to mimic the natural process. Oxylipin distribution is relatively wide within different diatoms and these compounds characterize an evident species-dependent specificity of the metabolic signature that arises from the variability of both the fatty acids recognized as lipoxygenase (LOX) substrates and the enzymatic activities downstream of the LOX processing (Wichard et al., 2005b; d'Ippolito et al., 2005). Generally, isolation and characterization of new secondary metabolites, such as polyketides, terpenes and alkaloids, in marine natural product research relies on a combination of different chromatographic methods, mass spectrometry and nuclear magnetic resonance (NMR) techniques. The structures of previously described oxylipins were unambiguously elucidated by these procedures. However, these methods are time consuming and labour intensive and do not allow the processing of large numbers of samples for metabolic profiling. In order to clarify metabolic pathways and detect non-volatile oxylipins in unknown microalgae communities and different isolated strains, a new sensitive and fast analytical approach was developed. It was based on the unique

combination of traditional chromatographic methods with advanced mass spectrometry (MS), ultraviolet (UV) and NMR techniques. The methodology was first tested on synthetic and commercial analogues of purified natural compounds and later on extracts of marine diatoms from laboratory cultures as well as phytoplankton samples collected in the Mediterranean Sea.

## II. 2. Materials and Methods

### II. 2. 1. Reagents and equipment

Solvents were purchased from Carlo Erba (Milan, Italy) and distilled before use. 5(S)-HEPE, 9(S)-HEPE, 12(S)-HEPE and 15(S)-HEPE standards were obtained from Cayman Chemicals (Ann Arbor, MI, USA). All other chemicals including *N*-methyl-*N*-(trimethylsilyl)-trifluoroacetamide and 16-hydroxyhexadecanoic acid were purchased from Sigma-Aldrich (Schnelldorf, Germany). Silica gel chromatography was performed by using precoated Merck F<sub>254</sub> plates and Merck Kieselgel 60 (Darmstadt, Germany). HPLC purifications were carried out on a Shimadzu chromatograph equipped with LC-10ADV pumps and a UV SPD-10AVP double wavelength detector. LC-MS analysis was performed on a *micro*-QToF mass spectrometer (Waters) equipped with an ESI source and coupled with a 2695 HPLC Alliance system. GC-MS data were obtained by a Thermo Electron, PolarisQ mass spectrometer equipped with a Thermo Electron, GCQ gas chromatograph using a 5% diphenyl column (Thermo Electron, Trace TR-5, 30m x 0.25mm x 0.25µm). NMR spectra were registered on a Bruker Avance DPX 300, Bruker AMX 400, Bruker DRX 600 equipped with inverse TCI Cryoprobe<sup>®</sup>.

### II. 2. 2. Synthetic oxylipin analogues

Synthetic non-volatile oxylipins were synthesized by Dr. Emiliano Manzo (CNR-Istituto di Chimica Biomolecolare of Pozzuoli, Italy) through a general procedure based on allylic oxidation of palmitoleic and oleic acid methyl esters according to Salvador et al. (1997). Briefly, fatty acid methyl esters were stirred overnight under argon with *tert*-butylhydroperoxide and catalytic copper (I) iodide in ACN at 50° C. After extraction with diethyl ether, en-one derivatives were purified on silica gel

followed by reverse phase HPLC. The resulting material was either reduced by DIBAL (Di-isoButyl Aluminium Hydride) in THF at -5° C to give the allylic alcohol or, alternatively, epoxy alcohols were prepared from the en-ones after reduction to allylic alcohols and following epoxidation with 3-chloroperbenzoic acid in dichloromethane for 2 h at 0° C. The reaction mixture was left to warm up to room temperature under stirring and then extracted. Final compounds were purified on silica gel and characterized by NMR assignment and mass spectroscopy (data are reported in the Appendix see Figures A.1-A.6).

### II. 2. 3. Cell culture samples

Cultures of *Thalassiosira rotula* (CCMP 1647) and *Skeletonema marinoi* (CCMP 2092) were obtained from the Provasoli-Guillard National Centre for Culture of Marine Phytoplankton (Boothbay Harbor, Maine, USA). *Pseudo-nitzschia delicatissima* (B321) was isolated from the Gulf of Naples (Italy) during the winter 2004 by the Ecology and Evolution of Plankton Department of the Stazione Zoologica Anton Dohrn (Naples, Italy).

Axenic cultures of marine diatoms were prepared as described in Ianora et al. (1996). Briefly, diatoms were grown in Guillard's (F/2) marine enrichment basal salt mixture powder medium (Guillard, 1983). The cultures were maintained in a growth chamber at 20° C on a 12:12 light:dark cycle under a photon flux density of 175  $\mu\text{mol quanta m}^{-2} \text{s}^{-1}$ . Cell cultures were allowed to grow until reaching the stationary growth phase in polycarbonate carboys under gentle air supply filtered through 0.22  $\mu\text{m}$  polycarbonate filters and then harvested by centrifugation at 1200 g for 10 min at 5° C using a swing-out rotor. The cell pellets were collected in 50 ml Falcon tubes and immediately processed for analysis or frozen in liquid nitrogen and kept at -80° C until further analysis.

### II. 2. 4. Marine phytoplankton samples

Phytoplankton was collected using a phytoplankton net (mesh size, 20  $\mu\text{m}$ ) in the North Adriatic Sea by the Functional and Evolutionary Ecology Department of the

Stazione Zoologica Anton Dohrn (Naples, Italy). Samples were collected during a ship cruise at the beginning and end of the 2005 spring bloom, March and May respectively. Samples were concentrated by gentle centrifugation at 1200 g for 10 min at 5° C. The cell pellets were collected in 50 ml Falcon tubes and immediately frozen in liquid nitrogen and kept at -80° C until further analysis. Phytoplankton cell numbers and species composition were determined on fixed samples (formaldehyde 4%) by Dr. Mauro Bastianini (CNR- Istituto di Scienze del Mare of Venice, Italy) after concentration by sedimentation according to Utermohl (1958), using an inverted microscope (Zeiss Axiovert 35), at magnification of 400x.

#### II. 2. 5. *Extraction procedure*

A cell pellet (about 5 g wet weight) was suspended in distilled water (1 ml/g of wet pellet), sonicated for 1 min at 4° C and left at room temperature in order to allow wound induced reactions to take place. After 30 min, acetone (equal volume with water) and the internal standard, 16-hydroxyhexadecanoic acid (30 µg/g of pellet) was added. The resulting suspension was centrifuged at 2000 g for 5 min at 5° C and successively extracted with dichloromethane (equal volume with aqueous phase). The combined organic phase was dried over Na<sub>2</sub>SO<sub>4</sub> and evaporated under reduced pressure with a rotary evaporator (Buchi, Rotavapor R-200). The raw residue was methylated with diazomethane in diethyl ether (0.4 ml per 10 mg extract) for 1 h at room temperature to convert free acids in methyl esters. After removing the organic solvent under N<sub>2</sub>, the resulting methylated extract was used for analysis of non-volatile oxylipins by LC-MS/MS and GC-MS.

#### II. 2. 6. *LC-MS analysis of non-volatile oxylipins*

Methylated extracts were dissolved in methanol to a final concentration of 100 µg/ml and directly analyzed by LC-MS. The MS method was based on a *micro*-QToF instrument equipped with an ESI source in positive ion mode and a UV photodiode array (DAD) detector (scan range 205-400 nm) for a dual monitoring of the chromatographic runs. For ESI-QToF-MS/MS experiments, argon was used as collision gas at a pressure of 22 mbar. Chromatographic analysis was carried out on a reverse

phase column (Phenomenex, C-18 Kromasil 4.6 x 250 mm, 100 Å) using a linear MeOH/H<sub>2</sub>O gradient (see Table II.1) with a column flow of 1 ml/min. 1/10 of the column flow was channelled by a post-column split to the ESI<sup>+</sup> Q-ToF MS analyzer and the remaining 9/10 to the UV DAD detector.

**Table II.1.** Solvent system and standard gradient employed for analytical HPLC-MS.

<i>Time (min)</i>	<i>Methanol (%)</i>	<i>Water (%)</i>
0	75	25
28	96	4
30	100	0
40	100	0

#### II. 2. 7. GC-MS analysis of non-volatile oxylipins

In order to obtain the GC-MS conditions methylated diatom extracts were purified on a RP-HPLC column (Phenomenex, C-18 Kromasil 4.6 x 250 mm, 100 Å) by a linear MeOH/H<sub>2</sub>O gradient. Analytical HPLC system specifications are given in Table II.2. HPLC peaks of hydroxy acid methyl esters were collected, evaporated to dryness under N<sub>2</sub>. The non-volatile oxylipin samples needed to be derivatized for analysis in the GC-MS. About 25-75 µg of purified compounds in 30 µl THF were directly incubated overnight at 4° C with 30 µg of *N*-methyl-*N*-(trimethylsilyl)-trifluoroacetamide (MSTFA). The same derivatization method adjusted for concentration was also used for the methylated diatom extracts run without previous purification.

**Table II.2.** Solvent system and standard gradient employed for HPLC. Flow rate: 1ml/min and UV detection at 235 nm.

<i>Time (min)</i>	<i>Methanol (%)</i>	<i>Water (%)</i>
0	70	30
10	80	20
60	80	20
65	100	0
75	100	0

The derivatized material was analysed in GC-MS with an ion-trap MS instrument in EI mode (70 eV) connected with a GC system, by using a 5% diphenyl column and helium as gas carrier. Elution of silyl derivatives required a temperature programme starting with 150° C for 2 min, followed by an increase of 20° C min<sup>-1</sup> till 230° C and 5° C min<sup>-1</sup> until 305° C was reached. 2 µl samples were directly injected using the split (1:10) mode, with a blank window of 3 minutes, inlet temperature of 270° C, transfer line set at 280° C and ion source temperature of 250° C.

#### II. 2. 8. *Oxylipin quantification*

Calibration curve standards for quantification with LC-MS were prepared in methanol by known amounts of the methyl esters of 15-HEPE and 16-hydroxyhexadecanoic acid. All calibration curves consisted of blank and standard samples in triplicates at concentrations ranging from 10 ng/ml to 3 µg/ml. The single concentration points were prepared by successive dilution of a bulk MeOH solution (10 µg/ml). The bulk samples were stored at -20° C. The calibration curves were constructed by plotting the peak areas of each standard against the concentrations. The standard and oxylipin quantifications were carried out by Waters QUANLINK software according to the manufacturer's instructions.

### II. 3. Results

#### II. 3. 1. *Oxylipin signature of Thalassiosira rotula*

In order to select representative oxylipins for LC-DAD-ESI<sup>+</sup>-MS/MS analysis, different single strain cultures of diatoms were chosen based on their reported characteristics in the literature. Axenic cultures of the marine diatom *T. rotula* (CCMP 1647) were obtained and worked as already described in the experimental section § II. 2. 5. A full set of MS, MS/MS and UV data of the oxylipin fraction was revealed by a single analytical run of the methylated extract of *T. rotula* (CCMP 1647) at a concentration of 100 µg/ml. The oxylipin signature of *T. rotula* (CCMP 1647) under the conditions described above (§ II. 2. 6) is presented in Figure II.1.

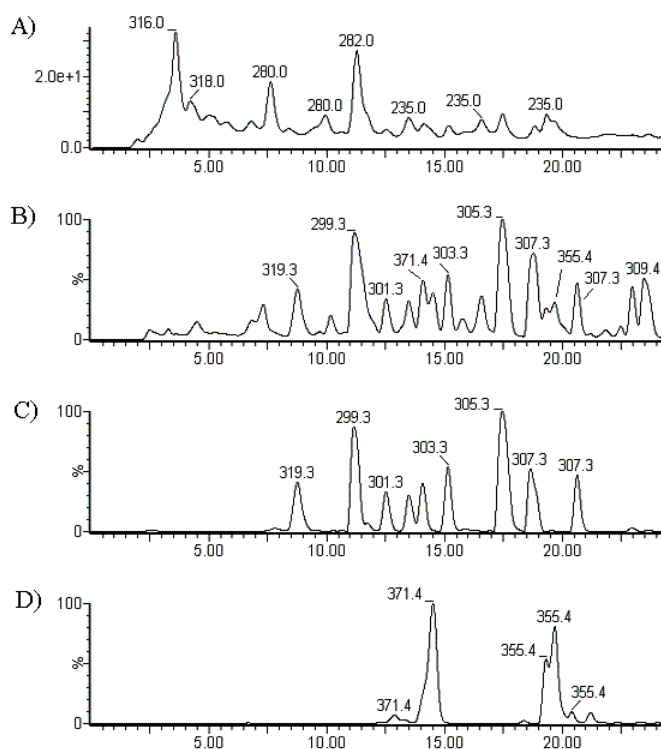


**Figure II.1.** LC-DAD-MS signature of *Thalassiosira rotula*. (A) UV-DAD profile. Numbers above peaks indicate maxima of absorbance in nm. (B) Total ion current (TIC) MS profile acquired in full scan MS. Numbers above peaks indicate the molecular weight of the most intense ion. (C) Extraction ion ( $m/z$  299, 301, 303, 305, 307, 317, 319) profile for the oxylipin family derived from of hexadeca-6Z,9Z,12Z,15-tetraenoic acid and hexadeca-6Z,9Z,12Z-trienoic acid. (D) Extraction ion ( $m/z$  355, 371) profile for the oxylipin family derived from eicosa-5Z,8Z,11Z,14Z,17Z-pentaenoic acid.

In agreement with d'Ippolito et al. (2005), two major series of compounds were detectable by ion extraction mode according to the origin from hexadeca-6Z,9Z,12Z-trienoic (C16:3, HTrA), hexadeca-6Z,9Z,12Z,15-tetraenoic (C16:4, HTA) acids (Figure II.1C) or eicosa-5Z,8Z,11Z,14Z,17Z-pentaenoic (C20:5, EPA) acid (Figure II.1D). Methyl esters of hydroperoxy fatty acids with a UV maxima at 235 nm were clustered in two families of isomeric compounds showing  $m/z$  371 ( $M+Na^+$ ) when they derive from EPA or  $m/z$  319 and 317 when they arise from HTrA and HTA, respectively. In the experimental conditions chosen for the analysis, oxylipins were revealed as sodium adducts ( $M+Na^+$ ) with a molecular ion at  $m/z$   $M+23$ . Sodium adducts stabilize the molecular ions thus reducing the molecular fragmentation and enabling determination of the molecular weight. Elution order of the different classes of oxylipins on reverse phase column C-18 depends on the number of double bonds and length of the alkyl chain with epoxy alcohols that precede keto- and hydroxy- fatty acid derivatives. It is

worth noting that under the described conditions, hydroperoxy fatty acid methyl esters were co-eluted with the corresponding hydroxy analogues that showed identical UV maximum at 235 nm. However, their presence could be easily detected by MS on the basis of the higher weight of the pseudo molecular ( $M+Na^+$ ) ion at  $m/z$  371 for the hydroperoxy derivative of EPA and  $m/z$  319 and 317 for the hydroperoxy derivatives of HTrA and HTA, respectively.

### II. 3. 2. UV data for structural elucidation

Characterization of oxylipins in complex mixtures takes also great advantage from UV data associated to the individual HPLC peaks. The UV profile is independent of the overall structure of molecules and the spectra allows to discriminate between isobaric compounds as in the case of the methyl esters of 15-hydroperoxy-eicosa-5Z,8Z,11Z,13E,17Z-pentaenoic acid (15-HpEPE) and 13-hydroxy-14,15-epoxy-eicosa-5Z,8Z,11Z,17Z-tetraenoic acid (13,14-HEpETE) from *S. marinoi* (CCMP 2092) and *P. delicatissima* (B321) (Figure II.2). The maxima at 236 and 205 nm of hydroperoxy fatty acids and epoxy alcohols, respectively, result only from the presence of the diene system, thus they provide quick and reliable markers in the structure assignment of the two classes of molecules apart from the fatty acid chain.

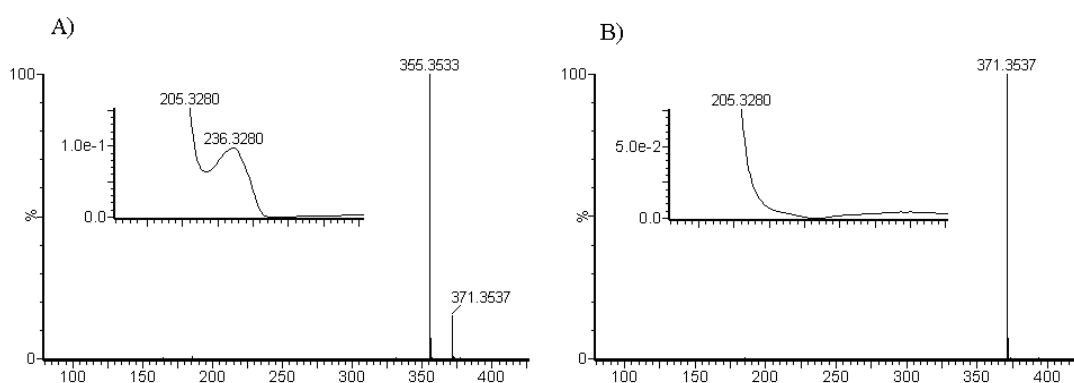


**Figure II.2.** UV assisted identification of isobaric epoxy alcohol and hydroperoxy acids. The figure reports the MS spectrum of 15-hydroxy-eicosa-5Z,8Z,11Z,13E,17Z-tetraenoic acid (15-HEPE) methyl ester with its corresponding hydroperoxy- (A) and 13-hydroxy-14,15-epoxy-eicosa-5Z,8Z,11Z,17Z-tetraenoic acid (13,14-HEpETE) methyl ester (B). The inserts describe the corresponding UV curves.

In addition to hydroxy- and epoxyhydroxy- derivatives,  $\alpha$ ,  $\beta$ - and  $\alpha$ ,  $\beta$ ,  $\gamma$ ,  $\delta$ -unsaturated keto-acids give also characteristically strong UV maxima around 250 nm or above in relation to the number of adjacent double bonds. A clear example of UV assisted identification of diatom oxylipins is provided by the analysis of 15-oxo-5Z,9E,11E,13E-pentadecatetraenoic acid methyl ester ( $m/z$  285  $M+Na^+$ , see Figure II.3), recently described in *P. delicatissima* (B321). This compound belongs to a family of molecules, generally named  $\omega$ -oxo acids (Wendel & Jüttner, 1996; Hombeck & Boland, 1998; Pohnert & Boland, 2002), which show diagnostically intense UV absorptions above 280 nm for the extended conjugation of the carbonyl moiety with two or three double bonds.

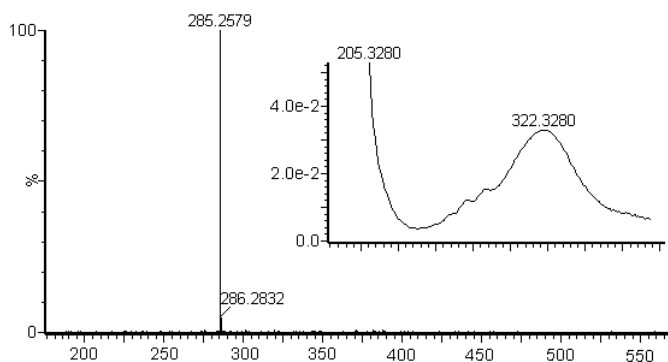
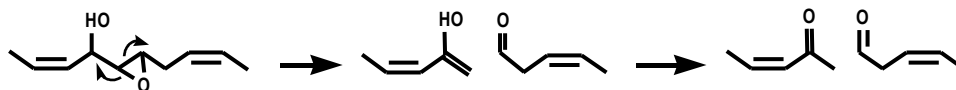


**Figure II.3.** UV assisted identification of  $\omega$ -oxo acid. The figure reports the MS spectrum of 15-oxo-5Z,9E,11E,13E-pentadecatetraenoic acid methyl ester. The inserts describe the corresponding UV maximum of absorbance in nm.

### II. 3. 3. LC-MS/MS analysis of epoxyde fatty acid derivatives

On the other side, induced fragmentation of epoxyhydroxy-derivatives provides useful information for structural elucidation. In MS/MS mode (collision energy = 35 V), synthetic fatty acid epoxydes, such as 8-hydroxy-9,10-epoxy-octadecanoic acid methyl ester ( $m/z$  351  $M+Na^+$ ) (data is reported in the Appendix see Figure A.4), typically give fragments arising by the heterolytic break of the carbon-carbon bond of the epoxyde ring. This cleavage is very specific and allows the positioning of the functional group (see Scheme II.1).



**Scheme II.1.** General mechanism of oxyrane ring breaking with the resulting neutral loss of unsaturated carbonyl compounds.

A similar fragmentation was observed with natural epoxy alcohol methyl esters, as deduced by MS/MS analysis (collision energy = 27 V) of 13,14-HEpETE, 16-hydroxy-14,15-epoxy-eicosa-5Z,8Z,11Z,17Z-tetraenoic acid (16,14-HEpETE) and 11-hydroxy-9,10-epoxy-hexadeca-6Z,12Z-dienoic acid (11,9-HEpHDE). Analogously, cleavages of natural epoxy alcohol derivatives of fatty acids provide information for the location of both the epoxy and the alcohol groups present on the fatty acid alkyl chain. Because the charge resides always on the daughter ion containing the ester function, the cleavage mechanism of both epoxide and epoxy alcohol derivatives of polyunsaturated fatty acid is very unambiguous and allows the positioning of the functional group. Fragmentation typically generates daughter ions arising from losses of oxygen ( $M-16$ ), rupture of C-C bond of the oxyrane ring and between alcoholic and epoxide functions, as described in Figure II.4.

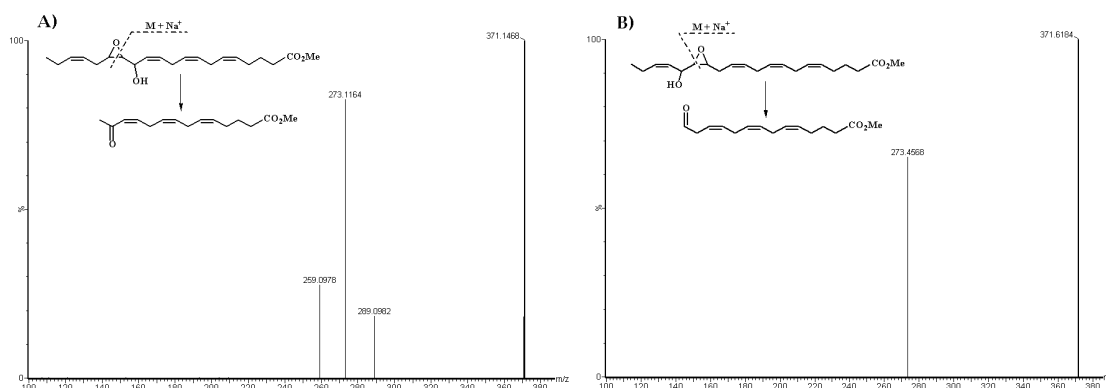


**Figure II.4.** Fragmentations of isomeric epoxy alcohol derivatives of EPA in MS/MS mode. Both compounds show parent pseudo-molecular ion ( $M+Na^+$ ) at  $m/z$  371. (A) MS/MS spectrum of 13-hydroxy-14,15-epoxy-eicosa-5Z,8Z,11Z,17Z-tetraenoic acid (13,14-HEpETE) methyl ester shows fragments at  $m/z$  289, 273 and 259 accounting for the occurrence of the methyl keto compound. (B) MS/MS spectrum of 16-hydroxy-14,15-epoxy-eicosa-5Z,8Z,11Z,17Z-tetraenoic acid (16,14-HEpETE) methyl ester reveals a single fragment at  $m/z$  273 due to formation of the aldehyde compound.

### II. 3. 4. LC-MS/MS analysis of keto fatty acid derivatives

Keto acid methyl esters gave also structurally significant product ions when collided with argon at a collision energy = 20 V. The MS/MS spectrum of natural 6-ketohexadeca-7*E*,9*Z*,12*Z*,15-tetraenoic acid (6-KHTE) methyl ester ( $m/z$  299  $M+Na^+$ ) showed ions which are derived from the  $\alpha$ -cleavage of the C-C bond adjacent to the keto group at  $m/z$  167 ( $M-C_{10}H_{13} + Na^+$ ) and at the vinyl positions at  $m/z$  219 ( $M-C_6H_9 + Na^+$ ) and 259, as depicted in Figure II.5. The fragmentation mechanism arising by  $\alpha$ -cleavage is common to other keto acids and is sufficiently diagnostic to assign the position of the functional group. Table II.3 illustrates molecular mass, fragment ions and UV maxima of synthetic analogues and natural oxylipins common in diatom extracts.

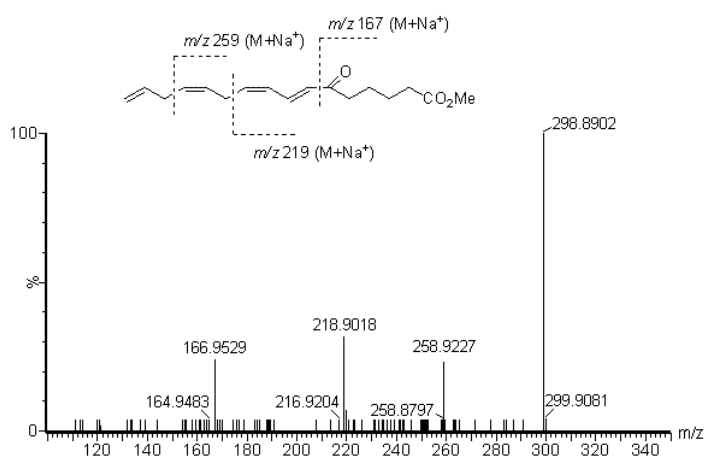


**Figure II.5.** ESI<sup>+</sup> MS/MS spectrum of 6-keto-hexadeca-7*E*,8*Z*,12*Z*,15-tetraenoic acid methyl ester resulting from  $\alpha$ -cleavage of the C-C bond. Parent ion at  $m/z$  299.

**Table II.3.** Diagnostic LC-DAD-ESI<sup>+</sup>-MS/MS data of common oxylipins from marine diatoms.

Fatty acid source	Chemical species <sup>a</sup>	M+Na <sup>+</sup> m/z	Fragment ions m/z	UV maxima nm
C16:2 <sup>b</sup>	9-KHME	305		235
C16:2 <sup>b</sup>	9-HHME	307		214
C16:3	6-KHTrE	301	221, 169	282
C16:3	6-HHTrE	303		234
C16:4	6-KHTE	299	259, 219, 167	282
C16:4	6-HHTE	301		234
C16:4	11,9-HEpHDE	319	221, 207	
C18:1	8-hydroxy-9,10-epoxy octadecanoic acid	351	223, 209, 195	
C20:5	15-oxo acid	285		322
C20:5	7,5-HEpETE	371	153	
C20:5	10,8-HEpETE	371	193	
C20:5	13,14-HEpETE	371	289, 273, 259	
C20:5	16,14-HEpETE	371	273	
C20:5	5-HEPE	355		236
C20:5	9-HEPE	355		236
C20:5	14-HEPE	355		236
C20:5	15-HEPE	355		236

<sup>a</sup> Analysis are performed on the corresponding methyl esters. <sup>b</sup> Biosynthesis not proven.

### II. 3. 5. GC-MS analysis of silyl-derivatives

The identity of isomeric alcohols has been ascertained by GC-EI MS after silylation of the methyl ester derivatives. The derivatization procedure is explained in the experimental section § II. 2. 7. Silyl derivatives possess excellent GC properties and produce useful EI mass spectra (Evershed, 1992; Mueller et al., 2006). Methyl silyl-derivatives of hydroxy fatty acids exhibited a weak molecular ion (M<sup>+</sup>) with predictable fragmentation pattern driven by the silyl group. The mechanism of cleavage occurs at the  $\alpha$  position to the siloxy group and allows one to assign the chain length and the positioning of the hydroxy function with a single chromatographic run. In the positive EI mode, the MS spectra of all trimethylsilyloxy (O-TMS) derivatives generate a characteristic ion at  $m/z$  73 due to the O-TMS fragment. Typically the charge is retained on the daughter ion bearing the trimethylsilyl-pentadienol moiety, as shown for the silyl derivative of natural 9-hydroxy-hexadeca-6Z-10E-12Z-trienoic acid methyl ester (9-HHTrE), which represents a distinctive diatom product. Figure II.6A shows a base peak at  $m/z$  197 and a lower intensity peak at  $m/z$  155 from  $\alpha$ -cleavage. A similar pattern of fragmentation was observed for the synthetic 8-keto-octadec-9Z-enoic acid

(8-KOME) methyl ester ( $m/z$  311 for  $M+H^+$ ) that showed fragments at  $m/z$  167 and 197 due to breaking next to the double bond and carbonyl group. Formal loss of MeOH and C=O from  $m/z$  197 generated the base peak of the spectrum at  $m/z$  137 (see Figure II.6B).

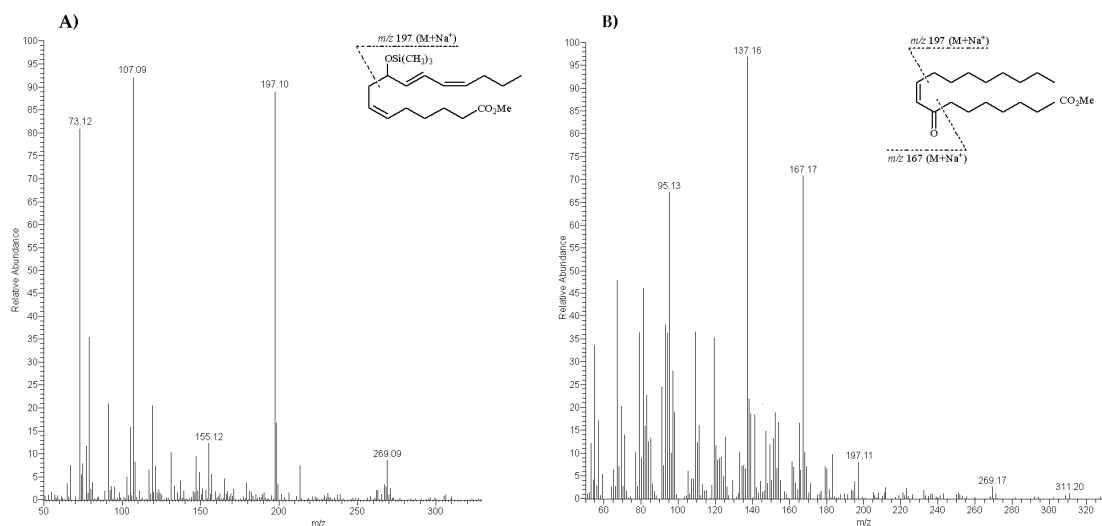


**Figure II.6.** GC-MS  $\alpha$ -fragmentation of oxylipins containing siloxy and keto moieties. Silyl derivatives of (A) 9-hydroxy-hexadeca-6Z-10E-12Z-trienoic acid (9-HHTre) methyl ester from *Skeletonema marinoi* and *Thalassiosira rotula* and (B) synthetic 8-keto-octadec-9Z-enoic acid (8-KOME) methyl ester.

The predictable fragmentation allows also to discriminate between isomeric synthetic keto-acids, like with the isomeric 8-keto-9E-hexadecenoic (8-KHME) and 11-keto-9E-hexadecenoic (11-KHME) derivatives (283  $m/z$   $M+H^+$ ), which exhibited the same chromatographic behaviour ( $R_t = 8.77$ ), but diagnostically differed in their fragments at  $m/z$  197 and 211 (data are reported in the Appendix see Figures A.1 and A.2, respectively).

Moreover, ion trap GC-EI MS analysis of natural and commercial hydroxy derivatives, such as 5-, 9-, 12-, 14- and 15-HEPEs, confirmed the diagnostic ions arising from  $\alpha$ -cleavage (Fox et al., 2000) and recognized by the hydroxy group position (data are reported in the Appendix see Figures A.8-A.10). GC-MS analysis provided additional data in the deconvolution of complex profiles of marine diatom oxylipins (Table II.4). In contrast to the isomeric keto-acid, the epoxy alcohol fatty acid methyl esters (either as natural compounds or silyl derivatives) gave complex mass spectra when analysed

in the same experimental GC-MS conditions due to the opening of the epoxide ring. Thus no further structural information was provided by the fragmentation pattern.

**Table II.4.** Diagnostic GC-MS data of silyl derivatives of natural oxylipins and synthetic analogues<sup>a</sup>.

Oxylipin source	Retention time (min)	MW	Diagnostic fragments (m/z)
8-KOME <sup>a</sup>	10.65	310	167, 197
8-KHME <sup>a</sup>	8.77	282	197, 139, 137
11-KHME <sup>a</sup>	8.77	282	211, 151, 125
8-HOME <sup>a</sup>	9.94	384	271, 241
11-HOME <sup>a</sup>	9.94	384	285
9-HHTrE	8.20	352	197
9-HHTE	8.12	354	270, 235
9-HODE	10.14	382	311, 259, 225
13-HODE	10.14	382	311, 207
13-HOTrE	10.21	380	311, 207
5-HEPE	11.91	404	303
8-HEPE	11.90	404	263
9-HEPE	11.85	404	255
12-HEPE	11.85	404	295
14-HEPE	11.84	404	183
15-HEPE	11.91	404	335

### II. 3. 6. Reproducibility and sensitivity in LC-MS

16-hydroxyhexadecanoic acid and 15-HEPE methyl esters were used i) to monitor extraction efficiency and measurement accuracy of the LC-MS protocol and ii) to determine the concentration of an unknown oxylipin sample by comparing it to a known concentration of the internal standard. Standard samples (injection volume 50  $\mu$ l) of 16-hydroxyhexadecanoic acid gave a linear MS response ( $r^2 = 0.9943$ ) within concentrations ranging from 100 ng/ml to 1  $\mu$ g/ml (Figure II.7A). Standard samples spiked at six concentrations ranging from 10 ng/ml to 3  $\mu$ g/ml in phytoplankton extracts gave linear response ( $r^2 = 0.9954$ ) from 300 ng/ml to 3  $\mu$ g/ml (Figure II.7B). The absolute detectable amount of 15-HEPE was ~500 pg (50  $\mu$ l from a solution 10 ng/ml) in total ion current and below 250 pg (50  $\mu$ l from a solution 5 ng/ml) by ion extraction. However, MS/MS analyses required more material and, for example, the detection limit with all epoxy alcohols was 2.5 ng (50  $\mu$ l from a solution 50 ng/ml).

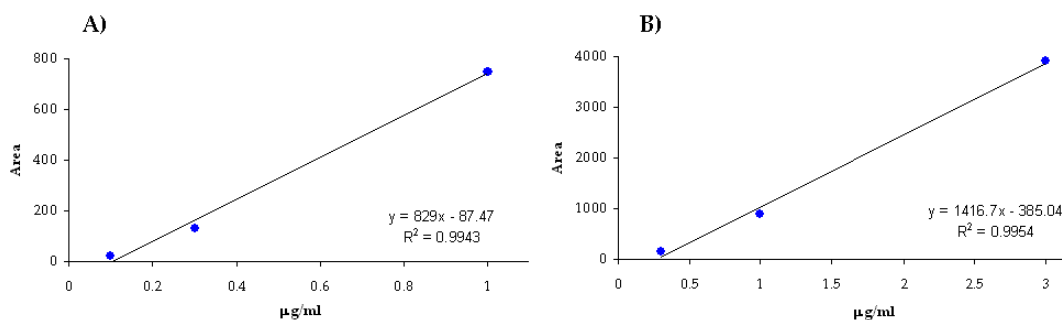


**Figure II.7.** Calibration curve standards. (A) Standard samples of 16-hydroxyhexadecanoic acid methyl ester gave linear MS response within concentrations ranging from 100 ng/ml to 1 µg/ml. (B) Calibration curve of 15-HEPE methyl esters gave linear MS response within concentrations ranging from 300 ng/ml to 3 µg/ml.

### II. 3. 7. Analysis of marine phytoplankton

Diatom composition of the phytoplankton sample collected in March 2005 included *Skeletonema marinoi* (79.9% in cell number), *Leptocylindrus danicus* (1.2% in cell number) and *Chaetoceros* sp. (18.3% in cell number). The sample from May 2005 comprised *Pseudo-nitzschia pseudodelicatissima* (85.7% in cell number), *Chaetoceros* sp. (13.4% in cell number) and *Cerataulina pelagica* (below 1% in cell number). In DAD detection, the profiles of phytoplankton samples were obtained in the wavelength range from 205 to 400 nm. ESI<sup>+</sup> MS/MS analysis indicated at least three oxylipin classes that, in relation to retention time, included epoxy alcohols, hydroxyacids and hydroperoxyacids (Figure II.8). As for hydroxy- and hydroperoxy fatty acids, mass spectra showed main pseudomolecular ions (M+Na<sup>+</sup>) consistent with EPA derivatives (*m/z* 355 and 371, UV<sub>max</sub> = 235 nm) running between 18.0 and 21.0 min. Furthermore, both samples contained the methyl derivative of hydroxy-hexadecenoic acid (HHME) (*m/z* 307.5, UV<sub>max</sub> = 214 nm). In the sample from May 2005, two major epoxy alcohols of EPA (*m/z* 371) were clearly detectable at 12.5 min and 14.4 min. In MS/MS mode, this last product gave fragment ions at *m/z* 289 (C<sub>15</sub>H<sub>22</sub>O<sub>4</sub>·Na<sup>+</sup>), 273 (C<sub>15</sub>H<sub>22</sub>O<sub>3</sub>·Na<sup>+</sup>) and 259 (C<sub>14</sub>H<sub>20</sub>O<sub>3</sub>·Na<sup>+</sup>) for the presence of 13,14-HEpETE, whereas the second epoxy alcohol (R<sub>t</sub> = 12.4 min) was associated with fragment ion at *m/z* 153 (C<sub>6</sub>H<sub>10</sub>O<sub>3</sub>·Na<sup>+</sup>) in agreement with the structure of 7-hydroxy-5,6-epoxy-eicosa-8Z,11Z,14Z,17Z-tetraenoic acid methyl ester (7,5-HEpETE). The phytoplankton sample collected in March 2005 showed a third epoxy alcohol (*m/z* 371) featured by a MS/MS fragment ion at *m/z* 193 (C<sub>9</sub>H<sub>14</sub>O<sub>3</sub>·Na<sup>+</sup>)

that agrees with the occurrence of 10-hydroxy-8,9-epoxy-eicosa-5Z,11Z,14Z,17Z-tetraenoic acid methyl ester (10,8-HEpETE).

After purification and silylation of the individual LC-MS peaks, the isobaric hydroxy-derivatives of EPA at 17.7 and 20.2 min in the phytoplankton sample of May 2005 gave parent ions at  $m/z$  404 and daughter ions at  $m/z$  335 and 303 for 15-HEPE and 5-HEPE, respectively. The peak eluted at 19.7 min in the sample of March 2005 was attributable to 8-hydroxy-eicosa-5Z,9E,11Z,14Z,17Z-tetraenoic acid (8-HEPE) for the characteristic presence of ions at  $m/z$  263 ( $C_{16}H_{27}OSi$ ) based on the expected fragmentation of the corresponding silyl derivative ( $m/z$  404).

The LC-MS protocol was also tested for the quantification of oxylipins using 16-hydroxyhexadecanoic acid as internal standard. In the phytoplankton sample of March, 0.22 pg/diatom cell and 0.45 pg/diatom cell are determined for 8-HEPE and 10,8-HEpETE, respectively. The amount of oxylipins in the sample of May were 2.72 and 1.13 pg/diatom cell for the major HEPES, and 2.80 and 1.08 pg/diatom cell for the epoxy alcohols. In both phytoplankton samples the level of HHME was about 2.45 pg/diatom cell.

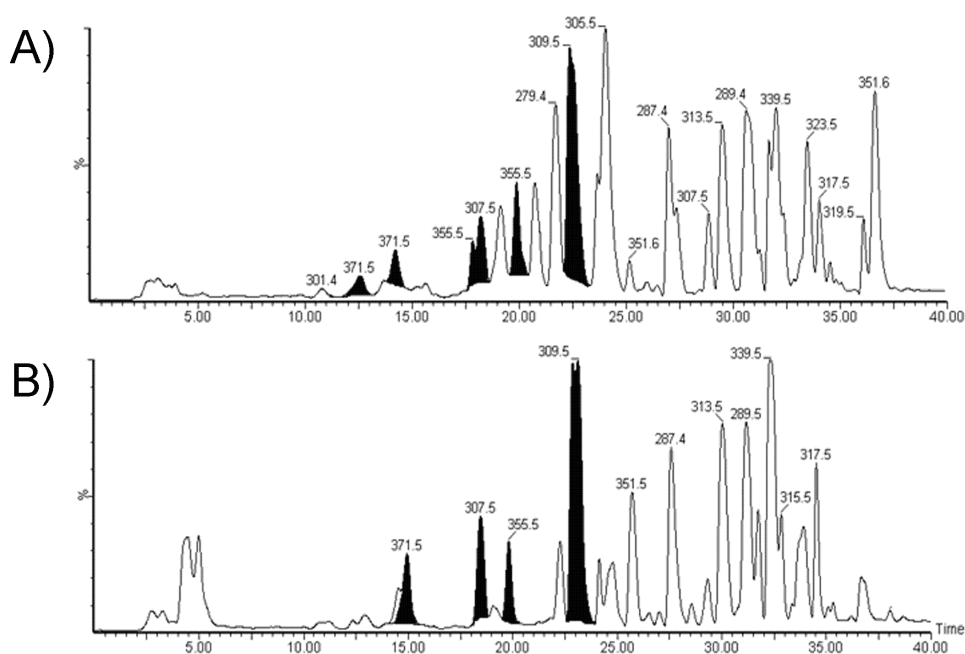


**Figure II.8.** Phytoplankton analysis (North Adriatic bloom). (A) Sample collected in May 2005 containing *Pseudo-nitzschia pseudodelicatissima* (85.7% in cell number), *Chaetoceros* sp. (13.4% in cell number) and *Cerataulina pelagic* (below 1% in cell number). (B) Sample collected in March 2005 containing *Skeletonema marinoi* (79.9% in cell number), *Chaetoceros* sp. (18.3% in cell number) and *Leptocylindrus danicus* (1.2% in cell number).

## II. 4. Discussion

The application of mass spectrometry (MS) for the analysis of cellular metabolites has dramatically increased over the last two decades and today MS is one of the most important analytical tools for the analysis of different classes of metabolites (Dunn & Ellis, 2005). MS combined with a separation technique offers many opportunities for analysis of biological samples because it enables the determination and identification of a large number of metabolites in a single analysis. However, two issues must be considered in connection with choosing an appropriate analysis method: i) resolution, because metabolites comprise different classes of molecules with distinct physical-chemical properties, and ii) sensitivity, since metabolite concentrations can be relatively low. The versatility of the different instrumental MS platforms commercially available allows an integrated approach that in many cases provides sufficient data for a qualitative and quantitative metabolite analysis in natural extracts (Niessen, 2003) and has been recently applied to plant oxylipins (Mueller et al., 2006). In marine diatoms, lipoxygenase-dependent pathways of fatty acid oxidation appear to be nearly ubiquitous, but the qualitative and quantitative composition of the final products vary both among species and in response to unknown physiological and environmental factors (d'Ippolito et al., 2005; Fontana et al., 2007b; d'Ippolito et al., 2009). The compounds hitherto characterized suggest the occurrence of two predominant families derived from C<sub>16</sub> and C<sub>20</sub> fatty acids, with an almost constant presence of isomeric epoxy alcohols and hydroxy- fatty acids. Using the combination of Q-ToF mass analyzer and UV photodiode array (DAD) detection, a complete characterization of these compounds is easily accomplished by LC-MS/MS techniques equipped with the "soft" electrospray ionization. This technology offers great improvement enabling to the analysis to a large number of different types of non-volatile molecules (polar, less-polar and neutral metabolites) with a reduced manipulation of the biological samples (Wheelan et al., 1995; Pérez Gilabert & García Carmona, 2002; Hwa Lee et al., 2003; Schulze et al., 2006). Common HPLC RP-18 columns allow a clear fractionation of the major classes of oxygenated fatty acids hitherto characterized in different marine diatoms by showing a predictable chromatographic behaviour that is extremely diagnostic for the analysis of unknown phytoplankton samples. LC-MS profiles do not

allow unambiguous discrimination among the positional isomers of hydroxy- fatty acids but, as reported in Table II.4, this pitfall is overcome by GC-MS analysis of the corresponding silyl derivatives (Mueller et al., 2006; Schulze et al., 2006). A complete identification of the metabolic content of a complex diatom extract can be accomplished only by a combination of LC-MS, GC-MS and MS/MS techniques, even if the fragmentation in LC-MS/MS analysis of  $\alpha$ -epoxy alcohol methyl esters is by itself a valid and reliable method to infer the lipoxygenase pathways in diatoms. In fact, sodium adducts of epoxy alcohol methyl esters generate main daughter ions, from the cleavage of the oxirane ring with a positive charge that typically resides on the fragment containing the ester function (Table II.3). As depicted in Figure II.4, the C-O bond proximal to the hydroxy function is the most susceptible to undergo heterolytic cleavage to give charged aldehydes and methylketones. These last two compounds, as illustrated with the isomeric 13,14-HEpETE and 16,14-HEpETE (Figures II.4A and II.4B), show different stabilities in the MS collision chamber. The aldehyde function is stable and does not undergo other cleavages (Figure II.4B), whereas the methylketones are further fragmented (Figure II.4A). The experimental results demonstrate that the MS/MS spectrum of epoxy alcohols leading to aldehydes show a single ion mass, whereas the fragmentation process leading to methylketones is characterized by predictable clusters of daughter ions. The mechanism is very specific (Table II.3) and allows to characterize the isomeric epoxy alcohols and consequently, on a biogenetical basis (Chang et al., 1996), the original hydroperoxy fatty acids and the corresponding position of the lipoxygenase-catalyzed insertion of oxygen.

Quantification of diatom oxylipins is achieved on pseudomolecular ions, using 16-hydroxyhexadecanoic acid as internal standard to monitor extraction efficiency. The lower limit of quantification of 15-HEPE was 100 ng/ml ( $\sim 0.3 \mu\text{M}$ ) in a raw extract of phytoplankton as surrogate matrix, but the absolute amount detected in a single chromatographic run was below 500 pg ( $\sim 1.5 \text{ pmol}$ ) in total ion current and below 250 pg ( $\sim 0.7 \text{ pmol}$ ) by ion extraction. This sensitivity was sufficient to screen and quantify oxylipins occurring at femtomolar range in diatom cells from phytoplankton samples collected before and after the apex of the spring blooms in the North Adriatic Sea. Identification of 13,14-HepETE, 7,5-HEpETE and 10,8-HEpETE in the phytoplankton

samples suggests the presence of three different eicosapentanoate-dependent lipoxygenase pathways leading to synthesis of 15-, 5- and 8-hydroperoxy-eicosapentaenoic acids. The pathways have been further confirmed by GC-MS analysis of the silyl derivatives of the corresponding HEPES purified by HPLC from the diatom extracts (data not shown). Oxylipins derived from putative 15- and 5R-LOX activities have been already reported in monoclonal cultures of *Pseudo-nitzschia delicatissima* and *Skeletonema marinoi* (d'Ippolito et al., 2009; Fontana et al., 2007b) whereas 8-LOX products have been hitherto described from the coral *Plexaura homomalla* (Brash et al., 1996).

## Chapter III

### Effects of diatom metabolites on the reproduction of zooplankton grazers

#### III. 1. Introduction

Several analogies and differences exist between animals, plants and diatoms with respect to the biosynthesis and function of oxylipins. While in animals and plants, oxylipins are produced by a peroxidation mechanism of polyunsaturated fatty acids via lipoxygenase (LOX) and cyclo-oxygenase-like activities, they solely originate from the LOX action in diatoms.

In mammals, oxylipins are formed mainly via the arachidonic acid (C<sub>20:4</sub> fatty acid) cascade and they play a major role in inflammatory processes, in stress responses to infection, allergy and immune exposure to food, drugs and environmental xenobiotics (Brash, 1999). Oxylipins from terrestrial plants, called phyto-oxylipins, are formed mainly via the C<sub>18</sub> polyunsaturated fatty acid metabolism and they act as signal molecules and protective compounds such as antibacterial and wound-healing agents (Blée, 2002). Although the eco-physiological role of oxylipins has been especially studied in mammalians and higher plants, a huge variety of “phyco-oxylipins” has been also reported from diatoms, where they originate from the oxygenation of C<sub>16</sub> and C<sub>20</sub> polyunsaturated fatty acids (Fontana et al., 2007a).

Diatoms are at the base of the marine food web and are thought to constitute a suitable food source for zooplankton grazers like copepods. This idea largely persisted until 1993 (Ban et al., 1997) when a world-wide group of researchers reported what is now known as the “*diatom-copepod paradox*”. Although copepods do consume diatoms to a large extent, pieces of evidence indicated that diatoms were not an optimal food for copepod growth, because their consumption lead to elongated generation times and increased mortality rates in offspring of their grazers (Paffenhöfer, 1970; Ianora & Poulet, 1993; Poulet et al., 1994). Further studies suggested that the anti-proliferative

effect of diatoms on copepod reproduction was not caused by nutritional deficiency, but rather by the presence of antimitotic compounds, which reduced egg viability in copepods by blocking mitotic division during the embryogenesis (Poulet et al., 1994). Initially, this inhibitory effects were correlated to polyunsaturated aldehydes (PUAs) (Miralto et al., 1999; d'Ippolito et al., 2002a, 2002b; Ianora et al., 2004), which are produced by diatoms in response to physical damage as occurred during copepod grazing (Pohnert, 2000). However, although PUAs compromised copepod egg hatching success and larval development *in vitro*, these unstable lipids alone were not sufficient to explain the ecological effect on zooplankton communities, since several species of diatoms that do not produce PUAs negatively affected copepod reproduction as well (Wichard et al., 2005b; Jones & Flynn, 2005; Ianora et al., 2006; Dutz et al, 2008). Recently, diatoms were described to produce an entirely new group of oxygenated fatty acid derivatives by lipoxygenases (d'Ippolito et al., 2005). The presence of these compounds clearly demonstrated that different oxygenase pathways could be active in marine diatoms, suggesting that the production of aldehydes in this group of microalgae could be accompanied or complemented by the synthesis of many other products derived from the enzymatic oxidation of membrane lipids. The aim of this part of the PhD thesis was: (i) to examine the effect of six marine diatom diets (*Skeletonema marinoi*, *Skeletonema pseudocostatum*, *Thalassiosira rotula* 1, *Thalassiosira rotula* 2, *Chaetoceros affinis* and *Chaetoceros socialis*) on egg production, hatching success and early larval stages of the calanoids *Temora stylifera* and *Calanus helgolandicus*; (ii) to analyse lipid derivatives composition in these marine diatoms during the experimental conditions used in previous studies to trigger the synthesis of PUAs; (iii) to examine the involvement of different classes of oxylipins other than PUAs in diatom-copepod interactions and (iv) to study the effect of the diatom lysis on LOX-mediated synthesis.

## **III. 2. Materials and Methods**

### *III. 2. 1. Cell culture samples*

The diatom species *S. marinoi* (SZN B118), *S. pseudocostatum* (SZN B77), *T. rotula* strain 1 (CCMP 1647) and *T. rotula* strain 2 (CCMP 1018), used in the feeding experiments described below, were obtained from the Functional and Evolutionary Ecology

Department of the Stazione Zoologica Anton Dohrn (Naples, Italy) and the Provasoli-Guillard National Centre for Culture of Marine Phytoplankton (Boothbay Harbor, Maine, USA), respectively. Axenic cultures of these microalgae were prepared in 2 L jars with 1 L of 0.22  $\mu\text{m}$  filtered and autoclaved seawater enriched with F/2 medium (Leftley et al., 1987) at 20° C under 12h:12h light:dark cycle. Cultures were diluted daily by replacing 25% of the culture with fresh media. Cultures of the dinoflagellate *Prorocentrum minimum*, which served as diet control in the experiment, were likewise prepared. Cell carbon content of *S. marinoi*, *T. rotula* 1 and *P. minimum* was considered to be the same as in Carotenuto et al. (2002). Cell carbon content of *S. pseudocostatum* was not determined, but it was assumed to be the same as *S. marinoi* due to its similar size.

*C. affinis* (SZN FE21) and *C. socialis* (SZN FE17), used in a second feeding experiment, were isolated in the North Adriatic Sea by the Functional and Evolutionary Ecology Department of the Stazione Zoologica Anton Dohrn (Naples, Italy) during the 2002 spring bloom, while *S. marinoi* (CCMP 2092) was purchased from the Provasoli-Guillard National Centre for Culture of Marine Phytoplankton (Boothbay Harbor, Maine, USA). Axenic cultures of these diatoms were grown as described in the experimental section § II. 2. 3 of chapter II. The dinoflagellate *P. minimum* served again as diet control and was grown in the same conditions.

### III. 2. 2. Marine zooplankton samples

The copepod samples of *T. stylifera* were collected weekly from October 4<sup>th</sup> to November 30<sup>th</sup> 2005 at a fixed station of the Gulf of Naples (Italy) by towing a 250  $\mu\text{m}$  mesh net with a non-filtering cod obliquely from a depth of 50 m to the surface. The copepods of *C. helgolandicus* were harvested as described above on several occasions in autumn and winter 2005 in the Gulf of Naples and Chioggia (Italy). All samples were poured in an insulated box and transported to the laboratory within 1 hour of collection.

### III. 2. 3. *Feeding experiments*

Dr. Aldo Barreiro (Facultad de Ciencias, University of Vigo, Spain) performed the first feeding experiment. Healthy adult female copepods of *T. stylifera* (n = 10) were sorted and transferred to crystallizing dishes containing 100 ml of 0.45 µm filtered seawater and kept at 20° C. Each dish contained a single animal and they were maintained in this suspension for 24 h. The next day, animals were transferred to new food suspensions with each of the target algae offered as the only food. The microalgae tested were *S. pseudocostatum* (SZN B118), *S. marinoi* (SZN B118), *T. rotula* 1 (CCMP 1647), *T. rotula* 2 (CCMP 1018) and the control diet *P. minimum*. This alga was used as a negative control, because *T. stylifera* fed with it retains a high and constant egg hatching success (Turner et al., 2001). Each day, copepods were transferred to new containers with fresh media and food suspensions. Cell concentrations of each alga were adjusted to keep the same carbon concentration (0.98 µg C ml<sup>-1</sup> and 1.24 µg C ml<sup>-1</sup> for both *Thalassiosira* and *Skeletonema* genus, respectively) close to natural bloom conditions. Egg production and hatching success were recorded daily under an inverted binocular microscope. Experiments were terminated after 12 to 15 days. Hatching success was estimated by maintaining egg production containers for an additional 48 h at 20° C and was calculated as the percentage of nauplii with regard to egg production.

The second feeding experiment was conducted at the Functional and Evolutionary Ecology Department of the Stazione Zoologica Anton Dohrn (Naples, Italy) in the same manner as above. The diatom species *C. affinis* (SZN FE21), *C. socialis* (SZN FE17), and two control diets, *S. marinoi* (CCMP 2092) and *P. minimum*, positive and negative control, respectively were used as food source for the experiment reported in the section § III. 3. 2. In addition to *T. stylifera*, possible dietary effects were also tested on the copepod *C. helgolandicus*.

### III. 2. 4. *Statistical analysis*

Statistical analysis was computed by Dr. Ylenia Carotenuto (Functional and Evolutionary Ecology Department of the Stazione Zoologica Anton Dohrn, Naples, Italy). Data of the first feeding experiment were analysed with an ANCOVA using time

(LN transformed) as covariate, daily egg production rate as dependent variable and algal species as factor. In order to test for differences among diet treatments in the second experiment, a one-way ANOVA test was applied, calculating mean values for 14 days and using 10 replicates for each feeding experiment.

### III. 2. 5. *Fluorescence labelling and confocal microscopy of copepods fed with diatoms*

Teratogenic and apoptotic experiments were performed by Dr. Giovanna Romano (Functional and Evolutionary Ecology Department of the Stazione Zoologica Anton Dohrn, Naples, Italy). To compare the effects of PUAs, oxylipins and hydroperoxides (FAHs) on teratogenesis, *C. hegolandicus* females (n = 6) were incubated individually in 2 ml tissue culture wells filled with 0.45  $\mu\text{m}$  filtered seawater (FSW) and increasing concentrations of compounds ranging from 7.0 to 35.0  $\mu\text{M}$  for the aldehyde pool, from 3.0 to 15  $\mu\text{M}$  for hydroperoxides and from 3.0 to 70  $\mu\text{M}$  for the oxylipin mixture. Each class of these metabolites was dissolved in methanol. Metabolite concentrations were adjusted to give a final solvent concentration in the experiment of 10  $\mu\text{l}$  methanol  $\text{ml}^{-1}$ . Control females (n = 6) were incubated in methanol and 0.45  $\mu\text{m}$  FSW. After spawning (< 24 h) test and control females were removed and eggs were allowed to develop until hatching took place. The percentage of abnormal nauplii and survivorship of females was recorded. Newly hatched nauplii, incubated in PUAs, oxylipins or FAHs, were washed three times in FSW before overnight fixation in 2–4% paraformaldehyde. Fixed larvae were rinsed several times in PBS and immediately stained with TUNEL (terminal-deoxynucleotidyl-transferase-mediated-dUTP Nick End Labelling; Roche Diagnostics GmbH, Mannheim, Germany), or stored at 4° C in PBS containing 0.02%  $\text{NaN}_3$ , until fluorescence labelling. Before TUNEL staining, copepod larvae were incubated for 24 h in 250  $\mu\text{l}$  of 1 U  $\text{ml}^{-1}$  chitinase enzyme (EC 3.2.1.14; Sigma-Aldrich, Schnellendorf, Germany) dissolved in 50 mM sodium citrate buffer (pH 6.0, at 25° C) to permeabilize the chitinous wall. After rinsing several times in PBS, embryos were incubated for 2 h in 0.1% Triton X-100 at room temperature, rinsed in PBS containing 1% BSA (bovine serum albumin; Sigma-Aldrich, Schnellendorf, Germany), and further incubated for 90 min in TUNEL solution at 37° C. To obtain TUNEL-positive samples, nauplii were incubated for 10 minutes in 50 mM Tris-HCl (pH 7.5), 10 mM  $\text{MgCl}_2$ , 0.1%

dithiothreitol, containing 250  $\mu\text{g ml}^{-1}$  bovine pancreatic DNase I (Boheringer GmbH, Mannheim, Germany), at room temperature. Negative controls were obtained by incubating nauplii in label solution only as recommended by the manufacturers of the TUNEL kit. After staining, copepod larvae were observed with an inverted Zeiss LSM-410 confocal laser scanning microscope equipped with a 40x water immersion objective (NA 1.2). Each image was acquired with an Argon 488 nm wavelength laser to detect TUNEL fluorescence (green), and with a 633 nm wavelength laser to visualize samples in transmitted light. Images were reconstructed three-dimensionally using the Zeiss software.

### III. 2. 6. *Chemical analysis*

Frozen pellets of all diatoms were extracted as previously reported in the experimental section § II. 2. 5 of chapter II. Part of these crude extracts were submitted to PUAs analysis by GC-MS as described in d'Ippolito et al. (2002b). The remaining extracts were methylated with ethereal diazomethane and, after removing organic solvent under  $\text{N}_2$ , the resulting materials were dissolved in MeOH (final concentration 1  $\mu\text{g}/\mu\text{l}$ ) and analysed by LC-MS analysis on a QToF-*micro* mass spectrometer (Waters S.pA., Milan, Italy) equipped with an ESI source in positive mode and coupled with a Waters Alliance HPLC system. In the section § II. 2. 6 of chapter II the gradient HPLC to identify the oxygenate derivatives was described. Quantification of PUAs and oxylipins was carried out by addition of the internal standards, *trans*-4-decenal (30  $\mu\text{g}/\text{g}$  of pellet) and 16-hydroxyhexadecanoic acid (30  $\mu\text{g}/\text{g}$  of pellet). The average and standard deviation of five measurements ( $n = 5$ ) was calculated for each species.

### III. 2. 7. *Oxylipin preparation*

Fresh diatoms were harvested by gentle centrifugation (1200 g for 10 min at 5° C using a swing-out rotor). The cell pellet was collected in 50 ml Falcon tubes and immediately processed for purifying the oxylipin fraction. The extraction procedure is reported in the experimental section § II. 2. 5 of chapter II. The methylated extract was fractionated on a silica gel column by a polarity gradient system (petroleum ether/ $\text{Et}_2\text{O}$ ) to give 1.3 mg from *S. marinoi*. For FAHs synthesis, EPA was methylated with ethereal

diazomethane and auto-oxidized at 42° C in the dark for two weeks in the presence of  $\alpha$ -tocopherol (Peers & Coxon, 1983). Isolation of the hydroperoxide mixture was performed by SP-HPLC with an isocratic solvent system of *n*-hexane/Et<sub>2</sub>O 85:15 (1 ml/min,  $\lambda$  = 236 nm), prior to hydrolysis with 10% NaOH in EtOH. Stock solutions of PUAs, oxylipins and FAHs were dissolved in MeOH, and stored under N<sub>2</sub> at -80° C until further analysis.

### III. 2. 8. LOX assay

LOX activity was determined by the method proposed by Anthon & Barrett (2001) using modifications according to d'Ippolito et al. (2006). The colorimetric response was optimized by a two-step assay using hemoglobin, 32.5  $\mu$ l of 25 mM EPA and algal suspensions containing different number of cells ( $1.42 \times 10^6$ ,  $2.13 \times 10^6$ ,  $2.84 \times 10^6$  and  $4.26 \times 10^6$  cells) in 200  $\mu$ l F/2 medium. LOX activity was recorded by spectrophotometric measurements at 598 nm and the FAH concentration was corrected for the blank control without EPA and normalized to the total amount of protein for each sample. The protein content was determined by using the Lowry protein assay following the manufacture's instructions (Bio-Rad) with BSA as standard. All measurements were performed in triplicates and data are presented as means  $\pm$  SD.

### III. 2. 9. hROS detection

*S. marinoi* (CCMP 2092) cells obtained from a 2 L culture were harvested as described above, re-suspended in 10 ml F/2 medium and divided in ten aliquots: five aliquots were used as controls whereas the other five were loaded with 30  $\mu$ l of HPF/H<sub>2</sub>O 1:8. After 30 min of incubation in the dark, cells were washed with 1 ml F/2 medium by three cycles of centrifugation (800 g, 5° C, 5 min) and then re-suspended in 2 ml F/2 medium before measuring the fluorescence. The fluorescent emission of these samples was measured at 515 nm by spectrofluorimeter with an excitation light of 488 nm (Setsukinai et al., 2003). Afterwards the samples were sonicated and fluorescent activity determined again, as described above. In the parallel experiment, the same measurements were acquired for dye-loaded cells as described above, but without removing the extracellular HPF. In the last experiment, *S. marinoi* (CCMP 2092) cells

were processed as above, but cell lysis was promoted by addition of increasing concentrations of SDS (from 1% to 10%). Cell images were acquired every 5 minutes by epifluorescence microscope.

### III. 3. Results

#### III. 3. 1. *Effects of diatom diets on copepod reproduction*

The impact of the five different diatom diets (*S. marinoi*, *S. pseudocostatum*, *T. rotula* 1, *T. rotula* 2 and the dinoflagellate *P. minimum*) was tested on the egg production and the hatching success of the calanoid copepod *T. stylifera*. Copepods fed on *T. rotula* 1 (CCMP 1647) and *T. rotula* 2 (CCMP 1018) induced the highest egg production rates, although there was a decrease from the first half of the experiment (mean days 2 - 7:  $61.9 \pm 12$  SD and  $59.5 \pm 11.7$  SD eggs female<sup>-1</sup> day<sup>-1</sup>) with respect to the second half (mean days 8 - 15:  $31.8 \pm 9.8$  SD and  $35.4 \pm 15.5$  SD eggs female<sup>-1</sup> day<sup>-1</sup>), representing a decrease of 48.7% and 40.4%, respectively. In contrast, *S. marioni* (SZN B118) and *S. pseudocostatum* (SZN B77) diets had an even more pronounced inhibitory effect on egg production rates (mean days 2 - 7:  $21.7 \pm 9.6$  SD and  $26.4 \pm 17.5$  SD eggs female<sup>-1</sup> day<sup>-1</sup>; mean days 8 - 15:  $4.5 \pm 2.2$  SD and  $1.5 \pm 2.7$  SD eggs female<sup>-1</sup> day<sup>-1</sup>), corresponding to a drastically decrease of 94.1% and 79.2%, respectively. The dinoflagellate *P. minimum* was used as negative control, because diet supported moderately low but constant egg production rates over the whole experimental period (mean days 2-7:  $13.6 \pm 5.3$  SD eggs female<sup>-1</sup> day<sup>-1</sup>; mean days 8-15:  $14.4 \pm 5.7$  SD eggs female<sup>-1</sup> day<sup>-1</sup>).

ANCOVA analyses (Table III.1) showed significant differences in egg production between all pair wise comparisons except *T. rotula* 1-*T. rotula* 2 and *S. marinoi*-*S. pseudocostatum* in *T. stylifera*.

**Table III.1.** ANCOVA analysis of egg production rate in *T. stylifera*. Covariate was always significant.

<i>T. stylifera</i>	<i>df (factor, error, total)</i>	<i>F</i>	<i>p</i>
TR1-TR2	1, 289, 292	1,14	0,286
TR1-SM	1, 311, 314	69,46	<0,001
TR1-SPC	1, 240, 243	34,55	<0,001
TR1-PRO	1, 273, 275	78,93	<0,001
TR2-SM	1, 291, 294	106,86	<0,001
TR2-SPC	1, 220, 223	56,29	<0,001
TR2-PRO	1, 253, 256	139,46	<0,001
SM-SPC	1, 242, 245	0,04	0,841
SM-PRO	1, 275, 278	4,37	0,035
SPC-PRO	1, 204, 207	5,34	0,022

Optimal hatching rates were observed after one day with all diets, but decreased thereafter for all diatoms tested. Only *P. minimum* supported constant egg hatching rates throughout the experiment (mean 89.9% ± 8.9 SD). After just two days, egg hatching success decreased somewhat when copepods fed on both *Thalassiosira* species, with a pronounced reduction to 37.6% ± 14 SD in *T. rotula* 1 and 15.7% ± 5.3 SD in *T. rotula* 2 within 15 days. However, diets of *S. marioni* and *S. pseudocostatum* induced a much stronger egg hatching inhibition after just three days with a drastic decrease reaching values of 4.6 %± 9.2 SD and 0%, respectively, in the same period.

ANCOVA analyses (Table III.2) showed significant differences between all pair wise comparisons for hatching success except for *T. rotula* 2-*S. marinoi*, *T. rotula* 2-*S. pseudocostatum* and *S. marinoi*-*S. pseudocostatum*.

**Table III.2.** ANCOVA analysis of egg hatching success in *T. stylifera*. Covariate was always significant.

<i>T. stylifera</i>	<i>df (factor, error, total)</i>	<i>F</i>	<i>p</i>
TR1-TR2	1, 247, 250	57,15	<0,001
TR1-SM	1, 184, 187	25,84	<0,001
TR1-SPC	1, 222, 225	39,83	<0,001
TR1-PRO	1, 215, 218	28,84	<0,001
TR2-SM	1, 176, 179	0,157	0,639
TR2-PRO	1, 207, 210	207,29	<0,001
SM-SPC	1, 151, 154	0,41	0,52
SM-PRO	1, 144, 147	93,9	<0,001
SPC-PRO	1, 182, 185	131,94	<0,001

### III. 3. 2. Effects of non-PUA producing diatoms on copepod reproduction

*C. affinis* (SZN FE21) and *C. socialis* (SZN FE17), which did not produce PUAs (Fontana et al., 2007b), were tested on egg hatching success and early larval stages of the calanoid copepods *T. stylifera* and *C. helgolandicus*. The results were compared with the toxic activity of the PUAs-producing diatom species *S. marinoi* (CCMP 2092; positive control) using the dinoflagellate *P. minimum* as a negative control. *C. socialis* moderately affected copepod egg viability that decreased to 45% compared to 78% initial hatching success after 14 days of feeding on this diet. In contrast, copepod egg viability declined dramatically from > 80% to 0% when copepods were fed on *C. affinis*, similar to the effect induced by *S. marinoi* (Figure III.1). All diets tested were significantly different (one-way ANOVA,  $p < 0.0001$ ) from one another for both copepod species tested.

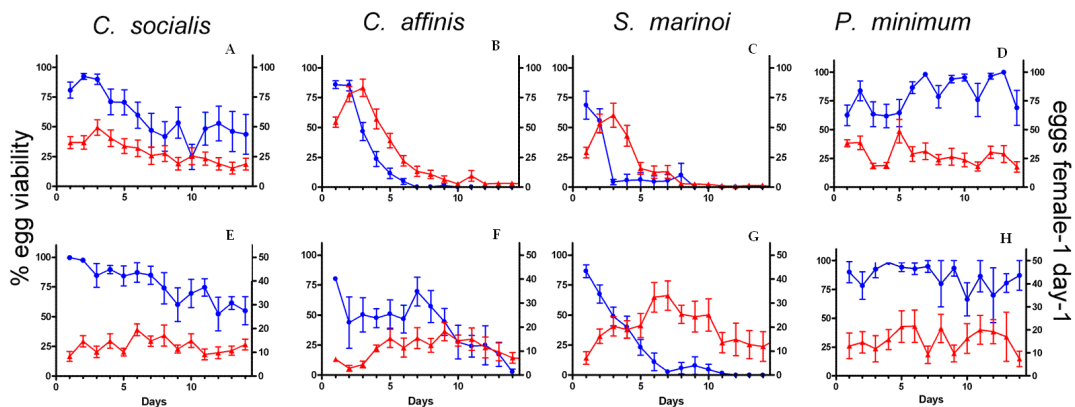


**Figure III.1.** Effect of diatom diets on egg production (red) and % egg viability (blue) in the copepods *T. stylifera* (A-D) and *C. helgolandicus* (E-H) fed with the diatoms *C. socialis*, *C. affinis*, *S. marinoi* (positive control) and *P. minimum* (negative control).

Moreover, the feeding experiment showed that the decline in egg viability is accompanied by a concomitant rise in the number of hatched teratogenic nauplii. Mothers fed on *C. affinis* and *S. marinoi* produced nauplii with strong teratogenic birth defects. Abnormal nauplii had asymmetrical bodies and malformed or reduced numbers of appendages. Some died within a few hours after hatching, whereas others died about one day later, at naupliar stage NII, because they were unable to swim or feed properly. Cell death through apoptosis had occurred in many tissues of the body, especially in appendages with strong structural malformations, as revealed utilizing

confocal laser microscope and the fluorescent TUNEL probe, specific for apoptosis (Figure III.2), as apoptotic regions corresponded to those of developmental aberrations. Conversely, females reared with *C. socialis* and *P. minimum* (negative control diet) produced only morphologically normal nauplii that showed no fluorescence.

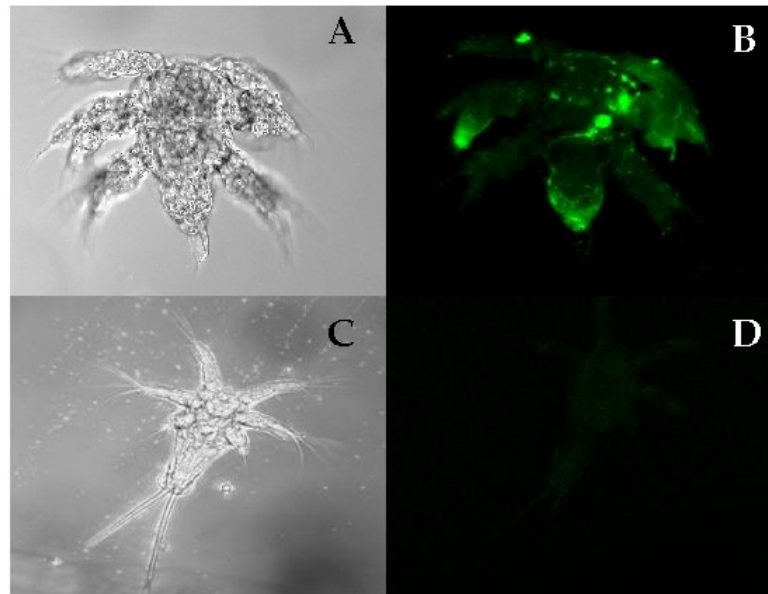


**Figure III.2.** Morphological anomalies and apoptosis (TUNEL staining) induced by toxic diatoms. Transmitted light and fluorescent images of nauplii generated from *T. stylifera* females reared with *C. affinis* (A and B) and *P. minimum* (C and D) (negative control).

### III. 3. 3. *Chemical analysis of lipoxygenase products*

For an ecological interpretation of the deleterious effect of diatoms on their grazers, it was essential to quantify the oxylipin and aldehyde production in these algal diets. Within 5 minutes, cell damage triggered LOX activity and the resulting fatty acid derivatives were detected by monitoring the level of oxylipin methyl esters on reverse-phase LC-MS/MS and the carbethoxyethylidene-aldehydes on GC-MS. Quantitative composition and distribution of total oxylipin and aldehyde contents in *T. rotula* 1, *T. rotula* 2, *S. marinoi* and *S. pseudocostatum* are shown in Figure III.3.

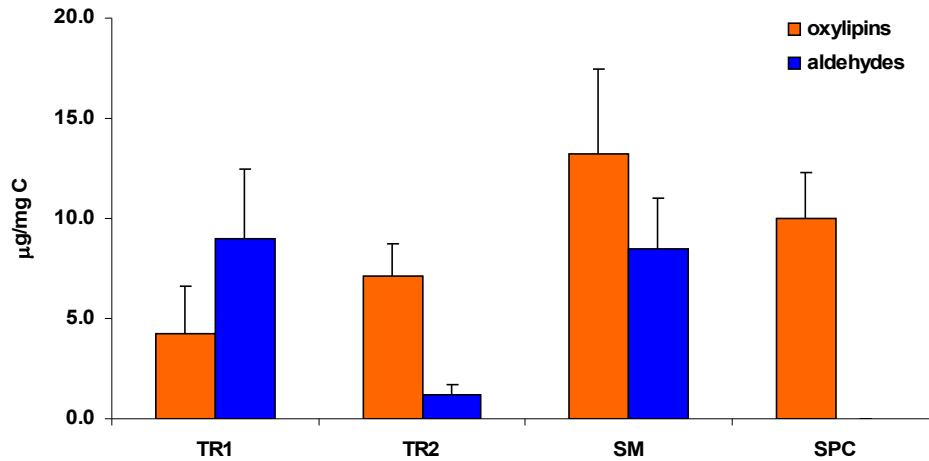


**Figure III.3.** Quantitative analysis of phyco-oxylipins (orange) and PUAs (blue) in *T. rotula* 1 (TR1), *T. rotula* 2 (TR2), *S. marinoi* (SM), and *S. pseudocostatum* (SPC). No LOX derivatives were detectable in *P. minimum*. (n = 5 ± SD).

Sample replicates (n = 5) of each different species were collected in the growth stationary phase and then extracted as described in the experimental section III. 2. 6. Levels of oxylipins, in a weight/biomass basis, differed among the diatom species tested (one way ANOVA,  $F_{3,11} = 7.8$ ,  $p < 0.01$ ). However, this difference was due to the much lower amount of oxylipins produced by *T. rotula* 1 ( $4.2 \pm 2.4 \mu\text{g mg C}^{-1}$ ) compared to *S. marinoi* ( $13.2 \pm 4.3 \mu\text{g mg C}^{-1}$ ) and *S. pseudocostatum* ( $10.0 \pm 2.3 \mu\text{g mg C}^{-1}$ ). On the contrary, PUAs accounted for 39% of the total carbon content in *S. marinoi* ( $8.5 \pm 2.5 \mu\text{g mg C}^{-1}$ ), and 68% of the total carbon content in *T. rotula* 1 ( $9.0 \pm 3.5 \mu\text{g mg C}^{-1}$ ). PUA content in both diatoms was not statistically different from oxylipin content (student's t-test:  $t_4 = 1.64$ ,  $p > 0.05$  for *S. marinoi*, and student's t-test:  $t_8 = 2.1$ ,  $p = 0.07$  for *T. rotula* 1, respectively), though at the edge of  $p$  value for *T. rotula* 1. Cultures of *T. rotula* 2, which have been reported as either able or unable to synthesize PUAs (Pohnert et al., 2002; Wichard et al., 2005b), showed low levels of PUA production ( $1.2 \pm 0.5 \mu\text{g mg C}^{-1}$ ), but much higher levels of oxylipins ( $7.1 \pm 1.6 \mu\text{g mg C}^{-1}$ ) (student's t-test:  $t_4 = 6.2$ ,  $p < 0.01$ ). There was an inverse linear regression between the amount of oxylipins produced by each diatom species, including the negative control (*P. minimum*), and mean hatching success of calanoid *T. stylifera* ( $r^2 = 0.85$ ). On the contrary, there was no relationship between the amount PUAs produced and mean hatching success ( $r^2 = 0.05$ ), as depicted in Figure III.4.

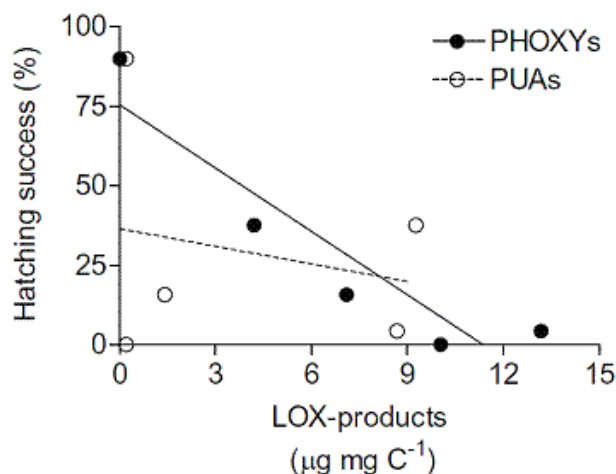


**Figure III.4.** Linear regressions between LOX-products, (phyco-oxylipins, dark circle and black line; PUAs, white circle and dotted line), and mean hatching success in *T. stylifera*.

### III. 3. 4. *Phyco-oxylipin profiling*

Apart from the total amount of PUAs, *T. rotula* 1, *T. rotula* 2 and *S. marinoi* had similar profiles of these compounds. Octatrienal, octadienal and heptadienal were the main compounds found in *S. marinoi* and *T. rotula* 2 by GC-MS profiling, whereas *T. rotula* 1 additionally produced decatrienal. *S. pseudocostatum* showed a high production of oxylipins, in quantities similar to *S. marinoi*, but PUAs were not detected in this species. Constitutive analysis of the PUA mixture in *T. rotula* 1 and *S. marinoi* was consistent with previous results (d'Ippolito et al., 2002a 2002b, 2003, 2004), whereas *T. rotula* 2 was previously characterized by only octadienal and octatrienal according to Wichard and co-workers (2005b).

Unlike the PUAs composition, the oxylipin patterns in the diatom species were significantly different. The oxygenated fatty acid derivatives showed a species-dependent composition suggesting the occurrence of species-specific lipoxygenase oxidation of C<sub>16</sub> and C<sub>20</sub> polyunsaturated fatty acids. Oxylipin profiles in *T. rotula* 1 and *S. marinoi* were identical to those previously described (d'Ippolito et al., 2005; Fontana et al., 2007b). In *S. pseudocostatum*, eicosapentanoate-dependent 15-LOX products, such as 15-oxo-5Z,9E,11E,13E-pentadecatetraenoic acid (285 *m/z* M+Na<sup>+</sup>, 15-oxoacid), 15-hydroxy-eicosa-5Z,8Z,11Z,13E,17Z-pentaenoic acid (355 *m/z* M+Na<sup>+</sup>, 15-HEPE) and 13-hydroxy-14,15-epoxy-eicosa-5Z,8Z,11Z,17Z-tetraenoic acid (371 *m/z* M+Na<sup>+</sup>, 13,14-HEpETE) were predominant (Figure III.5D). In contrast, 9-LOX metabolism of C<sub>16</sub> fatty

acids was central in *T. rotula* 2 with 9-hydroxy-hexadeca-6Z,10E,12Z-trienoic acid (9-HHTrE), 9-hydroxy-hexadeca-6Z,10E,12Z,15-tetraenoic acid (9-HHTE) and their corresponding epoxy alcohols as the major compounds (Figure III.5B). Neither PUAs nor oxylipins were detectable in *P. minimum* (data not shown). For estimation of the deleterious potential of diatom diets, the sum of several oxygenate derivatives was considered responsible for explaining the anti-proliferative effects of these diatoms. Both species of *Chaetoceros* did not produce PUAs, even though cell damage triggered the LOX pathways and the consequent synthesis of species-specific derivatives of EPA. In agreement with Fontana et al. 2007b, LC-MS analysis of methylated extracts of these two species contained several minor components of hydroxy-, hydroperoxy- and epoxyhydroxy- fatty acids (Figure III.5E and III.5F).

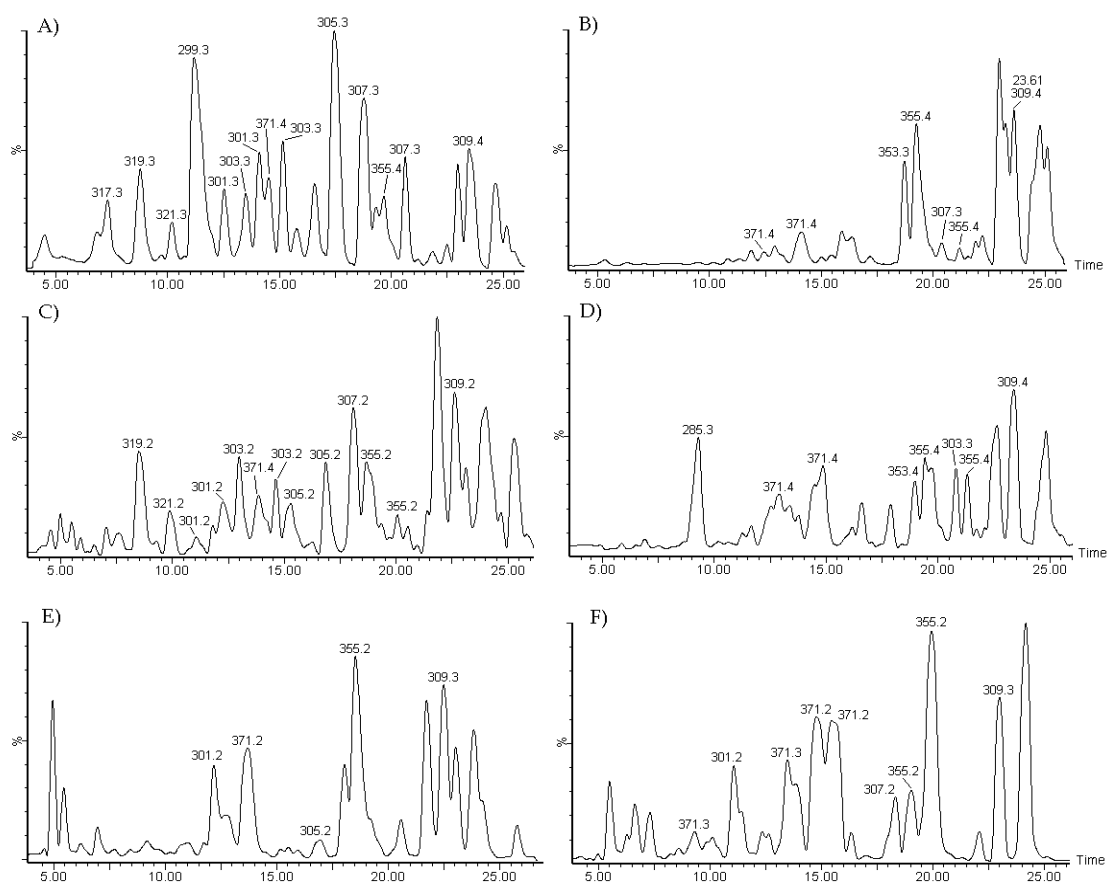


**Figure III.5.** Phyco-oxylipins signatures by LC-MS in *T. rotula* 1 (A), *T. rotula* 2 (B), *S. marinoi* (C), *S. pseudocostatum* (D), *C. affinis* (E) and *C. socialis* (F). Internal standard, 16-hydroxyhexadecanoic acid methyl ester, is shown by the mass peak at  $m/z$  309.

### III. 3. 5. Lipoxygenase activity

A direct measurement of LOX-induced synthesis of fatty acid hydroperoxides (FAHs) in the microalgal lysates was carried out according to the rapid and sensitive spectrophotometric method proposed by Anthon & Barrett (2001), slightly modified, because eicosapentaenoic acids (EPA) was used as the exogenous substrate. Within 5 minutes, cell damage elicited LOX activity and resulted in production of FAHs from undetectable levels to  $11.6 \pm 6.1 \mu\text{M}/\text{mg}$  of protein ( $25.2 \pm 6.1 \text{ ng}$ ) in *C. socialis*,  $15.0 \pm 4.6 \mu\text{M}/\text{mg}$  protein ( $33.5 \pm 9.5 \text{ ng}$ ) in *C. affinis* and  $19.2 \pm 8.6 \mu\text{M}/\text{mg}$  of protein ( $44.5 \pm 18.9 \text{ ng}$ ) in *S. marinoi* (Figure 2b). No LOX activity was observed in *P. minimum*. Figure III.6 shows the levels of LOX products.

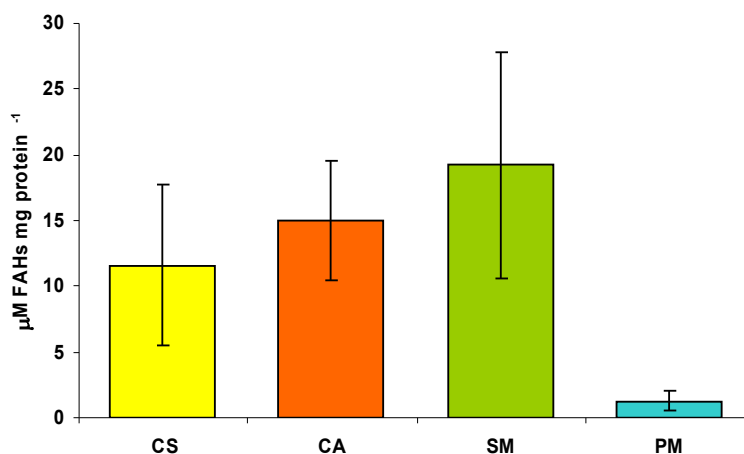
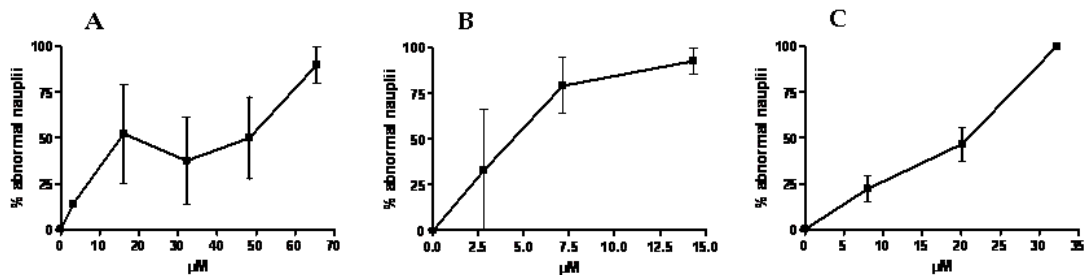


**Figure III.6.** Lipoxygenase activity in diatom cells. The activity is expressed as  $\mu\text{M}$  fatty acid hydroperoxides (FAHs) per mg protein. CS = *C. socialis*, CA = *C. affinis*, SM = *S. marinoi*, PM = *P. minimum*.

### III. 3. 6. Teratogenic and apoptotic activity of diatom products

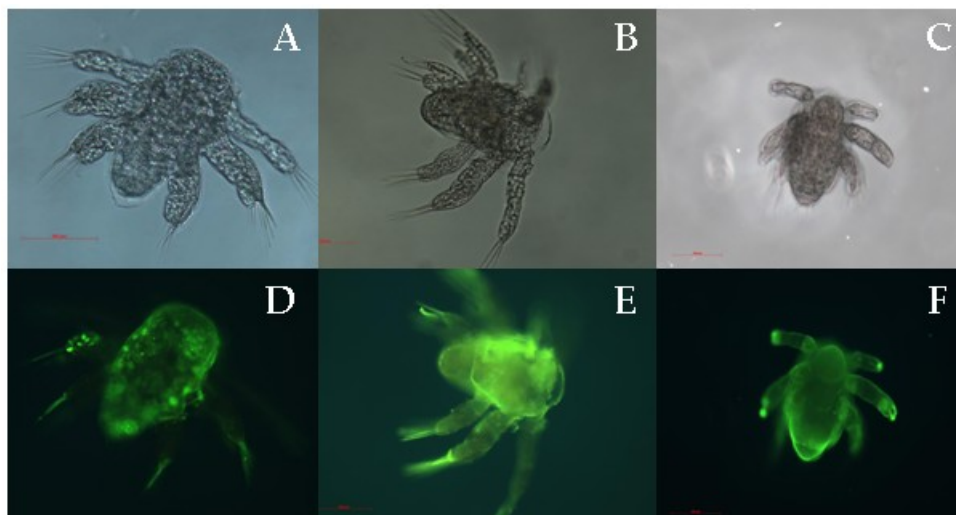
Substrates (EPA) and products of the LOX pathways, such as FAHs, PUAs and other oxylipins, were tested directly on newly spawned eggs of the copepod *C. helgolandicus*. These three classes of molecules reduced drastically egg-hatching success in a dose-dependent manner (Figure III.7). Furthermore, synthetic FAHs induced 100% abnormalities in newborn copepods at concentrations below  $14.5 \mu\text{M}$  (Figure III.7B), whereas the oxylipin fractions isolated from *S. marinoi* gave almost 100% abnormal nauplii only at concentrations higher than  $70 \mu\text{M}$  (Figure III.7A). The teratogenic effect of FAHs was significantly stronger than that induced by the mixture of commercial

aldehydes, for which 100% abnormal nauplii were achieved at concentrations 35  $\mu\text{M}$  (Figure III.7C).



**Figure III.7.** Teratogenic effects induced by LOX products on *C. helgolandicus*. Female copepods were incubated for 24 h with a mixture of FAHs (A), PUA fraction (B) and oxylipin mixture from *S. marinoi* (C).

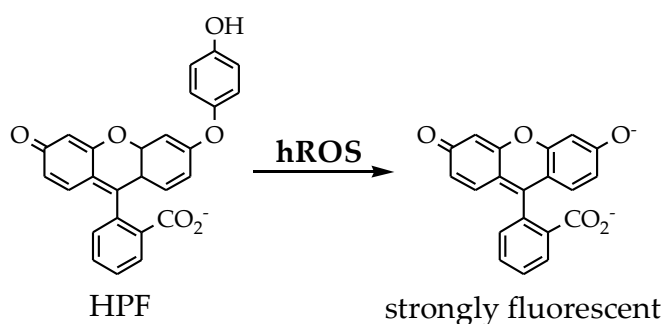
As previously described in feeding studies using toxic diatoms, FAH-induced teratogenesis was associated with evident apoptotic spots in correspondence to the morphological abnormalities (Figure III.8A-F). Incubation of nauplii with FAH fractions induced many apoptotic green areas, which were detected by TUNEL staining as depicted in Figure III.8E. Nauplii, which were generated from copepod females incubated for 24 h with oxylipin fraction, were apparently normal (Figure III.8A), but TUNEL-positive areas indicated possible internal lesions, not visible with conventional light microscopy (Figure III.8D).



**Figure III.8.** Nauplii generated from copepod females incubated for 24 h in 70  $\mu\text{M}$  oxylipins (A-D), 14.5  $\mu\text{M}$  FAHs (B-E) and 35  $\mu\text{M}$  PUA mixture (C-F). Transmitted light images (A-C) show evident malformations only after treatment with FAHs (E), although all LOX derivatives induced distinct apoptotic areas after TUNEL staining (D-F).

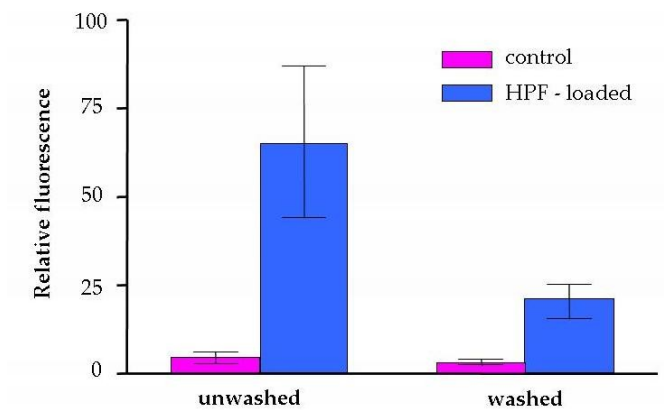
### III. 3. 7. Measurement of highly reactive oxygen species levels

Diatom-dependent toxicity is due to relatively short-lived products of lipid peroxidation. In particular, a specific class of radicals, called highly reactive oxygen species, was spotted for the first time in marine diatoms. The occurrence of radical progression in marine diatoms was detected by the fluorescent dye 2-[6-(4'-hydroxy)-phenoxy-3H-xanthen-3-on-9-yl]-benzoic acid (HPF). This probe is able to undergo oxidation only by highly reactive oxygen species (hROS), such as peroxynitrite (ONOO<sup>-</sup>) and hydroxy radical (<sup>•</sup>OH) (Scheme III.1).



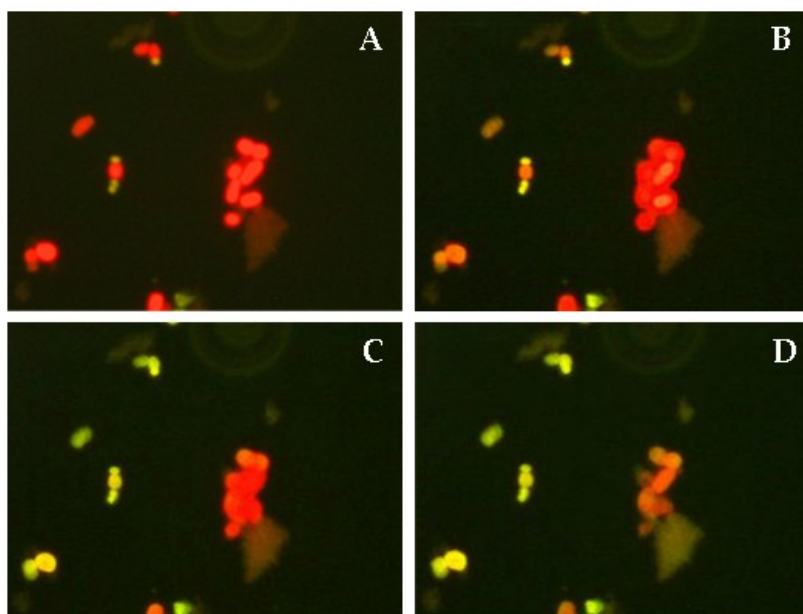
**Scheme III.1.** Fluorescence activation of 2-[6-(4'-hydroxy)-phenoxy-3H-xanthen-3-on-9-yl]benzoic acid (HPF) by hROS.

Figure III.9 summarizes the specific detection of hROS in *S. marinoi* by the membrane-permeable fluorescent dye HPF (Setsukinai et al., 2003). After 30 min incubation with HPF under dark condition, the physiologically undamaged cells were washed in order to remove the exceeding extracellular fluorescence dye. HPF-loaded cells weakly fluoresced if the system was not sonicated prior to illumination (Figure III.9, “washed” sample). In the parallel experiment with dye-loaded cells without removing the extracellular HPF (Figure III.9, “unwashed” sample), the difference between intact and crashed cells was even more evident, because fluorescence emission increased more than 10 times after wounding cells, from  $4.45 \pm 1.6$  ng/cell to  $65.4 \pm 21.4$  ng/cell ( $n = 5$ ).



**Figure III.9.** Levels of oxidizing radicals after dying with the fluorescent HPF, with and without washing out the extra cellular HPF. Pink bar = control cells, blue bars = HPF-loaded cells.

The result was in agreement with clearance of highly oxidizing radicals in the medium where the concentrations of HPF are evidently higher than in the intracellular lumen. Further evidence of hROS synthesis in damaged microalgae was obtained by a time-lapse experiment at the fluorescent microscope (Figure III.10), which revealed a progressive increase in the emission of HPF-loaded diatoms only after detergent-induced cell lysis. Within 20 min SDS rose up the amount of the fluorescent cells corroborating the production of highly reactive radicals under the same conditions that induced synthesis of PUAs and oxylipins.



**Figure III.10.** Fluorescent microscope images of cells after HPF loading and rupture with SDS recorded within 20 min (A: t=0; B: t=2; C: t=5; D: t=20). The red colour is due to chlorophyll of intact cells. Green colour is due to hROS-induced oxidation of HPF.

### III. 4. Discussion

Previous studies (Miralto et al., 1999; Ianora et al., 2004) reported the negative effect of PUAs produced by several species of bloom-forming marine diatom on reproduction and later larval development of dominant zooplankton grazers such as copepods. Unlike other defensive metabolites, PUAs are of low toxicity to adult or mature predators, but depress viability of gametes and offspring. This mechanism of chemical defence is new for the marine environment, where most of the known defence mechanisms are related to feeding deterrence or poisoning (leading in some cases to the death of grazers and predators), but never to reproductive failure.

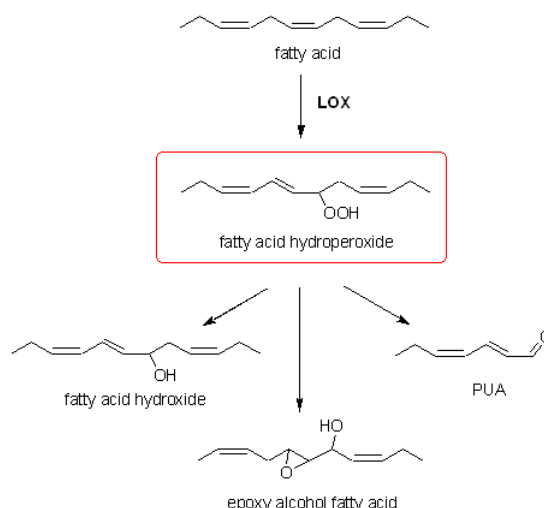
Nevertheless, PUAs production is not ubiquitous amongst diatoms. In a study of 71 strains belonging to 50 species by Wichard and co-workers (2005b) less than half of the diatoms produced PUAs. On the other hand, the chemistry of diatoms is more complex than previously thought, because besides PUAs these microalgae produce a large variety of other oxygenated fatty acid derivatives, generally named phyco-oxylipins, (Fontana et al., 2007a).

Diets on *T. rotula* 1 and *T. rotula* 2 sustained a higher egg production in *T. stylifera* compared to *P. minimum*, *S. marinoi* and *S. pseudocostatum* (Table III.1). High egg production rates with diets of *T. rotula* (Turner et al., 2001; Pohnert et al., 2002; Ceballos & Ianora, 2003) and low fecundity after feeding on *S. marinoi* and *S. pseudocostatum* (Ban et al., 1997; Ceballos & Ianora, 2003) are in agreement with previous results for this copepod species. Hence the results confirmed that the biological effects of the four diatoms have been conserved in respect to species or strains isolated previously. This is not a secondary aspect, since a few independent findings argue for variation of the ecological impact of diatoms as a result of strain differences (Pohnert et al., 2002; Wichard et al., 2005b; Ianora et al., 2006) or in response to physiological conditions of microalgal cells (Ribalet et al., 2007). Egg viability in *T. stylifera* was affected by all diatom species taken into consideration in this study (Table III.2). The diet with *S. marinoi* was already known to produce a strong reduction in copepod egg hatching (Ceballos & Ianora, 2003; Ianora et al., 2004). Feeding *S. pseudocostatum* and *T. rotula* 2 had significantly stronger negative effects on hatching viability than *T. rotula* 1 (Table III.2). Considering that PUAs show the highest levels in *T. rotula* 1 and are absent in *S.*

*pseudocostatum* (Figure III.3), the results of these experiments are a direct demonstration that these molecules *per se* cannot account for the reduced hatching success of copepod eggs, as other authors have recently noted (Wichard et al., 2005b and 2008; Dutz et al., 2008). On the other hand, the negative effect on copepod reproduction induced by diatoms becomes much clearer, when other lipoxygenase products rather than PUA content alone are taken into consideration (Figure III.5). In fact, in the absence of PUAs, the strong activity of *S. pseudocostatum* on copepod egg viability is fully explained by the large quantities of phyco-oxylipins (Figure III.3). Also in the case of the two strains of *T. rotula*, a higher production of phyco-oxylipins may compensate the significantly difference in the PUAs levels and account for the stronger toxicity of *T. rotula* 2. This is corroborated by regression analysis between hatching success and LOX-products that indicated a negative relationship only with phyco-oxylipins, but not with PUAs (Figure III.4).

The results of the second feeding experiment on a selection of non-PUA producing diatoms further demonstrated that these microalgae affect copepod reproduction through mechanisms that were independent of PUA production. In fact, *C. affinis* and *C. socialis*, though incapable of producing PUAs, compromise reproduction of natural grazers by blocking larval development and inducing strong larval malformations (Figure III.2). Oxylipin profiling shows that both diatoms experience strong, wound-induced lipid oxidation leading to LOX synthesis of HEPes (Fontana et al., 2007b).

Although the enzymatic specificity is dependent on the diatom species, all diatoms tested during this study show a comparable metabolism that is responsible for the synthesis of isomeric hydroxy- and epoxy alcohol derivatives as major products (Scheme III.2).



**Scheme III.2.** Biosynthetic sketch for the synthesis of oxylipins in marine diatoms.

In terrestrial plants, different classes of LOX products are crucial defence mediators, serving as signals necessary for gene activation or contributing to pathogen death (Maccarone et al., 2000; Knight et al., 2001; Cacas et al., 2005). In analogy with plant ecology, the results on diatoms suggest that LOX pathways have a key role in the molecular and cellular mechanisms linking oxidation of PUFAs to diatom-induced failure of copepod reproduction. It appears clear that (i) the levels of LOX activity (Figure III.6) correlates with the intensity of the diatom-induced toxicity that increases in the order *C. socialis* < *T. rotula* 1  $\approx$  *T. rotula* 2 < *C. affinis* < *S. pseudocostatum* < *S. marinoi*; (ii) LOX products are absent in non-toxic microalgae, such as *P. minimum* (Figure III.6); (iii) natural and synthetic LOX products other than PUAs show direct effects on copepod eggs, thus reducing hatching success and inducing teratogenesis in newly hatched nauplii (Figure III.7); (iv) in analogy with the effect of diatom diets (Miralto et al., 1999; Ianora et al., 2004; Romano et al., 2003), evident apoptotic progression is demonstrable in nauplii generated from eggs treated with products of LOX pathways, such as FAHs, PUAs and oxylipin mixtures (Figure III.8). In particular, FAHs, the primary product of LOX activity, compromise drastically egg viability and larval development of copepods through a dose-dependent effect that requires concentrations significantly lower than those necessary with the other oxylipins, including PUAs (Figure III.7).

The fact, that different classes of diatom oxylipins display negative maternal effect *in vitro*, implies that the ecological role of LOX activity does not necessarily depend on synthesis of PUAs as hitherto believed. In particular, since diatom cells are rich in PUFAs, the teratogenic and pro-apoptotic activity showed by FAHs on copepod eggs suggests that enzymatic peroxidation may have a primary role in diatom-copepod interactions. The mechanism of action of FAHs is not clear, but a current hypothesis suggests that the involvement of these unstable lipids is more likely due to propagation of radical reactions, rather than acting as exogenous signalling compounds. In plant ecology, a complex mixture of oxylipins and transient species, such as FAHs and ROS, can provide an highly oxidative status. FAHs are members of the ROS family and their accumulation has been reported in the early stages of some oxidative stress-induced processes in mammalian and plant systems (Tang et al., 2002; van Breusegem & Dat, 2006). Moreover, several studies have pointed out that enzymatic or autoxidative production of the reactive oxygen species are well-known mediator of a variety of distinct cellular responses. Recently, ROS synthesis has also been documented in marine diatoms in response to osmotic and chemical stimuli (Rijstenbil 2002, 2003 and 2005; Vardi et al., 2006; Wolfe-Simon et al., 2006). In the final experimental part of this chapter, the occurrence of radical progression in marine diatoms was tested by the fluorescent dye HPF (Scheme III.1). The choice of this probe was driven by the aim to detect highly reactive oxygen species (hROS), such as peroxynitrite (ONOO<sup>•</sup>) and hydroxy radical (•OH), that like FAHs are known to participate in various biological processes, including apoptosis and DNA damage (Wiseman & Halliwell, 1996; Ren et al., 2001). Fluorescence detection and time-lapse experiments revealed that diatom cells suffer massive hROS burst concurrent with lipid peroxidation (Figure III.9 and III.10). In particular, it is reasonable to suggest that the oxidative burst follows the activation of the LOX pathways, since the stereochemical purity of diatom FAHs and HEPes excludes the possibility that lipid peroxidation can be initially due to free radical mechanisms. Because HPF is able to penetrate into cell cytoplasm, the absence of fluorescence in intact diatoms proves activation of the process exclusively after the loss of cellular integrity, in agreement with the mode of action proposed by Pohnert for PUAs (2000). These results, taken

together, demonstrate that LOX activation in marine diatoms triggers a multi-phase mechanism responsible for the synthesis of at least two classes of pro-apoptotic and teratogenic products, FAHs and hROS, which can mimic the toxic effects of the microalgae on grazer copepods. It follows that during diatom blooms, both FAHs and hROS might have a direct effect on zooplankton populations by inducing physiological damage that apparently does not affect the parental genotype, but leads to trans-generational instability in young nauplii even in the absence of PUAs.

## Chapter IV

### Oxylipin production in the pennate diatom *Pseudo-nitzschia*

#### *delicatissima*

##### IV. 1. Introduction

Pennate planktonic diatoms of the genus *Pseudo-nitzschia* are common constituents of coastal and oceanic phytoplankton blooms (Hasle, 2002). Scientific interest in these diatoms has increased since 1985, when *Pseudo-nitzschia multiseriata* (= *Nitzschia pungens* f. *multiseriata*) caused an Amnesic Shellfish Poisoning (ASP) event (Bates et al., 1989). This species produces domoic acid, a neurotoxin which accumulates in filter feeders and, when passed to humans, may cause serious neurological disorders (Todd, 1993; Hampson & Manolo, 1998). Several other diatom species of its genus are notorious for the production of domoic acid and therefore are potential sources of ASP (Rhodes et al., 1996; Bates et al., 1998). In almost all species both toxic and non-toxic clones are present within the same morphospecies and domoic acid production varies quantitatively across conspecific clones which were maintained under the same culture conditions (Bates et al., 1998). Increased awareness of problems related to the presence of potentially toxic *Pseudo-nitzschia* species prompted several monitoring programmes, which, however, are hampered by the difficult identification of these species by light microscopy. A considerable level of genetic diversity has been recently detected amongst *P. delicatissima*-like isolates and distinct cryptic species have been described within what has been identified as *P. delicatissima*-complex (Lundholm et al., 2006; Amato et al., 2007). Furthermore, *Pseudo-nitzschia delicatissima* has been also reported as one of the diatom species capable of considerably impairing fecundity of zooplankton grazers as a result of the production of the polyunsaturated aldehydes (PUAs) (Miralto et al., 1999). The synthesis of these compounds in the centric diatom *Thalassiosira rotula* starts from lipoxygenase oxidation of EPA (d'Ippolito et al., 2005), but Barofsky & Pohnert (2007) recently suggested that the biosynthetic pathway differs from the one reported from higher plants and mammals. They proposed an unusual heterolytic

mechanism involving a lyase/lipoxygenase enzyme pair or a multifunctional lipoxygenase able to carry out both hydroperoxidation and cleavage of the resulting hydroperoxide.

In this chapter, the study of oxylipin metabolism in *Pseudo-nitzschia delicatissima* was undertaken along the growth curve of the diatom by oxylipin profiling and the analysis of lipoxygenase activity in order to provide clues about the role of oxylipins as chemo-physiological signals in diatom blooms.

## **IV. 2. Materials and Methods**

### *IV. 2. 1. Microalgal culturing*

Monoclonal cultures of *P. delicatissima* (Strain SZN B321 as AL-24 *sensu stricto* Amato et al. 2007, GenBank Accession no. DQ813830ITS) were isolated from the Gulf of Naples (Italy) during the winter 2004 by the Ecology and Evolution of Plankton Department of the Stazione Zoologica Anton Dohrn (Naples, Italy).

10 L jars filled with 0.22 µm filtered and sterile oligotrophic seawater enriched with F/2 medium (Guillard, 1983) were inoculated with an initial cell concentration of about 300-500 cells ml<sup>-1</sup>. Cultures were gently mixed by bubbling with sterile ambient air and grown at 20° C under 12h:12h light:dark cycle (100 µmol photons m<sup>2</sup> s<sup>-1</sup>). Every day, cell concentration was estimated by collecting a 2 ml subsample that was fixed with lugol solution for direct count of the cell number using a 1 ml Sedgwich-Rafter counting chamber and a Zeiss Axiophot microscope at a magnification of 100x. Cell cultures were grown in replicate (n ≥ 3). To obtain a sufficient amount of cell pellets for each phase along the growth curve, more replicates of *P. delicatissima* (strain SZN B321) were grown at the same time under identical conditions. The samples were collected from five points along the growth curve: (I) early exponential growth phase (day 3 after the inoculum); (II) mid exponential growth phase (from day 4 to 5); (III) late exponential growth phase (day 6); (IV) stationary phase (day 7 and 8); (V) declining phase, from day 9 onwards. Volumes ranging from 2 to 10 litres were harvested and concentrated by centrifugation at 1200 g for 10 min at 5° C. The cell pellets were collected in 50 ml Falcon tubes, immediately frozen in liquid nitrogen and kept at -80° C until use.

#### IV. 2. 2. *Extraction of lipoxygenase products*

The pellets were suspended in 50 mM phosphate buffer pH 6.5 (1 ml/g cell pellet) and sonicated for 1 min; after 30 min at room temperature, the homogenates were extracted as described in the experimental section § II. 2. 5. The crude extracts were divided and one part was submitted to PUAs analysis by GC-MS in agreement with d'Ippolito et al. (2002b). The remaining extracts were methylated with ethereal diazomethane in diethyl ether (0.4 ml 10 mg extract) for 1 h at room temperature. Methylated extracts were fractionated on RP-HPLC (Phenomenex, C-18 Kromasil 4.6 × 250 mm, 100 Å) using UV detection at 210 nm and the gradient solvent system reported in the Table IV.1.

**Table IV.1.** Gradient solvent system employed for RP-HPLC. Flow rate 1 ml/min.

<i>Time</i> ( <i>min</i> )	<i>Methanol</i> (%)	<i>Water</i> (%)
0	70	30
15	80	20
65	80	20
66	0	100
80	0	100

The purified fractions of 15S-hydroxy-eicosa-5Z,8Z,11Z,13E,17Z-pentaenoic acid (15S-HEPE), 13-hydroxy-14,15-epoxy-eicosa-5Z,8Z,11Z,17Z-tetraenoic acid (13,14-HEpETE) and 15-oxo-5Z,9E,11E,13E-pentadecatetraenoic acid (15-oxoacid) were then analysed by NMR. The 15S-hydroperoxy-eicosa-5Z,8Z,11Z,13E,17Z-pentaenoic acid (15S-HpEPE) was purified on an SP-HPLC column (Phenomenex, Si-5 Kromasil, 4.6 × 250 mm) by isocratic elution with *n*-hexane/Et<sub>2</sub>O 85:15 (flow rate 1 ml/min, UV detection at 236 nm).

#### IV. 2. 3. *Lipoxygenase assays*

Lipoxygenase activity along the growth curve was detected by monitoring the level of phyco-oxylipin methyl esters on reverse phase LC-MS/MS (Göbel et al., 2002; Montillet et al., 2004). Briefly, sample replicates collected along the growth curve ( $n \geq 3$ ) were extracted as described above and analyzed on a Q-ToF-*micro* mass spectrometer equipped with an ESI positive source and coupled with a HPLC system as reported in

the experimental section § II. 2. 6. Quantification of these metabolites was carried out by addition of 16-hydroxyhexadecanoic acid (30 µg/g of pellet) as internal standard. The average and standard deviation of the measurements ( $n \geq 3$ ) was calculated by Waters QUANLINK software according to the manufacturer's instructions.

Alternatively, diatom 15-LOX activity was assessed by measuring oxygen consumption according to Axelrod and co-workers (Axelrod et al., 1981). Briefly, oxygen consumption was measured with a Gilson model 5/6 oxygraph (Gilson Medical Electronics, Middleton, WI, USA) equipped with a Clark electrode (Yellow Spring) in a thermostated vessel at 22° C. Crude diatom lysates were added to 200 mM sodium borate buffer (pH 8.15) in a final volume of 1.9 ml. Oxygen uptake was initiated by the addition of 0.8 mM EPA prepared according to Anthon & Barrett (2001).

Protein content was determined with the method of Lowry (DC protein assay, Bio-Rad Laboratories) according to the manufacturer's instruction.

### **IV. 3. Results**

#### *IV. 3. 1. Phyco-oxylipin signature of *Pseudo-nitzschia delicatissima**

Unlike previously reported by Miralto and co-workers (1999), GC-MS analysis of *P. delicatissima* (B321) extracts, which were harvested in the stationary growth phase, revealed the total absence of polyunsaturated aldehydes (PUAs). After methylation with ethereal diazomethane, LC-MS analyses showed three major compounds corresponding to 15S-hydroxy-eicosa-5Z,8Z,11Z,13E,17Z-pentaenoic acid (15S-HEPE;  $R_t=19.64$  min), 13-hydroxy-14,15-epoxy-eicosa-5Z,8Z,11Z,17Z-tetraenoic acid (13,14-HEpETE;  $R_t=14.76$  min) and 15-oxo-5Z,9E,11E,13E-pentadecatetraenoic acid (15-oxoacid;  $R_t=9.54$  min) (Figure IV.1).

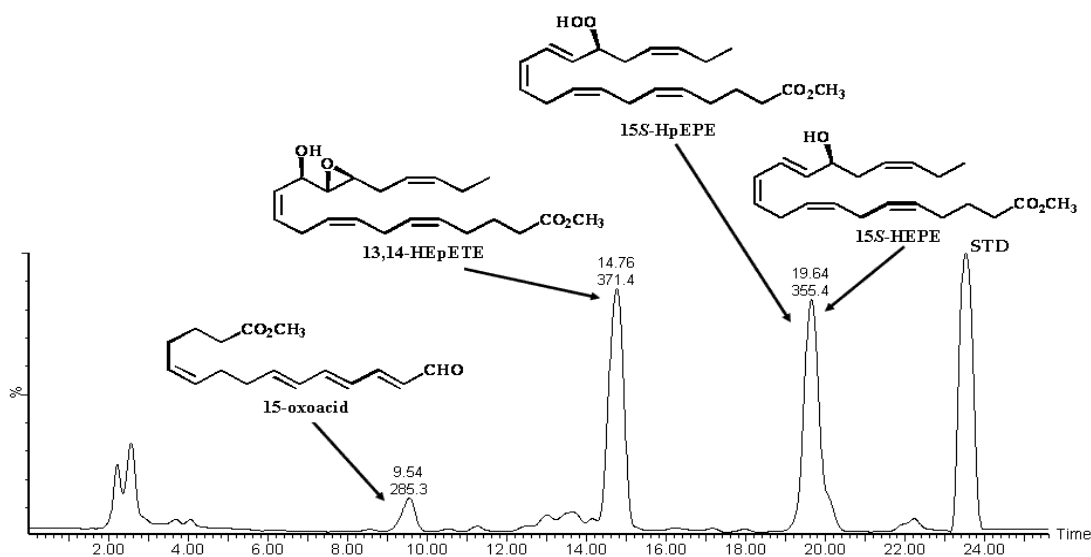


**Figure IV.1.** Reverse phase LC-MS profile of the *P. delicatissima* (B321) extract. Numbers above peaks indicate the molecular ion ( $M+Na^+$ ) as determined by ESI<sup>+</sup> ionization and retention time.

The *trans*-configuration of the 14,15 epoxide ring of 13,14-HEpETE was assigned on the basis of the coupling constant of 1.9 Hz between the oxirane protons H14 and H15 (NMR spectra are reported in the Appendix see Figure A.11). The NMR data ( $J_{13,14} = 5.1$ ; reported in the literature  $J_{threo} = 5.2$  and  $J_{erythro} = 3.4$ ) of this compound were similar to those for *threo*-13*S*-hydroxy-14*S*,15*S*-*trans*-epoxy-eicosa-5*Z*,8*Z*,11*Z*-trienoic acid derived from *in vitro* transformation of 15*S*-hydroperoxy-eicosa-5*Z*,8*Z*,11*Z*,13*E*-tetraenoic acid (15-HpETE) catalysed by cytochrome P450 (Chang et al., 1996). This supported the origin of the epoxy alcohol from the conversion of 15*S*-hydroperoxy-eicosa-5*Z*,8*Z*,11*Z*,13*E*,17*Z*-pentaenoic acid (15S-HpEPE) in agreement with the proposed enzymatic mechanism (Chang et al., 1996; Reynaud et al., 1999; Cristea & Oliw, 2006). This last compound co-eluted with 15S-HEPE on a reverse-phase column and showed a molecular ion at  $m/z$  371 ( $M+Na^+$ ) with a major fragment ion at  $m/z$  355 for the loss of oxygen as already reported in the chapter II of this thesis (see Figure II.2A). Despite the inherent instability of this product, a sufficient amount for NMR analysis was also purified on SP-HPLC. The <sup>1</sup>H-NMR spectrum of the purified compound was almost identical to that of 15-HEPE except for the chemical shift from 4.06 to 4.42 ppm (H15) of the hydroxymethine proton (Figure IV.2).

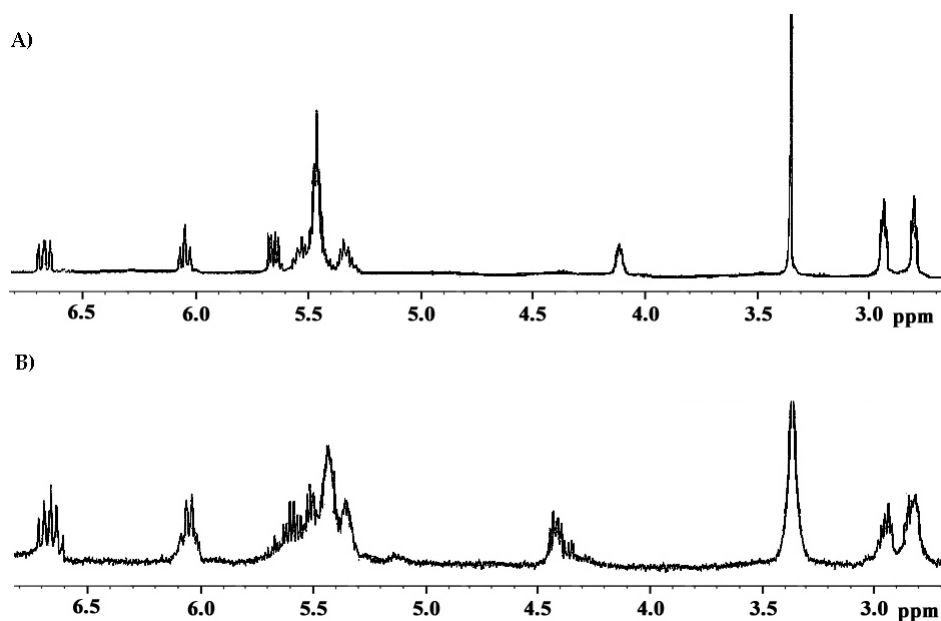


**Figure IV.2.** Downfield regions of  $^1\text{H-NMR}$  of (A) 15S-hydroxy-eicosa-5Z,8Z,11Z,13E,17Z-pentaenoic acid (15S-HEPE) and (B) 15S-hydroperoxy-eicosa-5Z,8Z,11Z,13E,17Z-pentaenoic acid (15S-HpEPE).

The presence of the hydroperoxy group at C15 was unambiguously determined by two dimensional NMR experiments that showed correlations of the proton H15 with two spin systems formed by the diene fragment from C14 to C11 and by the terminal pentenyl residue C16-C20 (data not shown).

The minor peak ( $R_t=9.54$  min) in the HPLC trace of *P. delicatissima* yielded a third stable compound characterized by ESI<sup>+</sup> MS pseudomolecular ion at  $m/z$  285.3 ( $\text{C}_{16}\text{H}_{22}\text{O}_3+\text{Na}^+$ ). Correlations observed in the COSY and TOCSY NMR spectra of this product indicated a triene spin system conjugated with a terminal aldehyde function ( $\delta$  9.41), which accounted for the strong UV maximum at 322 nm exhibited by this compound (UV spectra as depicted in the chapter II at Figure II.3). The remaining NMR signals contained an isolated double bond and four down-shifted methylenes in agreement with the structure of 15-oxo-5Z,9E,11E,13E-pentadecatetraenoic acid (15-oxoacid) methyl ester (NMR spectra is reported in the Appendix see Figure A.12). The all *trans* stereochemistry of the conjugated double bonds was inferred on the basis of the coupling constants that were all above 11 Hz.

#### IV. 3. 2. *Lipoxygenase products along the growth curve*

Figure IV.3 depicts the intergraded growth curve of *P. delicatissima* (B321) under the experimental conditions as reported above. The curve was characterized by an exponential growth phase lasting 6 days, followed by a short stationary phase (up to day 8 from the inoculum) and a declining phase from day 9 onwards. Only cells which showed an apparently undamaged cytoplasm and thus considered as alive were enumerated. Starting from day 8, increasingly high numbers of empty cells were present in the cultures, and this caused a very rapid collapse of the culture.

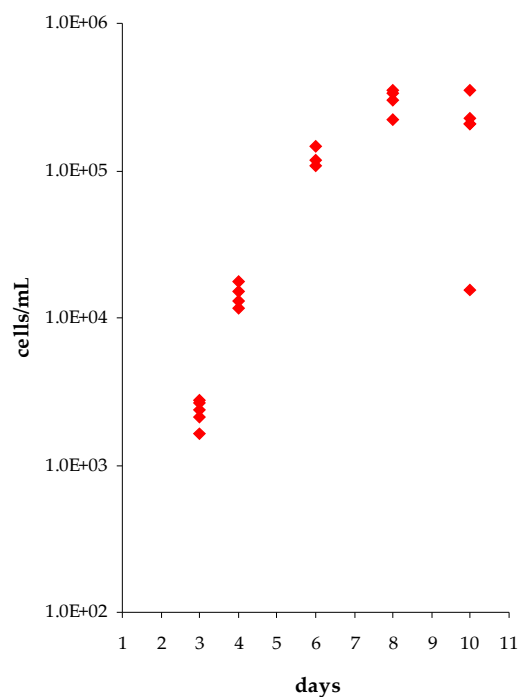


**Figure IV.3.** *Pseudo-nitzschia delicatissima* growth cycle. The diatom cells were collected in five distinct phases: early exponential (day 3 from the inoculum); mid-exponential (from day 4 to 5); late exponential (day 6); stationary (day 7 and 8); and declining (from day 9 onwards). Growth conditions are given in materials and methods section.

Free fatty acids, including EPA and polyunsaturated C<sub>16</sub> compounds were always present along the growth curve (data not shown) and their concentrations, as well as the cellular protein content, did not show significant variation during the time course experiment. Their amounts were largely predominant in respect to the levels of LOX products (data not shown).

*P. delicatissima* is a pennate diatom which possesses 15-LOX activity, as already reported for centric diatoms such as *Skeletonema costatum* and *Skeletonema pseudocostatum*, see section § III. 3. 4. of chapter III (Fontana et al., 2007b).

Measurements of 15-LOX activity along the growth curve were detectable by both oxylipin production (Figure IV.4A) and O<sub>2</sub> consumption in presence of exogenous EPA (Figure IV.4B). Nevertheless, the qualitative and quantitative composition of the oxylipin mixture produced by *P. delicatissima* was different in the diverse growth phases. The overall concentration of these metabolites ranged between  $3.6 \pm 1.3$  SD and  $8.6 \pm 1.2$  SD  $\mu\text{g mg}^{-1}$  of protein during the exponential growth, rising to  $22.9 \pm 1.3$   $\mu\text{g mg}^{-1}$  of protein in the stationary phase (Figure IV.4A).

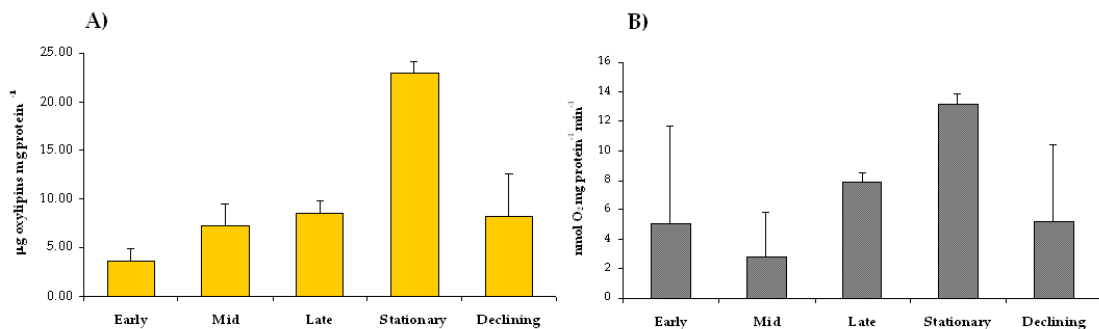


**Figure IV.4.** Time-course of phyco-oxylipin synthesis by 15S-lipoxygenase of *P. delicatissima*. (A) LC-MS quantification of LOX products in presence of 16-hydroxyhexadecanoic acid as internal standard and (B) oxygen consumption of cell lysates in presence of 0.8 mM exogenous EPA.

15S-HEPE and 13,14-HEpETE were always visible in LC-MS profiles and their concentrations progressively increased and reached their maximum in the stationary phase (Figure IV.5). The significant upsurge of oxylipins in the stationary phase was matched by the synthesis of 15-oxoacid ( $4.2 \pm 1.1$   $\mu\text{g mg}^{-1}$  protein), which was undetectable in other growth phases (Figure IV.5D), including the declining part.

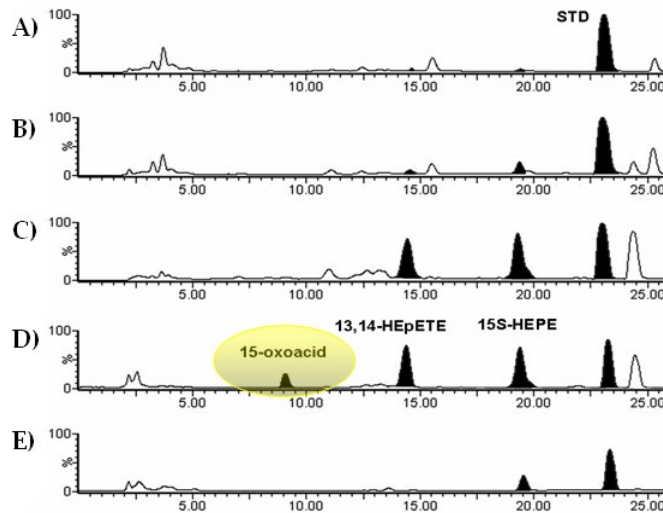


**Figure IV.5.** Oxylipin signature (total ion current profiles) along the growth curve of *Pseudonitzschia delicatissima*. (A) Early exponential phase, (B) mid-exponential phase, (C) late exponential phase, (D) stationary phase and (E) declining phase. Standard (STD): 16-hydroxyhexadecanoic acid.

Similar progress of the oxylipin levels was also observable in the stationary phase when metabolite concentration was expressed as cellular content (see Figure IV.6). The only differences between oxylipin concentration expressed on a cellular basis ( $0.47 \pm 0.3$  pg cell<sup>-1</sup>) or on the basis of protein content ( $8.2 \pm 4.4$   $\mu\text{g mg}^{-1}$  protein) was observed during the declining phase, when a drastic reduction of cell numbers was triggered by cell lysis. This discrepancy is easy to explain. The loss of cellular integrity did not stop the synthesis of oxylipins, which can continue for several minutes in marine water (Pohnert, 2000; Fontana et al., 2007a), thus leading to overestimates of oxylipin content per cell in the senescent phase.

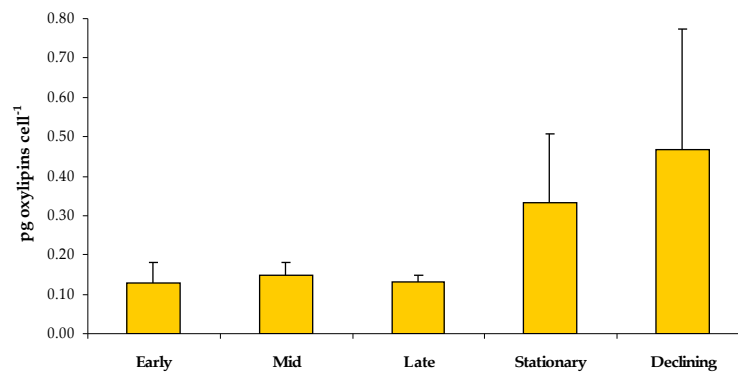


**Figure IV.6.** Time-course of phyco-oxylipin synthesis by 15S-lipoxygenase of *P. delicatissima*. LC-MS quantification of LOX products expressed as pg oxylipins cell<sup>-1</sup>.

#### IV. 4. Discussion

The presence and function of an eicosapentanoate-dependent 15(*S*)-lipoxygenase activity in the pennate marine diatom *P. delicatissima* is peculiar if one considers that only a few diatoms have hitherto been checked for oxylipins and, except for a few products in plants and algae (Bernart et al., 1993; Rorrer et al., 1997; Gerard et al., 2004), there are relatively few examples of oxylipins in non-mammalian systems that appear to arise from a 15-LOX. 15*S*-HpEPE, which was synthesized independently of the substrate availability (as verified by fatty acid analysis), was channelled downstream into three distinct pathways for oxylipin biosynthesis. Putative reductase and epoxy alcohol synthase were committed to the formation of 15*S*-HEPE and 13,14-HEpETE, whereas a hydroperoxide lyase (HPL) activity is responsible for the synthesis of 15-oxoacid only during the very short stationary phase that characterized the growth curve of *P. delicatissima*. As suggested by the absence of detectable volatile aldehydes in extracts of the diatom, synthesis of 15-oxoacid could not be related to the mechanism established for plant CYP74 HPLs, which would generate downstream aldehydic products (Hughes et al., 2008; Lee et al., 2008; Wasternack & Feussner, 2008). 15-oxoacid is a novel oxylipin and its formation is not explained by any known lyase process, even if the cleavage of the fatty acid hydroperoxide may follow mechanisms similar to those evoked for the release of  $\omega$ -oxoacids and unsaturated hydrocarbon derivatives in other diatoms and algae (Wendel & Jüttner, 1996; Hombeck & Boland, 1998; Hombeck et al., 1999; Pohnert & Boland, 2002; Wichard & Pohnert, 2006; Barofsky & Pohnert, 2007). The progression of oxylipin production in *P. delicatissima* along the growth follows two different physiological patterns. Production of 15*S*-HEPE and 13,14-HEpETE is linearly dependent on cell density, steadily increasing with the expansion of the diatom culture. Conversely, production of 15-oxoacid is constrained within the time-window of the stationary phase and, apparently, does not reflect a generic reaction to cell distress or death, since the compound is not produced during the declining phase when the fraction of suffering or dying cells is higher. Identification of the factors that elicit the synthesis of 15-oxoacid will require further studies, but it seems reasonable to assume that activation of the process may occur in response to a hitherto unknown physiological or environmental stimulus. Notably, production of

secondary metabolites in response to chemo-physical stressors, such as light or nutrient limitation, has been documented in a number of toxic microalgae, including a few species of the genus *Pseudo-nitzschia* (Cembella & John, 2006). Recently, it has been shown that production of LOX metabolites, such as PUAs in the diatom *S. marinoi*, increases during the stationary phase or by depletion of phosphorus and silica (Ribalet et al., 2007). Also activation of a stress-surveillance system in response to LOX-derived infochemicals has been reported for the diatom *Phaeodactylum tricornutum* (Vardi et al., 2006). In the oceans, persistence and success of diatom blooms are affected and controlled by a range of biotic and abiotic factors (Falkowski et al., 1998). The collapse of *P. delicatissima* cultures, accompanied by cell lysis and biomass degradation, occurred within a few days and reflected the abrupt termination recorded for some phytoplankton blooms (Berman-Frank et al., 2004; Bidle & Falkowski, 2004). It is tempting to suggest that population density-dependent synthesis of LOX products may control phase transition along the growth curve of *P. delicatissima*. In bacteria, autoinductive molecules produced in a cell density-dependent fashion are termed quorum sensing. In unicellular eukaryotes, diverse, small signalling molecules have also been shown to be critical for many processes during cellular differentiation and growth. Oxylipins have never been established as quorum sensing effectors (Tsitsigiannis & Keller, 2007; Noverr et al., 2008), although recently it has been reported that deletion of the LOX gene *AFlox* greatly diminished density-dependent morphological shifts in the fungus *Aspergillus flavus* (Brown et al., 2008). Furthermore, because oxylipins have a recognized role as chemical signals, these compounds although not having a direct responsibility as auto-inducers may still contribute to the modulation of cellular metabolism of diatoms as physiological mediators. The growth phase-induced synthesis of oxylipins, akin to the quorum-sensing in bacteria and fungi, may therefore monitor environmental conditions and regulate diverse cellular behaviours, including the synchronization of bloom demise.

## Chapter V

# Characterization of phyco-oxylipins as chemical markers for cryptic diatoms

### V. 1. Introduction

Diatoms are an ubiquitous class of unicellular microalgae, which play a crucial role in the biogeochemical cycling of minerals (e.g. silica) and the global carbon fixation (Smetacek, 1999). Biodiversity estimates for diatoms are based mainly on morphological features. Each diatom cell is surrounded by a rigid cell wall, called the frustule, which consists of two halves of amorphous polymerized silica resembling a box with an overlapping lid. The inner frustule is known as the hypotheca and the outer one is denoted the epitheca. In addition to the main valves (hypo- and epi-), the two thecae are held in place by a series of ring-like silica structures, the girdle bands (Figure V.1).

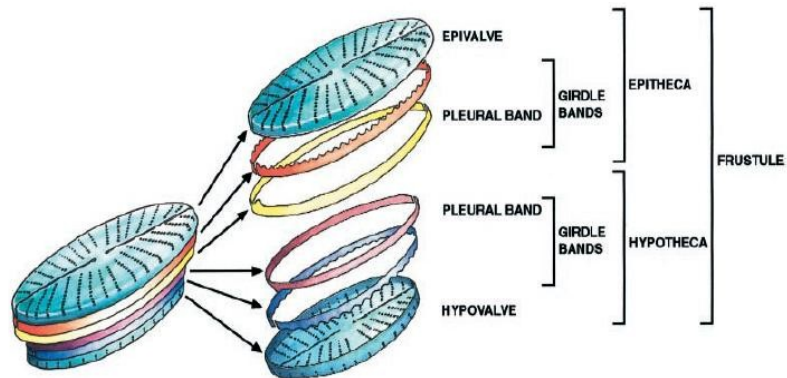


**Figure V.1.** Schematic overview of the siliceous components of diatom cell walls. Drawing by Ian Nettleton (Zurzolo & Bowler, 2001).

Taxonomically, diatoms are traditionally divided into two major groups depending on the symmetry of their frustules. Centric diatoms are radially symmetrical, whereas pennate diatoms are elongated and bilaterally symmetrical. By light microscopy only a few characters for species classification can be identified. Observation of the frustule in

electron microscopy allows further analysis of ultrastructural ornamentations, such as raphe, fibulae, striae and poroids can be seen, which are necessary for a detailed examination and an accurate species identification. Molecular studies have proven to be a powerful support to the morphological classification in diatoms for the revelation of the phylogenetic relationships at all taxonomic levels. Recent investigations highlighted the presence of an unsuspected level of cryptic or pseudo-cryptic diversity among different diatoms displaying that genetically distinct groups might exist within a single morpho-species (Behnke et al., 2004; Beszteri et al., 2005; Kooistra et al., 2008). What was considered to be a single species, based on cell morphology as observed in light microscopy, proved to consist of genetically distinct units (clades) differing only in minor morphological features. Importantly in view of the biological species concept, which defines species as reproductively isolated units, the reproductive isolation was proved in some cases (Amato et al., 2007; Vanormelingen et al., 2008). They can thus be defined as cryptic species.

In the case of the genus *Pseudo-nitzschia*, needle-chain pennate diatoms, several species appear to be highly similar under light microscopy. The needle-shaped cells form stepped chains by cells holding on to one another at their apices. Subtle morphological differences in cell shape and size as well as in the overlapping patterns of cell apices in the chain represent the only characters for identifying the different *Pseudo-nitzschia* species by light microscopy (Hasle & Syvertsen, 1997). Recent studies by Lundholm and co-workers (2003 and 2006) investigated *Pseudo-nitzschia delicatissima*-like and *Pseudo-nitzschia pseudodelicatissima*-like morphotypes using molecular genetic methods and electron microscopy. The results showed the heterogeneous composition of this species complex leading to the revision of the existing species and the description of new species based on sequence data and subtle ultrastructural differences. Amato et al. (2007) carried out mating experiments with multiple strains belonging to different genotypes and demonstrated that they were reproductively isolated entities, e.g. different biological species.

Pennate marine diatoms possess lipoxygenase pathways leading to oxygenate fatty acid derivatives (phyco-oxylipins). In the centric diatoms *Choetoceros* and *Thalassiosira* these pathways have shown a surprisingly high species-specificity which might serve as chemical markers for the characterization of cryptic species (d'Ippolito et al., 2005; Fontana et al., 2007b). In order to evaluate if a comparable level of diversity and specificity exists also in pennate diatoms, the patterns of phyco-oxylipins were assessed in five species of the genus *Pseudo-nitzschia*. Liquid chromatography coupled with photodiode array detection and mass spectrometry (LC-DAD-MS) in agreement with the method developed for oxylipins determination (see chapter II) was used to investigate phyco-oxylipin profiles. The strains of the five species have been obtained from the Stazione Zoologica Anton Dohrn (Naples, Italy) and consisted of multiple sympatric strains of the three *P. delicatissima*-like species complex (see Amato et al., 2007), *P. pseudodelicatissima* and *P. multistriata* isolated from the Gulf of Naples (Italy). At the Ecology and Evolution of Plankton Department of the Stazione Zoologica Anton Dohrn (Naples, Italy) a morphological and molecular investigation of these *Pseudo-nitzschia* morpho-species was carried out on the same strains and highlighted that the species are indeed split into distinct genotypes, distinguishable only by faint ultrastructural ornamentations in their frustule visible under the electron microscope (Amato et al., 2007). Members of biologically distinct clade were therefore chosen for phyco-oxylipin profiling in this part of the PhD thesis to allow a direct comparison and assess the value of phyco-oxylipins as chemical marker molecules.

## **V. 2. Materials and Methods**

### *V. 2. 1. Microalgal isolation and culturing*

Monoclonal cultures of five different *Pseudo-nitzschia* species were collected at the Long Term Ecological Research station MareChiara in the Gulf of Naples (Italy). Diatom cells were isolated by micro-pipettes from net samples and transferred singly to 24-well culture plates with sterile filtered seawater amended with F/2 nutrients (Guillard, 1983). F/2 culture medium was prepared with oligotrophic natural seawater at a salinity of 36 psu. The plates were maintained at a temperature of 20° C and a 14:10h light:dark cycle with a photon flux of 100  $\mu\text{mol photons m}^{-2} \text{ s}^{-1}$ . After 1-2 weeks the

established cultures were transferred in 2 L Erlenmeyer flasks filled with 1 L F/2 medium (Guillard, 1983) and were grown under the same conditions as described above. Every day, cell concentration was enumerated as described in the experimental section § IV. 2. 1. of chapter IV. Each species was cultured in replicate ( $n \geq 3$ ) and each replicate was considered a different strain for the chemical analysis. A subsample of 10 ml was collected from the culture in the exponential growth phase and used for the molecular analysis of the LSU (large ribosomal subunit) and ITS (internal transcribed spacer) rDNA. Cells were harvested at the stationary growth phase by centrifugation at 1200 g for 10 min at 5° C. Cell pellets were collected in 50 ml Falcon tubes and immediately frozen in liquid nitrogen and kept at -80° C until chemical analysis. 26 diatom strains belonging to the five different *Pseudo-nitzschia* species are reported below (see Table V.1).

#### V. 2. 2. *Molecular analysis*

DNA analysis were performed at the Ecology and Evolution of Plankton Department of the Stazione Zoologica Anton Dohrn (Naples, Italy). Briefly, genomic DNA was extracted following Kooistra et al. (2003) and then amplified by polymerase chain reaction (PCR) using the primers D1R and D3Ca (Lenaers et al., 1989; Scholin et al., 1994) for the hypervariable domains D1 and D3 of LSU rDNA and the universal primers ITS1 and ITS4 (White et al., 1990) for the ITS rDNA regions. Sequencing protocol of ribosomal (ITS2) and *rbcL* fragments was reported by Amato et al. (2007).

#### V. 2. 3. *Chemical analysis*

Cell pellets of the 26 diatom strains (see Table V.1) were dissolved in distilled water (1 ml/g of wet pellet) and sonicated for 1 min at 4° C prior to extraction with methanol (equal volume with water). The internal standard, 16-hydroxyhexadecanoic acid (15 µg/g of pellet) was added before the extraction and the resulting suspension was centrifuged at 2000 g for 5 min at 5° C. The organic extracts were dried under reduced pressure with a rotary evaporator (Buchi, Rotavapor R-200) and then methylated with ethereal diazomethane in diethyl ether (0.4 ml per 10 mg extract) for 1 h at room temperature. After removing the organic solvent under N<sub>2</sub>, the raw extract was used

for analysis of non-volatile oxylipins by LC-DAD-MS/MS as previously described in the experimental sections § II. 2. 6 and II. 2. 7 of chapter II.

**Table V.1.** List of strains used for the chemical analysis; strain code, LSU GenBank accession numbers, date of isolation and cell concentration (cells ml<sup>-1</sup>) at the stationary phase are reported.

Strain Code	GenBank Accession no.	Isolation Date	Cell Concentration (cells ml <sup>-1</sup> )
<i>P. delicatissima</i> clade 1 <i>sensu</i> Amato et al. (2007) (del1)			
Deli3 (=B284)	As AL-24 DQ813811	January 2007	312.400
AY-7 (=B286)	As AL-24	March 2007	324.800
AY-7 (=B286)	As AL-24	June 2007	146.800
73x79-6 (=B292)	As AL-24	January 2007	312.300
<i>P. delicatissima</i> clade 1 <i>sensu</i> Amato et al. (2007) (del1)			
B487	As AL-24	April 2009	947.600
B487	As AL-24	April 2009	743.900
B489	As AL-24	April 2009	1.697.500
B489	As AL-24	April 2009	3.876.700
<i>P. delicatissima</i> clade 2 <i>sensu</i> Amato et al. (2007) (del2) = <i>P. delicatissima sensu stricto</i>			
B247	As AL-22 DQ813810	November 2006	158.900
B241	As AL-22	January 2007	735.700
B247	As AL-22	March 2007	644.400
B247	As AL-22	June 2007	170.800
<i>P. dolorosa</i> clade 3 <i>sensu</i> Amato et al. (2007) (del3)			
B332	As AL-59 DQ813813	April 2007	690
B327	As AL-59	May 2007	37360
B327	As AL-59	June 2007	38850
<i>P. pseudodelicatissima</i> <i>sensu</i> Amato et al. (2007) (pse)			
B317	As AL-15 DQ813808	April 2007	178.400
B318	As AL-15	April 2007	137.800
B485	As AL-15	April 2009	214.600
B485	As AL-15	April 2009	280.000
B486	As AL-15	April 2009	234.000
<i>P. multistriata</i> <i>sensu</i> Orsini et al. (2002) (psm)			
DD12 (=B283)	As SZN-B27 AF416753	November 2006	68.700
AA11 (=B302)	As SZN-B27	January 2007	157.800
AA11 (=B302)	As SZN-B27	March 2007	79.800
B308	As SZN-B27	June 2007	70.400
B308	As SZN-B27	June 2007	83.200
B308	As SZN-B27	June 2007	145.200

### V. 3. Results

#### V. 3. 1. Morphological diversity

Examination of the frustule ultrastructures showed differences among all analysed *Pseudo-nitzschia* species (Figure V.2). The major part of the morphological differences were due to the densities of the striae and fibulae as well as cell width and poroid density. As reported by Lundholm et al. (2006), both *P. delicatissima* and *P. pseudodelicatissima* had a slit along the apical axis of the valve, called raphe, which is supported by the fibulae. The raphe is interrupted centrally by a small thickened nodule in the larger interspace. Striae were observed on the valve surfaces. In the species of the *P. delicatissima* complex (Figures V.2B, V.2C and V.2D) and in *P. multistriata* (Figure V.2I) each stria consisted of two rows of poroids; in *P. pseudodelicatissima* (Figures V.2F and V.2G) poroids are larger, arranged in a single line and split in different major sector. The hymen of the poroids was arranged in a hexagonal pattern (Figure V.2G). The *P. delicatissima*-like species were clustered into three distinct clades. In one of them (*P. delicatissima*, del2; Figure V.2C), the valve ultrastructure conformed to the description of *P. delicatissima sensu stricto* by Lundholm et al. (2006) and another one (*P. delicatissima*, del3; Figure V.2D) could be identified as *P. dolorosa* (Lundholm et al., 2006). The last one (*P. delicatissima*, del1; Figures V.2A and V.2B) presented very minor ultrastructurale differences from *P. delicatissima* del2 and it has been recently described as *Pseudo-nitzschia arenysensis* (Quijano-Scheggia et al., 2009). The species of *P. pseudodelicatissima* (pse, Figures V.2E, V.2F and V.2G) corresponded to *P. pseudodelicatissima sensu stricto* (Lundholm et al., 2003). Examination of *P. multistriata* (psm, Figures V.2H and V.2I) species fit the respective morphological characters described by Orsini et al. (2002).

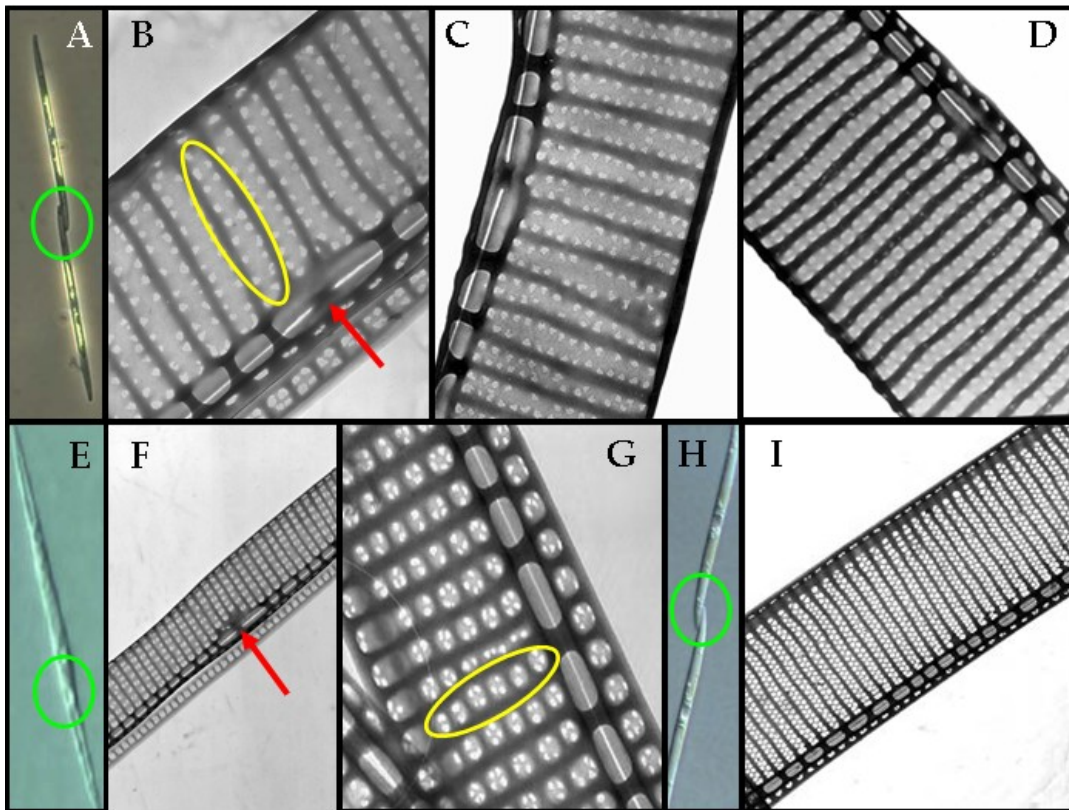


**Figure V.2.** Images from light (A, E, H; scale bars: 20  $\mu\text{m}$ ) and transmission electron microscopy (B, C, D, F, G, I; scale bars: 1  $\mu\text{m}$ ) of *P. delicatissima* del1 (A - B), *P. delicatissima* del2 (C), *P. dolorosa* del3 (D), *P. pseudodelicatissima* pse (E - G) and *P. multistriata* psm (H - I). Solid green circles indicate the overlapping region between two adjacent cells in a chain, solid red arrows the wider separation of the two central fibulae and solid yellow ellipses the striae.

### V. 3. 2. Genetic diversity

The results of the molecular analyses confirmed the attribution of the strains used for the chemical analyses to the three cryptic species of the *P. delicatissima* complex, *P. pseudodelicatissima* and *P. multistriata* (see Table V.1).

The strains of *P. delicatissima* clade 1 analyzed in two different periods (2007 and 2009) clustered into the same genetic clade for both genetic markers (LSU and ITS).

### V. 3. 3. Chemical diversity

A total of 26 diatom strains belonging to five *Pseudo-nitzschia* species were profiled for phyco-oxylipins by LC-DAD-MS/MS (see Table V.1 above). The oxylipin screening of these species revealed quantitative and qualitative differences. Figure V.3 represents the signatures of *P. delicatissima* clade 1 (del1, Figure V.3A), *P. delicatissima* clade 2 (del2, V.3B), *P. dolorosa* (del3, V.3C), *P. pseudodelicatissima* (pse, V.3D) and *P. multistriata* (psm, V.3E), which were identified under the analytical conditions described in the

experimental section § II. 2. 6 of chapter II. With this method it was possible to deduce the composition of each raw diatom extract.

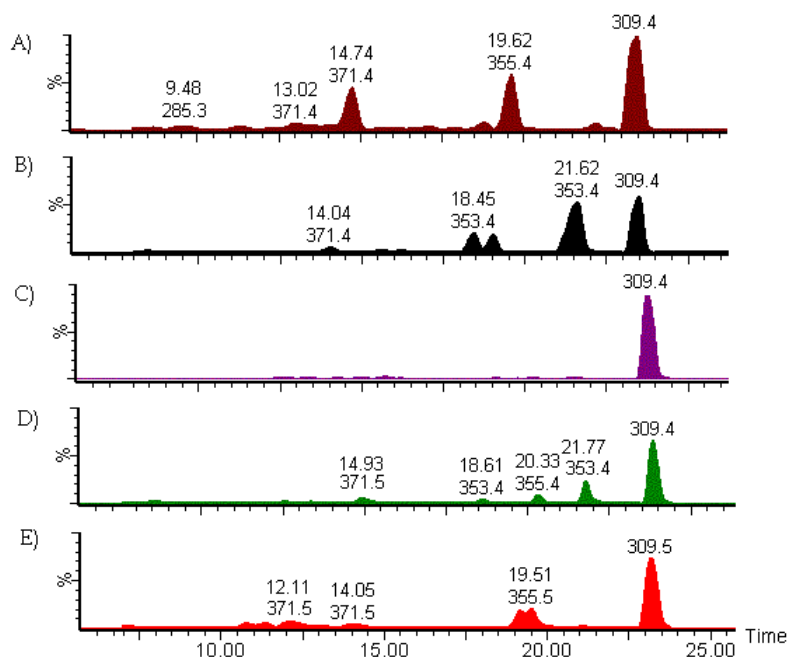


**Figure V.3.** LC-MS profile of different *Pseudo-nitzschia* species: (A) *P. delicatissima* clade 1 (del1), (B) *P. delicatissima* clade 2 (del2), (C) *P. dolorosa* (del3), (D) *P. pseudodelicatissima* (pse) and (E) *P. multistriata* (psm). Internal standard, 16-hydroxyhexadecanoic acid methyl ester, is shown by the peak at 23.5 min ( $m/z$  309.4).

Except for *P. dolorosa* (del3, Figure V.3C), all diatom strains had levels of phyco-oxylipins which allowed easy detection. As expected, *P. delicatissima* clade 1 (Figure V.3A) revealed an identical composition to the *P. delicatissima* strain B321, which was utilized for delineating the eco-physiological role of these metabolites as reported in the chapter IV of this thesis. Likewise *P. delicatissima* clade 1 (Figure V.3A) contained 15-hydroxy-eicosa-5Z,8Z,11Z,13E,17Z-pentaenoic acid (15-HEPE,  $R_t$ =19.62 min) and 15-oxo-5Z,9E,11E,13E-pentadecatetraenoic acid ( $R_t$ =9.48 min). Interestingly, when *P. delicatissima* clade 1 was re-isolated after two years (see Table V.1, samples B487 and B489), the LC-MS analyses confirmed the presence of these last two compounds, but revealed a second set of products featured by an unassigned HEPE (Figure V.4).

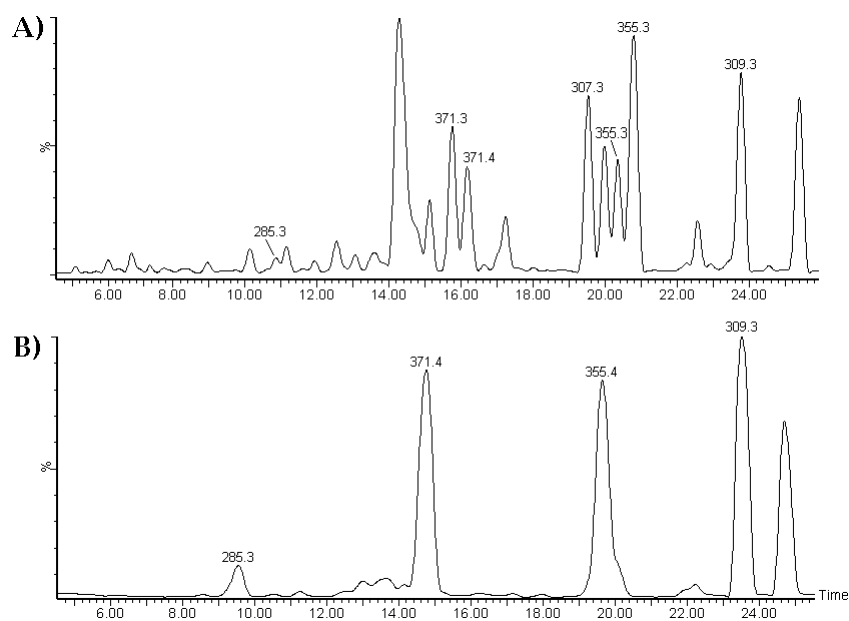


**Figure V.4.** Different LC-MS profiles of *P. delicatissima* clade 1. **(A)** Total ion current (TIC) MS profile of *P. delicatissima* isolated in the spring 2009 (B487). **(B)** Total ion current (TIC) MS profile of *P. delicatissima* isolated in the autumn 2007 (B286). Numbers above peaks indicate the molecular weight of the most intense ion.

The second clade of *P. delicatissima* (del2, Figure V.3B) was significantly different from the first clade, being featured by an unusual oxygenate derivative with a molecular mass of  $m/z$  353 ( $R_t=18.45$  and 21.62 min) and UV maximum at 248 nm (data not shown). This compound was also present in *P. pseudodelicatissima* (pse, Figure V.3D) together with another hydroxy- derivative of eicosapentaenoic acid (EPA). Other two different hydroxy derivatives ( $R_t=19.12$  and 19.51 min) of EPA, together with two epoxy alcohols ( $R_t=12.11$  and 14.05 min), composed the oxygenate fatty acid derivatives of *P. multistriata* (psm, Figure V.3E).

The above assignment of the HEPes were fully supported by GC-MS analysis of the corresponding trimethyl-silyl derivatives (data spectra are reported in the Appendix see Figures A.13 and A.14).

#### V. 3. 4. LC-MS/MS analysis of epoxy alcohols

After an initial profiling of the microalgae extracts, the species which showed the presence of epoxyhydroxy- derivatives ( $m/z$  371  $M+Na^+$ ) were successively analyzed in LC-MS/MS mode using a collision energy between 17 and 35 V. About 250-400  $\mu g$  of methylated extracts in 100  $\mu l$  MeOH were directly investigated for each species.

MS/MS fragmentation patterns arise from  $\alpha$ -cleavage of the oxirane ring and generate typical daughter ions that allow the identification of the structure. Further details of this mechanism was reported in the section § II. 3. 3 of chapter II.

The MS spectra of *P. delicatissima* clade 1 showed an epoxy alcohol derivative of EPA featured in MS/MS by fragmentation of the pseudo-molecular ions at  $m/z$  273 and 259 (Figure V.5A) deriving from 13-hydroxy-14,15-epoxy-eicosa-5Z,8Z,11Z,17Z-tetraenoic acid (13,14-HEpETE). In addition to this metabolite, samples of *P. delicatissima* clade 1 isolated in the spring 2009 (Table V.1, B487 and B489) were featured by a second C<sub>20</sub> epoxy alcohol (molecular ion at  $m/z$  371) that in MS/MS gave fragments at  $m/z$  249, 233 and 219 (Figure V.5B). These ions are not coherent with any known molecule and, therefore, the structure of this compound is left unresolved for the moment.

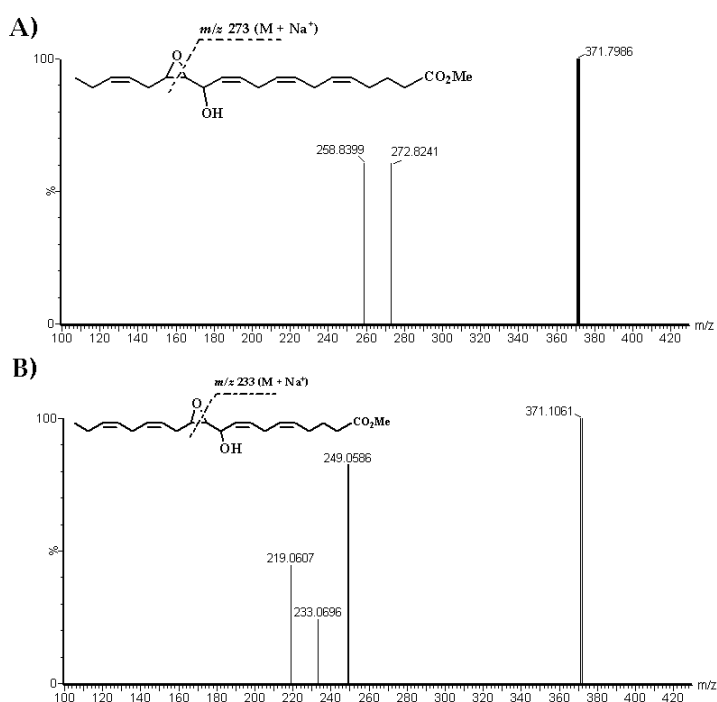


**Figure V.5.** MS/MS fragmentation of (A) 13-hydroxy-14,15-epoxy-eicosa-5Z,8Z,11Z,17Z-tetraenoic acid (13,14-HEpETE) isolated from *P. delicatissima* (B286) and (B) undetermined C<sub>20</sub> epoxy alcohol from *P. delicatissima* (B487).

In *P. multistriata*, the analysis revealed two C<sub>20</sub> epoxy alcohols attributable to 16-hydroxy-14,15-epoxy-eicosa-5Z,8Z,11Z,17Z-tetraenoic acid (16,14-HEpETE) (Figure V.6) and 12-hydroxy-10,11-epoxy-eicosa-5Z,8Z,14Z,17Z-tetraenoic acid methyl ester (12,10-HEpETE) on the basis of the diagnostic fragments found in MS/MS analysis.

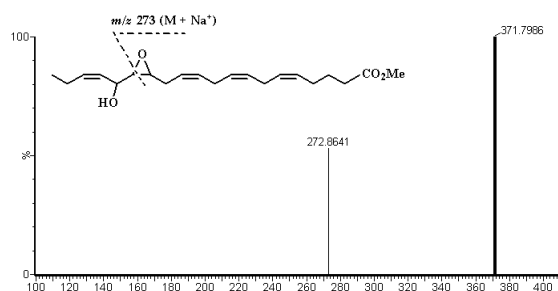


**Figure V.6.** MS/MS fragmentation of 16-hydroxy-14,15-epoxy-eicosa-5Z,8Z,11Z,17Z-tetraenoic acid (16,14-HEpETE).

The presence of an unusual oxygenate derivative showing molecular mass at  $m/z$  353 ( $M+Na^+$ ) in *P. delicatissima* clade 2 and *P. pseudodelicatissima* suggested a certain degree of similarity between the two species, although the pattern of the other oxylipins was significantly different. In *P. delicatissima* clade 2, the fragment ion at  $m/z$  153 ( $C_6H_{10}O_3 \cdot Na^+$ ) was associated with the structure of 7-hydroxy-5,6-epoxy-eicosa-8Z,11Z,14Z,17Z-tetraenoic acid methyl ester (7,5-HEpETE) (Figure V.7A), whereas the fragment ion at  $m/z$  193 ( $C_9H_{14}O_3 \cdot Na^+$ ) is inferred to derive from 10-hydroxy-8,9-epoxy-eicosa-5Z,11Z,14Z,17Z-tetraenoic acid methyl ester (10,8-HEpETE) (Figure V.7B) in the extract of *P. pseudodelicatissima*.

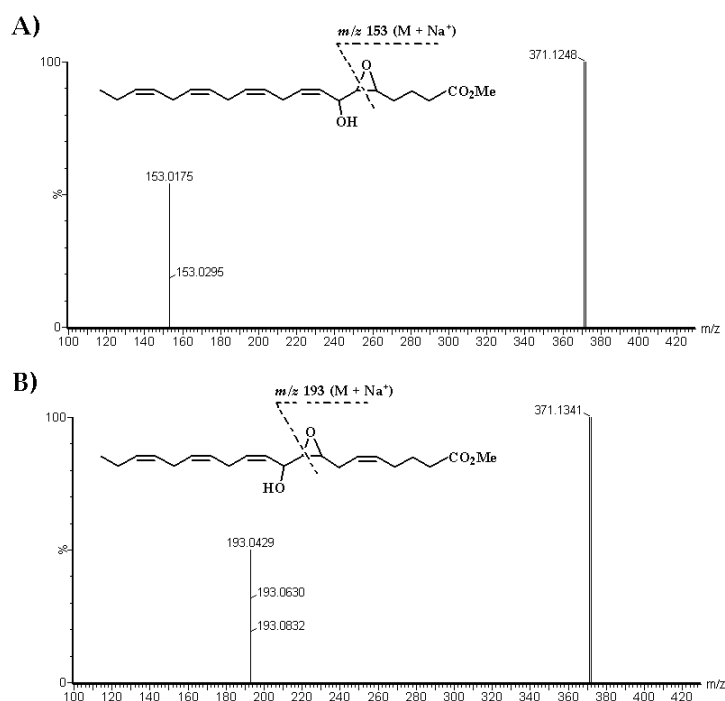


**Figure V.7.** MS/MS fragmentation of (A) 7-hydroxy-5,6-epoxy-eicosa-8Z,11Z,14Z,17Z-tetraenoic acid (7,5-HEpETE) and (B) 10-hydroxy-8,9-epoxy-eicosa-5Z,11Z,14Z,17Z-tetraenoic acid (10,8-HEpETE).

#### V. 4. Discussion

According to the literature (d'Ippolito et al., 2005; Fontana et al., 2007b), the oxylipin pathways in different diatoms revealed a species-specific distribution, either for the preferential substrate involved (HTrA, HTA and EPA), for the regio- and stereospecificity of lipoxygenases or considering the different metabolic fate of hydroperoxides in dependence of the enzymatic activities able of metabolizing these unstable intermediates (hydroperoxide-lyase, peroxygenase or epoxy alcohol synthase).

Diatoms of the genus *Pseudo-nitzschia* show a common lipoxygenase metabolism leading to the production of oxygenated derivatives of C<sub>20</sub> fatty acids featured by hydroxy eicosapentenoic acids (HEPEs),  $\alpha$ -hydroxy epoxy moieties (HEpETEs) and  $\omega$ -oxo acids. Nevertheless, structural characteristics and levels of these metabolites were found to be significantly different in the sympatric species taken into consideration in this study. All chemical analyses were performed on diatoms harvested in the stationary growth phase since lipoxygenase metabolism significantly varies during cell growth (Ribalet et al., 2007; d'Ippolito et al., 2009). As explained in the second chapter of this thesis, the LC-DAD-MS method has directly allowed the observation of phyco-oxylipins in crude extracts of these microalgae, resolving species of the same molecular mass or with the same retention time. Clear identification of the metabolic content of these extracts is completed by a combination of liquid chromatography with MS/MS techniques. Fragmentation of each  $\alpha$ -epoxy alcohol methyl ester is used as a valid and reliable tool to infer the oxidation position of the LOX pathways (see chapter II). These results, however, were corroborated by GC-MS analysis of the silyl derivatives of the isolated HEPEs. As summarized in the Table V.2, the phyco-oxylipin diversity was high and the identification of each  $\alpha$ -epoxy alcohol suggests the presence of six different eicosapentanoate-dependent lipoxygenase pathways in the five species analysed.

Table V.2. Distribution of phyco-oxylipins in five different *Pseudo-nitzschia* species.

	del 1		del 2	del 3	pse	psm
	autumn 2006	spring 2009				
15-oxoacid	+	+	-	-	-	-
7,5-HEpETE	-	-	+	-	-	-
10,8-HEpETE	-	-	-	-	+	-
12,10-HEpETE	-	-	-	-	-	+
13,14-HEpETE	+	+	-	-	-	-
16,14-HEpETE	-	-	-	-	-	+
5-HEPE	-	-	+	-	-	-
8-HEPE	-	-	-	-	+	-
11-HEPE	-	-	-	-	-	+
14-HEPE	-	-	-	-	-	+
15-HEPE	+	+	-	-	-	-
compound <i>m/z</i> 353	-	-	+	-	+	-
unknown HEPE	-	+	-	-	-	-

The genetically distinct species within the *P. delicatissima*-complex revealed subtle ultrastructural differences in the density of poroids under the electron microscope (Figure V.2), and minor differences – such as shape of poroids, density of striae and fibulae - characterized the other two species, *P. pseudodelicatissima* and *P. multistriata* (Figures V.2G and V.2I). Identification with the help of electron microscopy proved to be extremely difficult in the species belonging to the *P. delicatissima*-complex (Figures V.2B, V.2C and V.2D) due to the often occurring overlap in the ranges of the examined morphometric characters. The small, but consistent ultrastructural differences in their frustule architecture have been the principal traits for their taxonomy since 1965 (Hasle, 1965; Hasle et al., 1996). Thus, the species within each of these groups can be defined as a pseudo-cryptic (semicryptic *sensu* Mann, 1999) species. On the basis of four molecular markers, using three nuclear and one plastid markers, Amato and co-workers (2007) tested genetic relatedness among these different strains isolated from the Gulf of Naples (Italy). Of these four markers, ITS-2 appeared to be the only one that discriminated accurately between biological species. Furthermore, their tests of mating compatibility showed the existence of reproductive isolation between morphologically related, but genetically distinct sympatric populations suggesting the existence of evolutionary mechanisms that prevent interbreeding and explain the ecological meaning of their hidden diversity.

Classical ecological competition theory predicts that species, including cryptic species, can coexist at equilibrium only if they show some level of ecological specialization (Hutchinson, 1978; Tilman, 2004). Although the understanding of the biological characteristics of marine plankton is rather limited, there are data supporting the idea that different cryptic species occupy distinct ecological niches. During bloom conditions the cell concentration increases greatly, thus, if the timing of the bloom differs among different genotypes, the chances of finding conspecific cells within the bloom will be high and may largely or completely prevent interbreeding. If, on the other hand, blooms are mixed, then efficient recognition systems should evolve, allowing discrimination between members of the same species and others. Orsini and co-workers (2004) carried out a study during a spring bloom of *P. delicatissima* in the Gulf of Naples. Three “*P. delicatissima*” ITS types (corresponding to del1, del2, and del3 here) were recorded together in pre-bloom conditions, but only one of them (del1) contributed substantially to the spring bloom. The distribution of these distinct genotypes between different temporal windows in an annual or multi-annual cycle might represent a strategy for sharing the same environment. As an example, different populations of the diatom *Skeletonema costatum* (possibly pseudo-cryptic species, Sarno et al., 2005) characterized by distinct isozyme banding patterns were recorded during the spring and autumn blooms in Narragansett Bay (Gallagher, 1980). Cryptic diversity may explain the observed strain-specific differences in the capacity for producing toxins (Mos, 2001) or secondary metabolites, as described in this chapter, which may confer selective advantages to particular genotypes.

Ecologists identify and enumerate phytoplankton using light microscopy, but the finding of cryptic or pseudo-cryptic diversity cannot be recognized by these standard tools. This research has shown that the combination of HPLC and ESI<sup>+</sup> MS/MS can yield a considerable amount of information about taxonomy of diatoms, detecting simultaneously and with comparable sensitivity to the DNA markers a range of different LOX-derived fatty acid metabolites, as described for *P. delicatissima* clade 1 and *P. delicatissima* clade 2. This advance opens the possibility of more detailed investigations of lipoxygenase products as chemical markers of cryptic and pseudo-

cryptic species. The profiling strategies, illustrated with the results in this chapter, present several practical advantages including being relatively cheap on a per sample basis, high throughput and fully automated with analytical acquisition times typically taking less than three hour. Polyunsaturated fatty acids account for a large component of diatom cells and it is therefore extremely easy to perform analysis of their derivatives even with very little number of cells. Furthermore, the use of internal standards, such as 16-hydroxyhexadecanoic acid, allows the phyco-oxylin fingerprint of one species to be easily compared with another without the need for recalibration.

## Chapter VI

### Identification and preliminary purification of a galactolipid-hydrolyzing enzyme from *Thalassiosira rotula*

#### VI. 1. Introduction

Production of oxygenated derivatives of lipids is a common phenomenon in higher organisms and evidence for diverse roles of the oxylipins in plants is accumulating (Bl  e, 1998: see also chapter III and IV of this thesis). Volatile C<sub>6</sub> and C<sub>9</sub> aldehydes, for example, together with lipoxygenase derived compounds like jasmonates are reported to be involved in the hypersensitive resistance response of plants towards pathogens (Croft et al., 1993; Noordermeer et al., 2001; Bl  e, 2002). They also induce expression of a subset of genes involved in the defence response against insect herbivores (Pare & Tumlinson, 1999). Matsui et al. (2000) identified a not further-characterized lipid-hydrolyzing activity acting on galactolipids involved in the formation of the green leaf-volatile aldehyde hexanal in *Arabidopsis thaliana*. Other lipid-hydrolyzing activities, like those by phospholipases, are involved in the regulation of the jasmonates and other phyto-oxylipins (Dhondt et al. 2000; Ishiguro et al., 2001; Wang, 2001).

Recently, the occurrence of volatile PUAs was reported in several marine diatoms (Miralto et al., 1999; d'Ippolito et al., 2002a and 2002b; Pohnert et al., 2002; Wichard et al., 2005b). In the absence of genetic data on the lipid metabolism, the only information of aldehyde synthesis in these microalgae stems from chemical investigations (Pohnert, 2000; d'Ippolito et al., 2003 and 2004; Cutignano et al., 2006). The production of phyco-oxylipins in diatoms, including PUAs, is only activated after mechanical stress or cell disruption (Fontana et al., 2007a). In healthy, intact diatom cells free fatty acids are generally not found, because they are physiologically bound to the complex lipids. In analogy to plants, their release from membranes seem to be an important step in controlling the lipid peroxidation process, but when and how these fatty acids are made available for the enzymatic cascade is not well understood yet. On the basis of the analysis of site-specific transformations of fluorescent analogues of phospholipids

in crude cell preparations, a wound-activated defence mechanism triggered by phospholipase A<sub>2</sub> (PLA<sub>2</sub>) activity was proposed to account for the synthesis of PUAs in *T. rotula* (Pohnert, 2002). However, the presence of such a wound-inducible PLA<sub>2</sub> activity has not been characterized in this or other diatom species. In contrast to Pohnert's conclusion, Cutignano and co-workers (2006) showed that glycolipids are the only class of complex lipids that gives rise to the complete aldehydic pattern of *T. rotula* including the formation of the major aldehydes, such as octadienal and decatrienal, and the minor compounds heptadienal and octatrienal. The role of phospholipids was apparently less crucial, because they were only involved in the partial formation of the decatrienal. On the basis of the previous work by Cutignano and co-workers (2006) in this last chapter the preliminary purification of a galactolipid-hydrolyzing enzyme from *T. rotula* is reported.

## **VI. 2. Materials and Methods**

### *VI. 2. 1. Reagents and equipment*

Chromatography pre-packed columns (MonoQ HR 5/5, MonoQ™ 5/50 GL and Superdex 200 10/300 GL) were purchased from GE Healthcare, Uppsala, Sweden. FPLC purifications were carried out on a Amersham Biosciences ÄKTA-FPLC equipped with pumps (P-920), detector (UPC-900) and fraction collector (FRAC-900). HPLC purifications were carried out on a Thermo Electron chromatograph coupled with P4000 pumps and a UV2000 double wavelength detector. Standard proteins, such as bovine serum albumin (BSA), turkey egg albumin (ovoalbumin), trypsin inhibitor, vitamin B<sub>12</sub> and ribonuclease from bovine pancreas used for calibration of gel filtration columns were obtained from Sigma-Aldrich Chemie GmbH (Steinheim, Germany). Others standard proteins (aldolase, catalase and ferritine) and low molecular weight (LMW) marker proteins for SDS-PAGE were purchased from Amersham Biosciences, Uppsala, Sweden. Materials used for the protein purification (SDS-PAGE), such as acrylamide-Bis solution 30%, TEMED, β-mercaptoethanol, fixating, staining and destaining solutions, and Mini Protean II electrophoresis apparatus were obtained from Bio-Rad Laboratories (Hercules, CA, USA). The Bradford ready solution for protein assays was obtained from Bio-Rad Laboratories GmbH (München, Germany).

Glycerol, ammonium peroxide sulphate (APS) and membrane dialysis tube (cut-off 12 kDa) were purchased from Sigma Chemical (St. Louis, MO, USA). Concentration of protein samples was performed by different centrifugal filter devices: Centricon 10000 and 30000 MCWO (Amicon, Bedford, MA, USA), Vivaspin 15R (Sartorius, Hannover, Germany) and Amicon ultra 10K (Millipore, Cork, Ireland). Commercial L- $\alpha$ -phosphatidyl-d,l-glyceroldioleoyl and L- $\alpha$ -phosphatidyl-d,l-glyceroldioleoyl/tristearine were purchased from Sigma-Aldrich (Schnelldorf, Germany).

#### VI. 2. 2. *Cell culture samples*

Cultures of *T. rotula* (CCMP 1647) were purchased from the Provasoli-Guillard National Centre for Culture of Marine Phytoplankton (Boothbay Harbor, Maine, USA). Axenic cultures of marine diatoms were grown as described in Ianora et al. (1996). After a week the cells were harvested by centrifugation at 1200 g for 10 min at 5° C using a swing-out rotor. The cell pellets were collected in 50 ml Falcon tubes, immediately frozen and kept at -80° C until use.

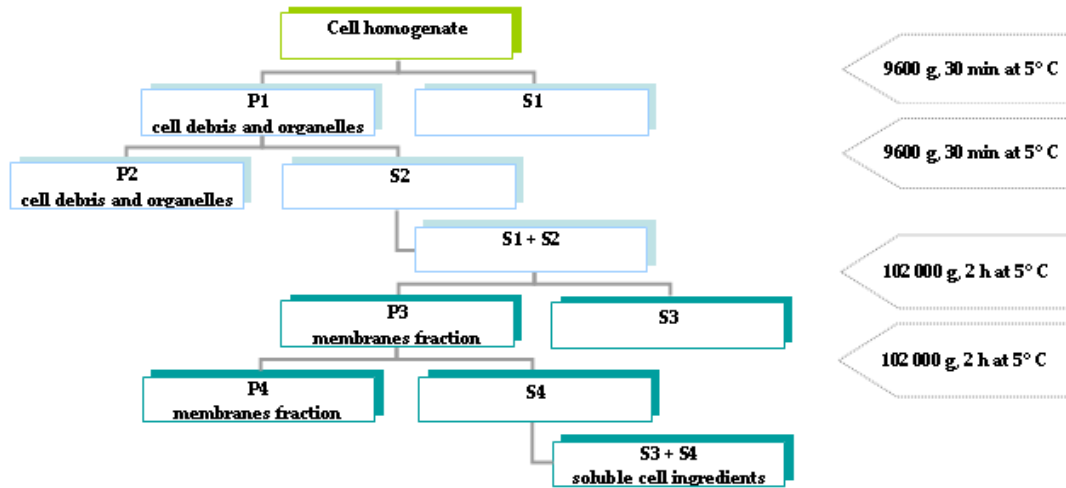
#### VI. 2. 3. *Extraction and isolation of the glycolipids from Posidonia oceanica*

About 1 Kg (wet weight) of *P. oceanica* leaves were cut into small pieces (0.5 cm length) and suspended in 0.5 L CHCl<sub>3</sub>/MeOH 1:1. The suspension was sonicated for 5 min in an ultrasonic bath cooled by ice and then ground with a mortar and pestle. The extract was filtered through a Whatman no. 1 filter paper and transferred into a separation funnel. The plant residue was extracted again in the same way (in total five-times). The extracts were combined after filtration in the separation funnel. The water phase was removed and the organic layer was evaporated under reduced pressure with a rotary evaporator (Buchi, Rotavapor R-200). The raw extract was purified by size exclusion chromatography. The sample was dissolved in CHCl<sub>3</sub>/MeOH 1:1 and loaded on a Sephadex LH20 column (3.0 x 126 cm, CHCl<sub>3</sub>/MeOH 1:1) for isolation of monogalactosyldiacylglycerols (MGDG), digalactosyldiacylglycerols (DGDG) and sulphoquinovosyldiacylglycerols (SQDG). Fractions were collected by a fraction collector and each one was analysed on TLC (silica gel, solvent system: CHCl<sub>3</sub>/MeOH/H<sub>2</sub>O 85:15:2) in order to combine similar fractions. The TLC pattern was detected under

an UV lamp at 254 nm and with two different spray reagents (ceric-sulphate-H<sub>2</sub>SO<sub>4</sub> and  $\alpha$ -naftol-H<sub>2</sub>SO<sub>4</sub> for sugar detection). MGDG were separated from DGDG by a further chromatographic step utilizing the centrifugal preparative thin-layer chromatography apparatus (CPTLC, Harrison Research inc, Palo Alto, CA, USA) with an elution solvent mixture of CHCl<sub>3</sub>/MeOH/H<sub>2</sub>O 85:15:2. Fractions were collected by a fraction collector and then analysed by TLC for combining as described above. MGDG and DGDG fractions were also examined by NMR and LC-MS techniques (data spectra are reported in the Appendix see Figures A.15 and A.16). In order to determine the fatty acid composition of each glycoylcerolipid class (0.5 mg), alkaline methanolyses (saponification) were carried out in 500  $\mu$ l of MeOH by Na<sub>2</sub>CO<sub>3</sub> at a final concentration of about 100 mM. The reaction mixtures were incubated over night at 42° C before neutralization with 1% H<sub>2</sub>SO<sub>4</sub> and extraction with diethyl ether. After removal of the organic solvent at reduced pressure, the residues were dissolved in *n*-hexane and analysed by GC-MS as reported in the section § VI. 2. 7 (data spectra are reported in the Appendix see Figures A.15 and A.16).

#### VI. 2. 4. *Fractionation of crude enzymatic extract*

About 25 g of wet weight *T. rotula* (CCMP 1647) cells were suspended in 20 mM Tris-HCl buffer pH 8.4 (1 ml/g of wet pellet). The suspension was sonicated three times for 30 sec and the resulting homogenate was centrifuged at 9600 g at 5° C for 30 min in order to remove insoluble material, cell debris and cell organelles. The pellet (P1, as depicted in the Scheme VI.1) was re-suspended in the same buffer (2 ml/g of wet pellet) and centrifuged again under the same conditions. The two supernatants (S1 + S2) were combined and ultracentrifuged twice (Sorvall Discovery, Rotor Ti60, Beckmann) at 102000 g for 2 h (5° C) yielding the membrane fractions (P3 and P4) and soluble cell ingredients in the supernatants (S3 + S4). The two supernatants were finally combined to give the crude enzyme. This preparation was performed for each different purification described through this research thesis.



Scheme VI.1. Overview of the differential centrifugation steps.

#### VI. 2. 5. Protein quantification

The protein concentrations were measured by Bradford assay following the manufacture's instructions (Bio-Rad). BSA was used as standard to establish calibration curves for protein quantification. Different volumes of BSA (250 µg/ml) were mixed with water to a final volume of 800 µl (Table VI.1) in 1.5 ml Eppendorf tubes. In order to correct for pipetting errors, these samples were prepared in duplicates. 200 µl Bradford ready-to-use solution (Bio-Rad Laboratories) was added and mixed properly with each sample. After an incubation time of 10 min at room temperature, absorbance was measured at 595 nm. Protein dilutions were adjusted to give absorptions between 0.100 and 1.000, since the Bradford assay is linear only within this range. For determining sample protein concentrations, the deionised water was used for preparing the samples in 1.5 ml Eppendorf tubes (final volume 800 µl). For samples with a high protein concentration a dilution was necessary. To each sample 200 µl of Bradford solution were added and samples mixed thoroughly. After 10 min incubation the absorbance was measured as described above.

**Table VI.1.** Dilution scheme for BSA standard.

<i>BSA</i> ( $\mu$ l)	<i>Water</i> ( $\mu$ l)
0	800
10	790
20	780
30	770
40	760
60	740
80	720

#### VI. 2. 6. Assay for galactolipid-hydrolyzing activity

MGDG from *P. oceanica* was used as a substrate in the routine assay for galactolipid-hydrolyzing activity. The respective protein samples were added to an Eppendorf tubes, and filled with 20 mM Tris-HCl buffer, pH 8.4, to reach a final volume of 300  $\mu$ l. Volumes of protein solutions added to the assay varied depending on the protein concentration of the respective sample as measured in the Bradford assay (see above). Substrate were dissolved in MeOH at the final concentration of 10  $\mu$ l/ml and added to the lid of the Eppendorf tubes containing the protein sample. In general, substrate controls (300  $\mu$ l buffer containing 3  $\mu$ l substrate) was included in all assays. After brief mixing of all components, samples were incubated for 40 min at room temperature. After incubation, EPA (0.7  $\mu$ g in 7  $\mu$ l methanol) was added as internal standard and the reaction was stopped by addition of equal volume of ethyl acetate. Each reaction mixture was then extracted by centrifugation at 2400 g for 5 min. The crude extract was methylated and analysed by GC-MS as described below. Activity was quantified plotting the peak areas of free fatty acid ( $C_{18:3}$ ) against the standard concentration (EPA).

#### VI. 2. 7. GC-MS analysis of free fatty acids

The extracts of enzymatic products were dissolved in 20  $\mu$ l of *n*-hexane and analysed by GC-MS equipped with an ion-trap, on a 5% diphenyl column, in EI (70 eV) and negative mode analyzer. Elution of free fatty acid methyl esters required an increasing gradient of temperature according to the following programme: 200° C for 2.5 min then 15° C min<sup>-1</sup> till 290° C, followed by 7 min at 290° C. 5  $\mu$ l samples were directly injected

in split mode (1:10), with a blink window of 3 minutes (inlet temperature of 270° C, transfer line set at 280° C and ion source temperature of 250° C).

#### VI. 2. 8. *SDS polyacrylamide gel electrophoresis (SDS-PAGE)*

After each purification protein fractions that showed activity and neighbouring fractions were submitted to SDS polyacrylamide gel electrophoresis (SDS-PAGE). SDS gels were used to monitor differences in the band patterns of active versus inactive fractions. Table VI.2 shows the composition of gels and buffers used for SDS-PAGE.  $\beta$ -mercaptoethanol was added to the sample buffer as reducing agent. Protein amounts loaded to the gel depended on the step of purification. Generally, a total volume of 10-20  $\mu$ l was applied for each sample, consisting of 2-4  $\mu$ l of 5x sample buffer and respective volumes of protein solution and deionised water, if necessary, to reach the final volume. On each gel, the LMW protein marker (Amersham Biosciences) consisting of a protein ladder ranging from 14.4 kDa to 97 kDa was run as size standard. After mixing sample buffer and protein solution, proteins were denatured for 5 min in a water bath at 100° C. The gel was run at 120 V until marker bands reached the resolving gel and then voltage was set to 150 V. Electrophoresis was stopped before the lower marker band reached the end of the gel. After electrophoresis, gels were incubated in the fixing and staining solution (Bio-Rad Laboratories) for 30 min. Slight background staining was removed by first washing the gel with destaining solution (Bio-Rad Laboratories) for 30 min and then with fresh destaining solution over night. In cases where target proteins were subject to further analysis, the target proteins were cut out of the gel after scanning the gels, cut into pieces of approximately 1 mm<sup>3</sup> and stored at -20° C until analysis by Matrix Assisted Laser Desorption/Ionization–Time of Flight (MALDI-ToF) mass spectrometry and nano-Electrospray-MS/MS (nESI-MS/MS).

**Table VI.2.** Gels and buffers used for SDS-PAGE.

<i>Description</i>	<i>Components</i>	<i>Volum e</i>
<b>Stacking gel 6% (10 ml)</b>	1 M Tris-HCl pH 6.8	2.5 ml
	30% Acrylamide/Bis solution	2 ml
	10% (w/v) SDS solution	0.1 ml
	deionised H <sub>2</sub> O	5.3 ml
	10% (w/v) APS solution	0.1 ml
	TEMED	0.01 ml
<b>Resolving gel 10% (10 ml)</b>	1.5 M Tris-HCl pH 8.8	2.5 ml
	30% Acrylamide/Bis solution	3.3 ml
	Glycerol	0.2 ml
	10% (w/v) SDS solution	0.1 ml
	deionised H <sub>2</sub> O	3.8 ml
	10% (w/v) APS solution	0.1 ml
<b>Sample buffer 5x (10 ml)</b>	TEMED	0.01 ml
	0.5 M Tris-HCl, pH 6.8	1.25 ml
	deionised H <sub>2</sub> O	2.75 ml
	Glycerol	2.5 ml
	10 % (w/v) SDS solution	2.0 ml
	0.5 % (w/v) bromophenol blue	1.0 ml
<b>SDS-Running buffer 5x (1 L)</b>	$\beta$ -mercaptoethanol	0.5 ml
	Tris base	15.1 g
	Glycin	94 g
	deionised H <sub>2</sub> O	950 ml
	10 % (w/v) SDS solution	50 ml

#### VI. 2. 9. *Trypsin digestion of SDS-PAGE separated proteins*

Trypsin digestion and MALDI-ToF mass analysis were performed by Dr. Gianluca Picariello (CNR- Istituto di Scienze dell'Alimentazione of Avellino, Italy). After thawing, the gel pieces were washed twice with 50  $\mu$ l deionised water and was completely destained by repeated immersion into a solution 50 mM NH<sub>4</sub>HCO<sub>3</sub> in 50% (v/v) aqueous acetonitrile (ACN) . The destained spots were dehydrated by submersion into ACN and dried under vacuum until ACN removal. Before digestion, the proteins were in-gel reduced with 10 mM dithiothreitol in 25 mM NH<sub>4</sub>HCO<sub>3</sub> for 45 min at 55° C and then S-alkylated with 55 mM iodoacetamide in 25 mM NH<sub>4</sub>HCO<sub>3</sub> under dark condition for 30 min at room temperature. The dried gel pieces were re-hydrated by 15  $\mu$ l 50 mM NH<sub>4</sub>HCO<sub>3</sub> containing 12 ng/ $\mu$ l trypsin in an ice-cold bath. After 45 min, the excess of trypsin solution was removed, the gel pieces were covered with 30  $\mu$ l 50 mM NH<sub>4</sub>HCO<sub>3</sub> and incubated overnight at 37° C. The tryptic digest was

three-fold extracted with 40  $\mu$ l of ACN/5% (v/v) formic acid solution (1:1, v/v). The recovered solutions were then pooled, concentrated in a speed-vac centrifuge and then lyophilized. Finally, peptides were re-dissolved in 15  $\mu$ l of 0.5% formic acid. Before mass spectrometric analysis peptides were desalted by C<sub>18</sub> reversed-phase Zip-Tip<sup>®</sup> microcolumns, washing with 0.1% trifluoroacetic acid (TFA) and eluting with 50% acetonitrile (v/v)/ 0.1% TFA.

#### VI. 2. 10. *MALDI-ToF analysis, peptide mass fingerprinting, nESI-MS/M and protein identification*

Peptides obtained after trypsin digestion were analysed by MALDI-ToF mass spectrometry. Mass spectra were acquired on a Voyager DE-Pro spectrometer (PerSeptive BioSystems, Framingham, MA, USA) equipped with a N<sub>2</sub> laser ( $\lambda$  = 337 nm), using  $\alpha$ -cyano-4-hydroxy-cinnamic acid (prepared by dissolving 10 mg in 1 ml of aqueous 50% (v/v) ACN/0.1% (v/v) TFA). The instrument operated with an accelerating voltage of 20 kV. External mass calibration was performed with the signal of matrix dimer at  $m/z$  379.05 and with the mono-isotopic masses of peptide standards including angiotensin I ( $m/z$  = 1296.68) and ovine  $\alpha$ <sub>s</sub>1-casein 1-23 peptide ( $m/z$  = 2754.55). The mass spectra were acquired in the reflector mode using Delay Extraction (DE) technology. Raw data were elaborated using the Data Explorer 4.1 software provided by the manufacturer.

Attempts of identifying proteins by peptide mass fingerprinting were carried out searching by the Mascot (Matrix Science, London, UK) and Protein Prospector MS-FIT (<http://prospector.ucsf.edu/>) search engines the non redundant National Center for Biotechnology Information (nrNCBI) and Swiss-Prot/TrEMBL databases. In all searches, a mass tolerance of 0.3 Da and carbamidomethylation of cysteines as fixed modification were set, whereas one missed tryptic cleavage was accepted. No restrictions for taxonomic protein origin were introduced. nESI-Q-TOF-MS and nESI-Q-TOF-MS/MS analysis of peptide mixtures were performed using a hybrid quadruple-orthogonal acceleration time of flight QStar Pulsar (Perkin-Elmer SCIEX, Toronto, ON, Canada) equipped with a nanospray source (Proxeon, Odense, Denmark) operating in the positive ion mode. Sample solutions (2  $\mu$ l) were introduced through

borosilicate capillary needles (Proxeon). The needle and orifice voltages were 800 V and 40 V, respectively. Air at a pressure of 10 psi was used as curtain gas. Selected peptide ions were fragmented in nESI-MS/MS experiments using N<sub>2</sub> as the collision gas; the Q0 and Q2 quadrupole voltages were 58.0 and 9.9 V, respectively. Data were processed using Analyst-QS V1.0 software furnished with the spectrometer.

MS/MS spectra were reconstructed either manually or with the aid of the software. The aminoacid sequences were used to search the NCBI and Swiss-Prot protein and translated genomic databases using BLAST and Protein Prospector MS-pattern.

### **VI. 3. Results**

#### *VI. 3. 1. First purification of galactolipid-hydrolyzing enzyme*

The combined supernatants S3 and S4 (53 ml) obtained after differential centrifugation (see Scheme VI.1) were concentrated on Centricon 10000 by repeated cycles of centrifugation at 3000 g for 1 h (10° C). Desalination was done by dialysis against 3 L of 20 mM Tris-HCl buffer (pH 8.0) for 18 h at 4° C using membrane tube with a cut-off of 12 kDa.

High performance ion exchange chromatography (MonoQ HR 5/5) was used to purify the dialysate (13 ml) of about 50 mg of proteins by using a mobile phase composed by 20 mM Tris-HCl buffer at pH 8.0 (buffer A) and 0.75 M NaCl in 20 mM Tris-HCl buffer at pH 8.0 (buffer B). Elution was detected at 280 nm UV. Column was washed with 5 ml deionised water and then equilibrated with buffer A for at least 10 column volumes with a flow rate of 1 ml/min. The sample was applied via a 10 ml SuperLoop injection device with a flow rate of 0.5 ml/min. After washing off protein not bound to the column with 5 column volumes of buffer A (5 ml) elution of proteins was achieved by a gradient of buffer A and B as given in the Table VI.3. 5 ml fractions were collected by a fraction collector.

**Table VI.3.** FPLC gradient. Flow rate: 1 ml/min.

Volume (ml)	Buffer A (%)	Buffer B (%)	Fraction size (ml)
0	100	0	5
25	100	0	5
30	60	40	5
60	0	100	5
75	0	100	5

The chromatographic profile obtained from this purification of 102000 g supernatants is reported in Figure VI.1. Fractions 5-10 were concentrated on centrifugal filter devices and the proteins recovered from the membranes were checked for the hydrolytic activity on GC-MS by using MGDG from *P. oceanica* as substrate (see experimental sections § VI. 2. 6 and § VI. 2. 7).

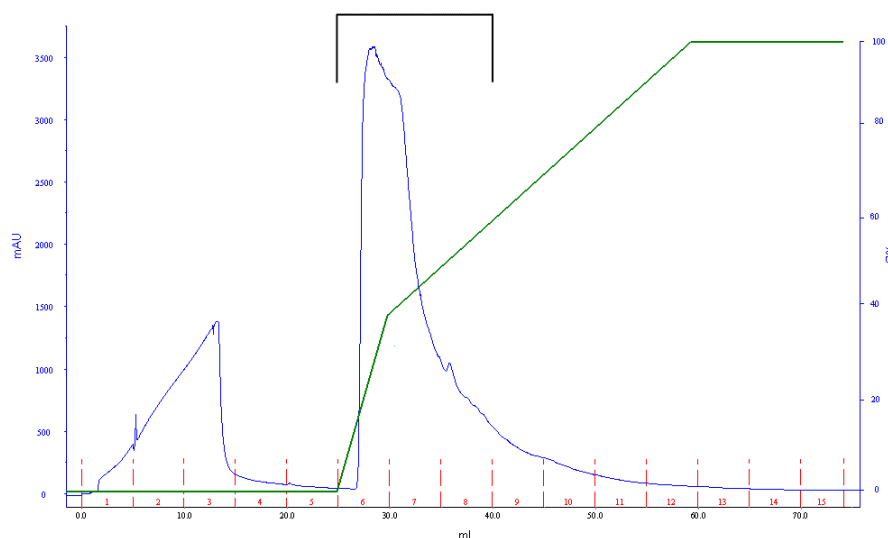


**Figure VI.1.** Chromatogram obtained for the purification of dialysate over an anion exchange column (detection at 280 nm, blue line). The mobile phase gradient of buffer A (20 mM Tris-HCl buffer pH 8.0) and B (buffer A plus 0.75 M NaCl) is represented by the green line. Active fractions (6-8) are marked by the black line.

Figure VI.2 summarises the activity profile of the assayed fractions (5-10). Proteins eluted from the column at approximately 300 mM NaCl (fraction #6) showed the highest activity, while the specific activity was totally absent when the NaCl concentration reached 500 mM. Since the green-brown diatom pigments eluted together with the central fractions (6-10), the purification via MonoQ HR 5/5 column

was just considered as a first purification step and was followed by a second chromatographic step under native conditions.

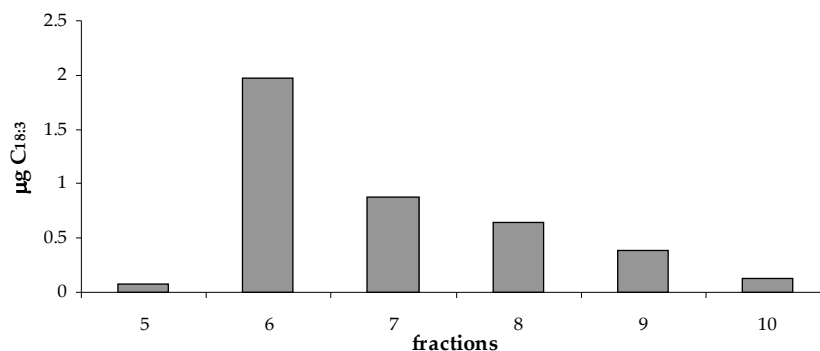


**Figure VI.2.** Hydrolyzing activity of the fractions (5-10) obtained from anion exchange chromatography.

Gel filtration was carried out on the active fractions (fraction #6, 4.63 mg) by a Superdex 200 10/300 GL column. The column was cleaned with at least 48 ml deionised water at a flow rate of 0.5 ml/min prior to usage and then equilibrated with 48 ml of 150 mM NaCl in 20 mM Tris-HCl buffer at pH 8.0. Fractions of 0.5 ml volume were collected by a fraction collector. Gel filtration showed a good resolution of the enzymatic separation. Fractions 16-23 obtained from the gel filtration were concentrated on centrifugal filter devices and tested in the activity assay as reported above. Only three fractions collected between 17 and 19 minutes (Figure VI.3) showed an hydrolyzing activity by GC-MS analysis.

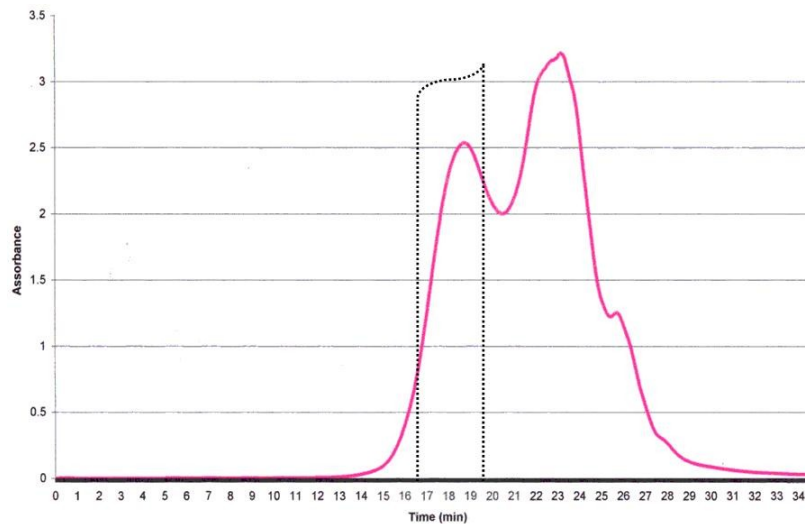


**Figure VI.3.** Gel filtration chromatogram obtained from purification of fraction #6 from the ion exchange chromatography. Flow rate 0.5 ml/min and detection at 280 nm. Fractions collected between 17-19 minutes showed hydrolyzing activity (indicated in black).

The specific activity was significantly higher (see Figure VI.4) but the protein amount was rather low (about 250  $\mu\text{g}$ ).

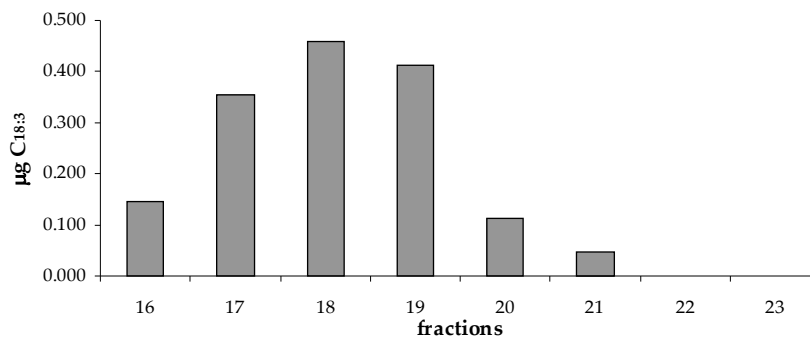


**Figure VI.4.** Hydrolyzing activity of the fractions 16-23 obtained from Superdex 200 10/300 GL.

Thus, fractions (17-19) were combined and run on 10% SDS-PAGE to monitor the band pattern of the active fractions. The SDS-PAGE was performed as described in the experimental section § VI. 2. 8. The gel showed one prominent band which represented a protein of approximately 39 kDa (Figure VI.5).

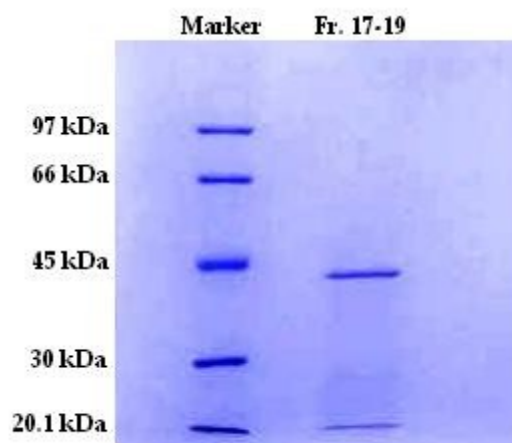


**Figure VI.5.** 10% SDS-PAGE of 10  $\mu$ g of protein of the combined fractions 17-19 obtained by gel filtration.

Attempts in identifying the 39 kDa protein by peptide mass fingerprinting were unsuccessful, although the quality of the MALDI-ToF spectra of the tryptic digest was excellent (data spectra are reported in the Appendix see Figure A.17). In order to search database for homologous proteins, the nESI-MS/MS fragmentation of selected peptide ions was carried out, as described in the experimental section § VI. 2. 10.

Peptide sequences (Table VI.4) were inferred from the MS/MS spectra. Homologous sequences were found both in eukaryotic species (*Arabidopsis thaliana* and *Hypericum perforatum*) and in prokaryotic species (*Pseudomonas fluorescens*). Some peptide sequences showed a perfect alignment with the N-terminal region of germin-like binding protein (GPL-binding, PAN Q84V99) of *A. thaliana*. Due to the presence of only a fragment of 55 aminoacids in the database, it was not possible to confirm extensive homology with the remaining part of the protein. Significant homologies were also found with protein entries in turn homologue to the GLP-binding protein, for example the P27SJ protein from *H. perforatum* (PAN Q5G1J7) and the DING periplasmic phosphate-binding protein of *P. fluorescens* (PAN Q4KD17).

**Table VI.4.** Peptide sequences obtained after trypsin digestion and subsequent mass analysis.

Mass peptide	Peptide sequence of galactolipid-hydrolyze	GPL sequence in <i>A. Thaliana</i>	P27SJ sequence in <i>H. perforatum</i>	DING protein in <i>P. fluorescens</i>
1412.7	LTATELSTYATNK	LTATELSTYATNK	LSATELSTYASAK	
1005.6	TGP[I/L]TVVYR		TGAIITVVYR	TGAIITVVYR
1110.5	NVHWAGSDSK	NVHWAGSDSK	NVHWAGSDSK	NVHWAGSDSK
1143.6	AAFLTNDYTK	AAFLTNDYTK	AAFLNNDYTK	AAFLNNDYTK
1219.6	ITDWSAVSQGR		ITDWSGISGGR	
1314.6	SESSGTTELFTR		SESSGTTELFTR	NESSGTTELFTR
1773.8	HFGDTNNNNDA[I/L]TSVR			
	HFGDTN[I/L]DNDA[I/L]TSVR			

### VI. 3. 2. *Second purification of galactolipid-hydrolyzing enzyme*

The combined supernatants S3 and S4 (58 ml) obtained after differential centrifugation (see Scheme VI.1) were concentrated on Vivaspin 15R by repeated cycles of centrifugation at 3000 g for 1 h (5° C). Desalination was done by against 2.5 L of 20 mM Tris-HCl buffer (pH 9.0) for 18 h at 4° C using the same membrane dialysis tube (cut-off 12 kDa) as reported above.

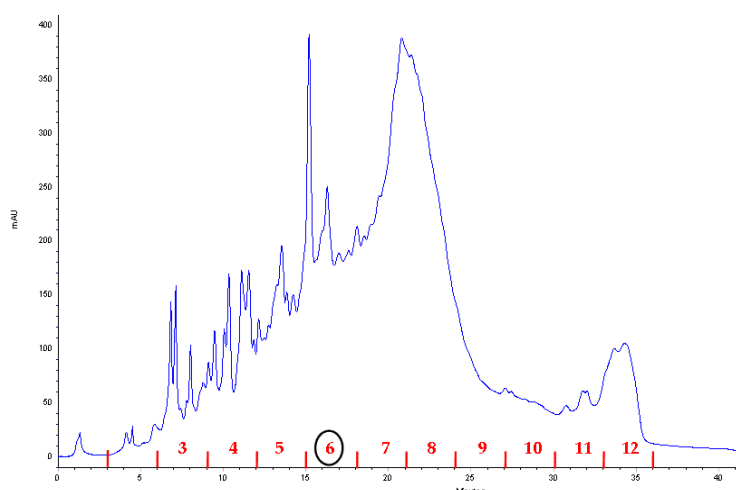
As above, high performance anion exchange chromatography was carried out for the first purification step of the dialysate (6.6 ml), which contained about 55 mg of proteins. Elution was achieved by using of 20 mM Tris-HCl buffer pH 9.0 (buffer A) and buffer A together with 1 M NaCl (buffer B) as the mobile phase. The purification was carried on Thermo HPLC system coupled with UV-detector at 280 nm. After washing with 5 column volumes deionised water (5 ml), the MonoQ™ 5/50 GL column was equilibrated with buffer A for at least 5 column volumes with a flow rate of 1 ml/min. A total of twenty chromatographic runs each with 250 µl of the dialysate was performed. Unlike the first purification a linear gradient was chosen for this separation (see Table VI.5). The good reproducibility of the run spectra allowed the combinations of fractions obtained from different runs. The fractions of 2.4 ml volumes were collected by a fraction collector every 3 min. After cleaning the column with 5 column volumes buffer B (5 ml), the column was re-equilibrated with 5 column volumes buffer A for a subsequent injection.

**Table VI.5.** HPLC gradient. Flow rate: 0.8 ml/min.

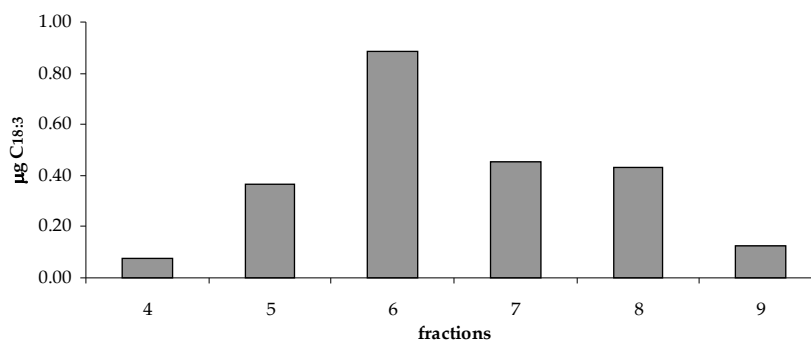
<i>Time (min)</i>	<i>Buffer A (%)</i>	<i>Buffer B (%)</i>	<i>Fraction size (ml)</i>
0	100	0	2.4
5	100	0	2.4
45	0	100	2.4
50	0	100	2.4

Figure VI.6 shows the chromatogram obtained for this anion exchange chromatography. Fractions 3-12 were concentrated on centrifugal filter devices and the proteins recovered from the membrane were checked for the activity.

Figure VI.7 summarises the activity of the assayed fractions (4-9) which was obtained as described in the section § VI. 2. 6 and § VI. 2. 7.



**Figure VI.6.** Chromatogram obtained from the purification of dialysate over an anion exchange column (detection at 280 nm). The active fraction (#6) is reported in the black circle.



**Figure VI.7.** Hydrolyzing activity of the fractions (4-9) obtained from anion exchange chromatography.

Like in the first purification, size exclusion chromatography was performed as next purification step. The active fraction #6 obtained from the ion exchange chromatography (2.45 mg) was loaded to a Superdex 200 10/300 GL column utilizing the same HPLC system and UV-detector at 280 nm. The column was equilibrated with 48 ml of 150 mM NaCl in 20 mM Tris-HCl buffer (pH 9.0), at a flow rate of 0.5 ml/min prior to purification. The void volume was collected in a Falcon tube, while subsequently 0.5 ml fractions (one fraction/min) were collected by a fraction collector. The obtained chromatogram was quite clear, even if it is quite different than the one recorded before (Figure VI.8). Fractions, which represented the same peak, were combined together and then concentrated.

Activity of the fractions C-G was assayed as described above and the fraction F showed the highest activity (Figure VI.9).

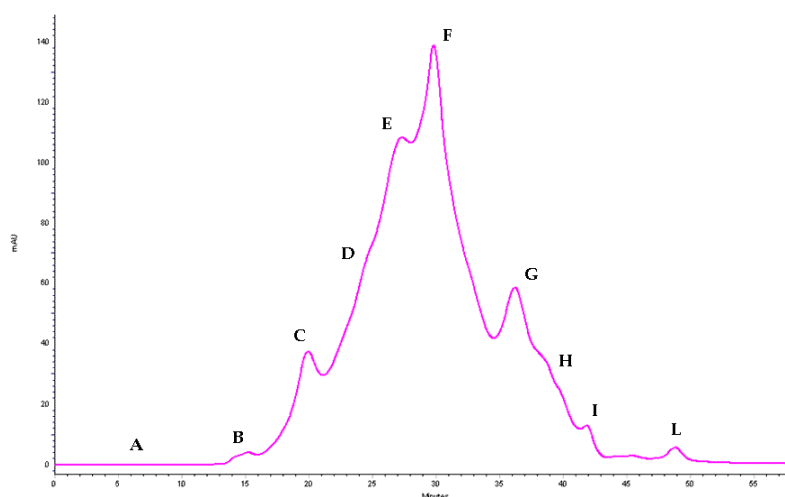


**Figure VI.8.** Gel filtration chromatogram obtained for the purification of fraction #6 from anion exchange chromatography. Flow rate 0.5 ml/min and detection at 280 nm. The peak F was the active fraction.

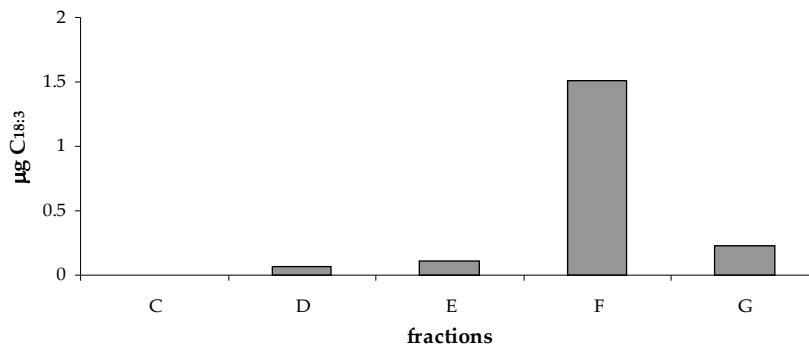


**Figure VI.9.** Hydrolyzing activity of the fractions C-G obtained from Superdex 200 10/300 GL.

In order to compare the hydrolyzing active fractions of the two protein purification showing (fractions #6 and F), they were applied to 10% SDS-PAGE for the screening of their band patterns. Figure VI.10 shows the 10% SDS-PAGE prepared as reported in the experimental section VI. 2. 8.

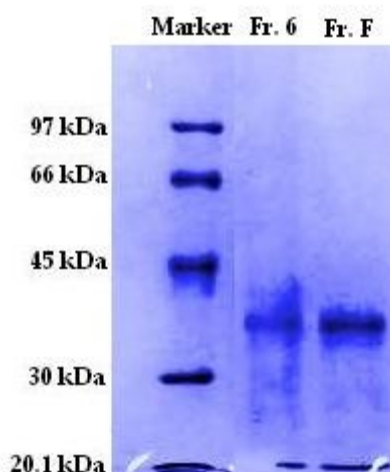


**Figure VI.10.** 10% SDS-PAGE of the active fraction obtained from anion exchange chromatography (Fr. 6) and gel filtration (Fr. F). 10 µg protein was applied onto the gel.

In contrast to the first purification, the amount of most hydrolyzing active fraction (F) allowed a further purification. Therefore another anion exchange chromatography was performed with this fraction. About 450 µg of the protein sample were loaded to a MonoQ™ 5/50 GL column using 20 mM Tris-HCl buffer pH 9.0 (buffer A) and buffer A together with 1 M NaCl (buffer B) as the mobile phase and HPLC system as described above. The selected gradient is given in the Table VI.6.

**Table VI.6.** HPLC gradient. Flow rate: 0.8 ml/min.

<i>Time (min)</i>	<i>Buffer A (%)</i>	<i>Buffer B (%)</i>
0	80	20
5	80	20
35	50	50
45	0	100
50	0	100

The resulting chromatographic run of the apparently single band of the SDS-PAGE (see Figure VI.10, lane Fr. F) showed two main peaks (Figure VI.11). Each peak was collected in two parts (rise and fall of the 280 nm adsorbance). The four different fractions were concentrated on centrifugal filter devices. Protein content was extremely low in the fractions #3 and #4, instead no proteins were detected in the fractions #1 and #2. Nevertheless, the specific activity was evident when the samples were incubated as described above. Figure VI.12 shows the activity in the fractions (1-4).

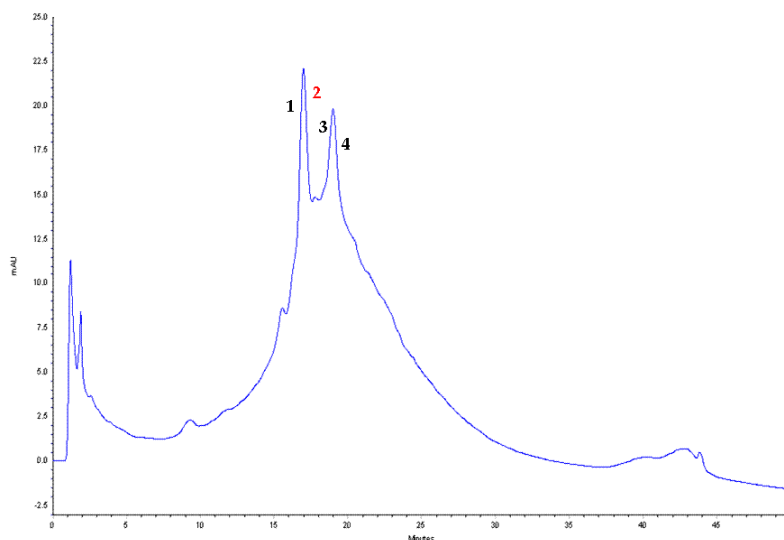


**Figure VI.11.** Chromatogram obtained from the purification of fraction F. Fraction #2 (red number) contained the activity.

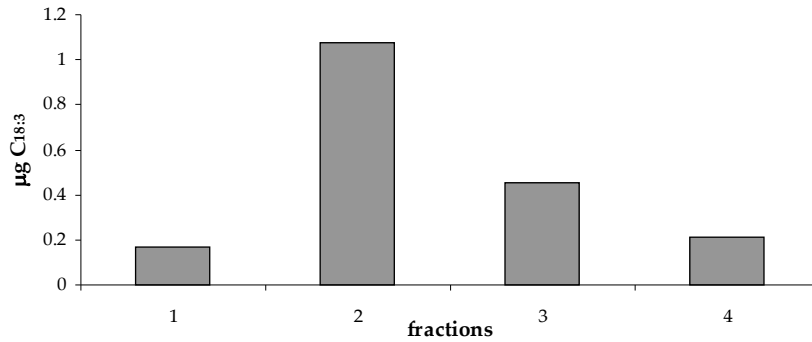


**Figure VI.12.** Hydrolyzing activity of the fractions (1-4) obtained from the second anion exchange chromatography.

Since there was evidence of proteins in the fractions #1 and #2, they were not applied to the SDS-PAGE gel. Fractions #3 and #4 showed a band, which represented a protein of approximately 35 kDa (Figure VI.13) suggesting there were more proteins which might co-migrate on the gel.

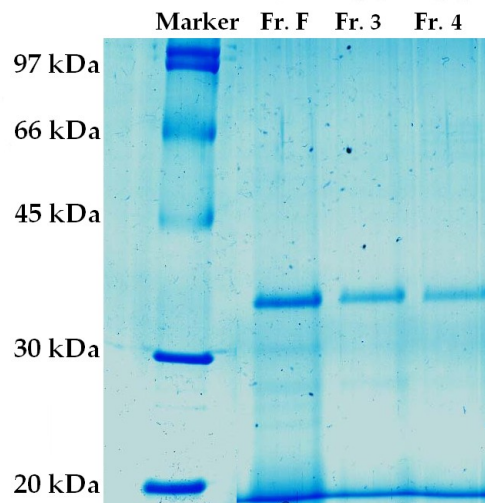


**Figure VI.13.** 10% SDS-PAGE of the fractions obtained from the second ion exchange chromatography (Fr. 3 and 4) and gel filtration (Fr. F).

The MALDI-ToF analysis of the not-hydrolyzed protein also provided a signal at molecular mass of 35.1 kDa (data spectrum is reported in the Appendix see Figure A.18). The peptide mass fingerprinting in this case allowed to identify the protein, with significant sequence coverage, as the ferredoxin-NADP-reductase from *Chlamydomonas reinhardtii* (PAN P53991), with a real MW of 35.3 kDa and highly homologue to the ferredoxin-NADP-reductase from *Thalassiosira pseudonana* (PAN B8C0N7, real MW 36.1

kDa). The identification was confirmed by nESI-MS/MS sequencing of selected peptide sequences. Table VI.7 shows the peptide sequences deduced by nESI-MS/MS and their homology sequencing.

**Table VI.7.** Peptide sequences obtained after trypsin digestion and subsequent mass analysis.

Mass peptide	Peptide sequence	Ferredoxin-NADP-reductase in <i>T. pseudonana</i>	Ferredoxin-NADP-reductase in <i>C. reinhardtii</i>
837.5	LDYALSR	LDYALSR	LDYALSR
896.5	LYSIASSR	LYSIASSR	LYSIASSR
1478.7	LDYALSREQNNR	-	LDYALSREQNNR
960.5	QWHVEVY*	QWHVEVY	QWHVEVY
1662.7	YGDDFTGNTGSLCVR	YGDDFTGNTGSLCVR	YGDD <b>GDGQT</b> ASLCVR
809.4	FPENFR	FP <b>D</b> NFR	-
1036.7	VKFPENFR	SKFP <b>D</b> NFR	-

\* Peptide sequence of (C-terminal)

### VI. 3. 3. Third purification of galactolipid-hydrolyzing enzyme

Supernatants S3 and S4 (140 ml) from the differential centrifugation (see Scheme VI.1) were concentrated on Centricon 10000 as described above. Desalination was done by dialysis against 3 L of 20 mM Tris-HCl buffer (pH 9.0) for 18 h at 4° C using membrane tube with a cut-off of 12 kDa as reported for the second preparation.

The dialysate (32 ml), which contained about 120 mg of proteins, was purified by only two different ion exchange chromatography steps. Elution was performed by using 20 mM Tris-HCl buffer pH 9.0 (buffer A) and 1 M NaCl in 20 mM Tris-HCl buffer pH 9.0 (buffer B) as the mobile phase. The sample elution was monitored by UV-detector at 280 nm on the ÄKTA-FPLC system. After washing with 5 column volumes deionised water (5 ml) the MonoQ<sup>TM</sup> 5/50 GL column was equilibrated with buffer A with 5 column volumes. The sample was applied with a flow rate of 0.3 ml/min. After the wash out of the unbound proteins (5 column volumes) the elution of proteins was achieved with a linear gradient of buffer A and B as given in the Table VI.8. Fractions of 2 ml were collected by a fraction collector. After cleaning the column with 15 column volumes buffer B (15 ml), the column was re-equilibrated with 5 column volumes buffer A for subsequent injection (3 injections of 10 ml each were performed).

**Table VI.8.** FPLC gradient. Flow rate: 0.3 ml/min.

Volume (ml)	Buffer A (%)	Buffer B (%)	Fraction size (ml)
0	100	0	2
15	100	0	2
55	0	100	2
70	0	100	2

Figure VI.14 shows the chromatogram obtained from this first ion exchange chromatography. Fractions 5-18 were concentrated on Amicon ultra 10k and after recovering the sample from the membrane, the activity of each fraction was assayed. Figure VI.15 summarises the activity assay of the these fractions.

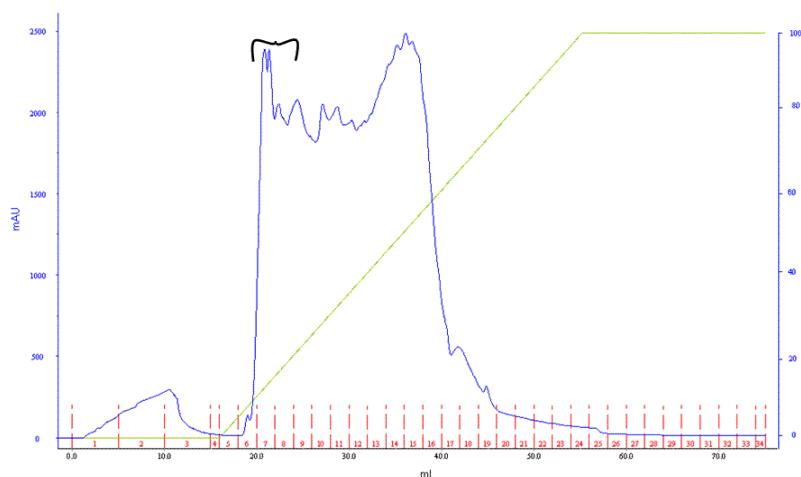


**Figure VI.14.** Chromatogram of dialysate purified over an anion exchange column (detection at 280 nm, blue line). The mobile phase gradient of buffer A (20 mM Tris-HCl buffer pH 9.0) and B (buffer A plus 1 M NaCl) is represented by the green line. Active fractions (6-8) are marked by the black line.

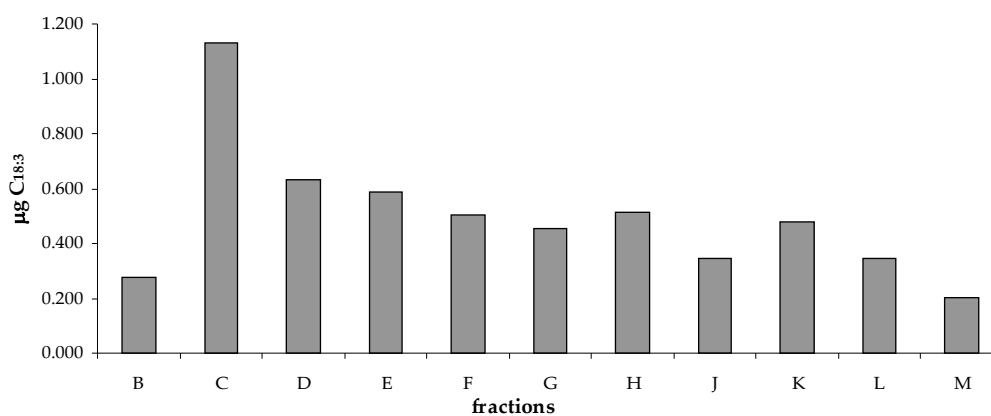


**Figure VI.15.** Hydrolyzing activity of the fractions (6-16 correspond to B-M) obtained from the anion exchange chromatography.

The fraction C was the most active among all fractions, even if the hydrolyzing activity was detected in all fractions tested. In order to monitor the protein composition of each fraction, comparable amounts of proteins from each fraction were used in a 10% SDS-PAGE. The gel was prepared as reported above. Figure VI.16 shows the gel after Commassie staining. The complexity of band patterns hampered the identification of bands that might correlate to the activity of fractions.

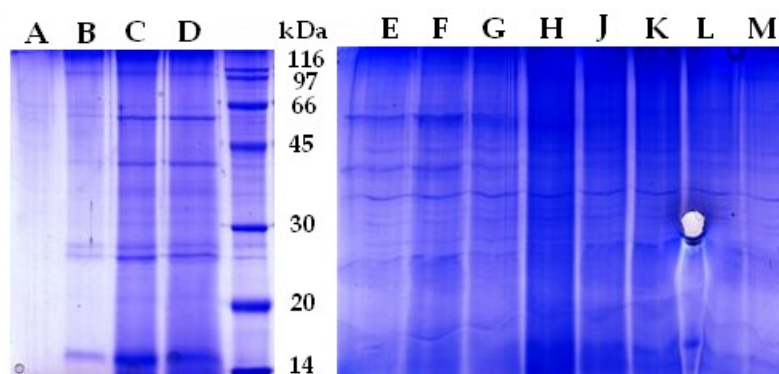


**Figure VI.16.** 10% SDS-PAGE of the fractions obtained from the ion exchange chromatography (5-16 correspond to A-M).

In contrast to the previous two purification, another anion exchange chromatography step was directly used as the second purification step. Fractions C and D were combined together and desalted again by membrane dialysis (cut-off 12 kDa) against 1 L of 20 mM Tris-HCl buffer (pH 9.0) for 12 h at 4° C. The dialysate (5.06 mg in 3 ml) was loaded to the MonoQ 5/50<sup>TM</sup> GL column and elution was achieved by using of 20 mM Tris-HCl buffer pH 9.0 (buffer A) and buffer A containing 0.5 M NaCl (buffer B) as the mobile phase. Before injection the column was equilibrated with 5 column volumes of 20 mM Tris-HCl buffer pH 9.0 (buffer A) with a flow rate at 0.5 ml/min. After the wash-out of the unbound proteins, the elution was carried out through two different gradient steps, as depicted in the Table VI.9. Fractions of 1 ml were collected by a fraction collector.

**Table VI.9.** FPLC gradient. Flow rate: 1 ml/min.

<i>Volume (ml)</i>	<i>Buffer A (%)</i>	<i>Buffer B (%)</i>	<i>Fraction size (ml)</i>
0	100	0	1
8	100	0	1
23	70	30	1
38	0	100	1
48	0	100	1

Figure VI.17 shows the resulting chromatogram of this second step of purification. Fractions 19-34 were concentrated on Amicon ultra 10K and after recovering the sample from the membrane, the activity of each fraction was assayed. Figure VI.18 summarises the activity of the fractions between 22 to 28.

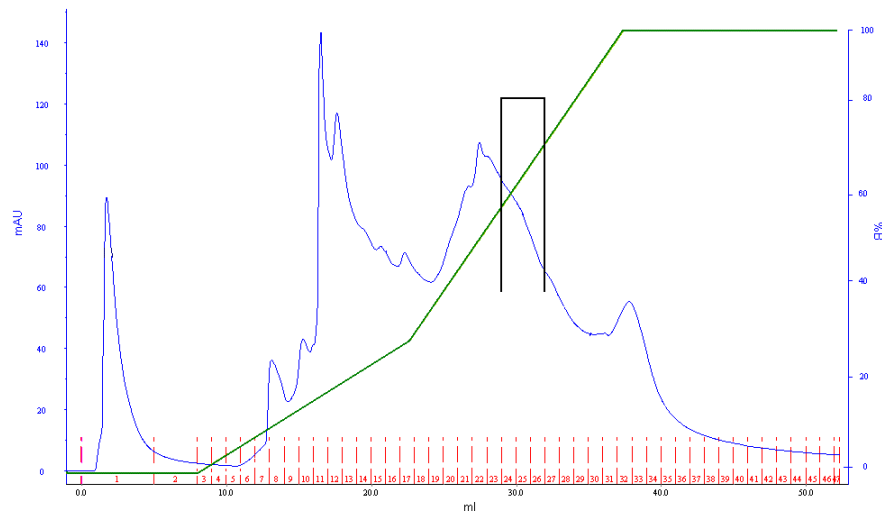


**Figure VI.17.** Chromatogram of the purification of dialysate from the combined fraction C and D over an (detection at 280 nm, blue line). The mobile phase gradient of buffer A (20 mM Tris-HCl buffer pH 9.0) and B (buffer A plus 0.5 M NaCl) is represented by the green line. Active fractions (24-26) are marked by the black line.

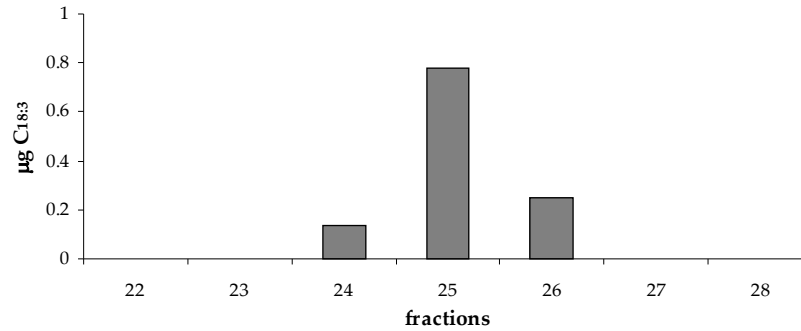


**Figure VI.18.** Hydrolyzing activity of the fractions (22-28) obtained from the second anion exchange chromatography.

The fractions 22 to 28 were run in a 10% SDS-PAGE (Figure VI.19). The band patterns of these fractions showed that a band at approximately of 30-35 kDa was only present in the active fractions (25-26). Thus, these bands were cut out of the gel and treated as described in the experimental section VI. 2. 9 and VI. 2. 10. But the attempts in identifying the protein by peptide mass fingerprinting were unsuccessful, and no significant homology were found by the analysis of the tryptic digest. This result was affected by massive concentration of co-migrating proteins that gave confused mass spectra unsuitable for peptide mass fingerprinting.

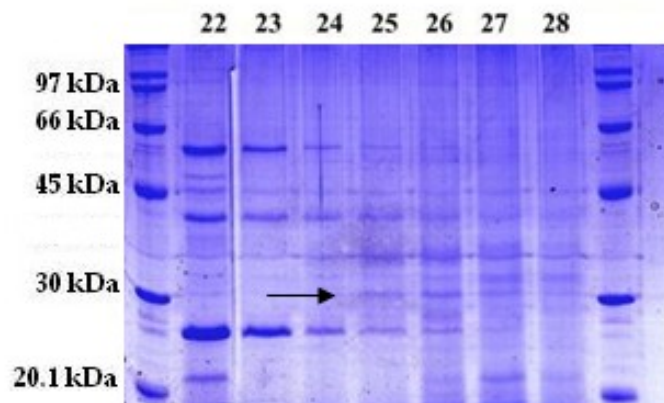


**Figure VI.19.** 10% SDS-PAGE of the fractions obtained from the ion exchange chromatography (22-28). The arrows indicates the bands which were cut from the gel.

#### VI. 3. 4. Solubilisation of galactolipid-hydrolyzing enzyme from cell membranes

Despite the presence of a few differences in the purification protocols, such as pH and NaCl concentration of the mobile phase, gradient systems or columns, the recovery of the galactolipid hydrolyzing activity after just two purification steps was in general drastically reduced, as depicted in Table VI.10. Each activity guided purification lead to the isolation of insufficient amount of the active proteins.

**Table VI.10.** Summary of protein contents which were recovered in different phases of purification.

<i>Biomass</i>	<i>Dialysate</i>	<i>First step</i>	<i>Second step</i>	<i>Final content</i>
12.1 g	48 mg	4.63 mg	-	0.25 mg
14.5 g	55 mg	2.45 mg	0.45 mg	no detected
40.5 g	120 mg	5.06 mg	-	0.63 mg

Since a large amount of the activity was still detected in the differential centrifuge fraction of the cell debris and cell organelles (P1 and P2), attempts to washing off the protein from the membranes with a non-ionic detergent were carried out.

Detergents are amphiphilic molecules which attach with their hydrophobic ends to the hydrophobic parts of protein molecules. When an adequate number of amphiphilic molecules has attached to the protein, the membrane proteins detach from the membrane and are solubilised. When solubilising a membrane protein, there are two important things that must be avoided, (1) that the protein aggregates (and is not solubilised), and (2) that the protein is denatured. Since every protein requires different conditions for its solubilisation while maintaining its native form (e.g. in terms of the detergent used, the detergent concentration, pH, buffer), preliminary tests were performed with different concentration of Triton X-100. The functionality of the protein after treatment with the detergent was controlled by the hydrolytic assay (see Figure VI.20). Pellet P2 (see Scheme VI.1) was treated with 0.1% (v/v) Triton in 20 mM Tris-HCl buffer pH 8.4 for 30 min at room temperature and then centrifuged at 9600 g for 30 min at 5° C. The resulting supernatant (S3) showed a hydrolyzing activity as strong as supernatant S1.

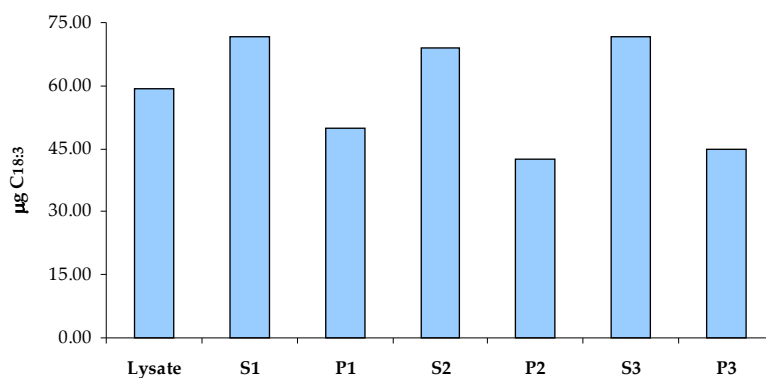


**Figure VI.20.** Relative amount of the C<sub>18:3</sub> detected in pellet (P3) and supernatant (S3) derived after incubation of the membrane fraction P2 with 0.1% (v/v) Triton solution in 20 mM Tris-HCl buffer pH 8.4 and subsequent centrifugation at 9600 g.

The last pellet P3 was diluted with 7 ml 20 mM Tris-HCl buffer pH 8.4 and divided into subsamples of 1 ml volume. The subsamples were incubated with different Triton concentrations ranging from 0% to 6% (v/v) in 20 mM Tris-HCl buffer pH 8.4 for 18 h at 4° under stirring. After the detergent incubation all subsamples were centrifuged as described above and the hydrolyzing activity was assayed. As reported in Figure VI.21 the hydrolyzing activity of the protein was maintained even at high Triton concentration (6%). Supernatant activity was always higher than the respective pellet activity. Major difference between the activity of pellet and supernatant and highest overall supernatant activity were obtained by using a 0.1% Triton solution, which therefore represents the best concentration for solubilisation of the hydrolyzing active protein from the membranes.

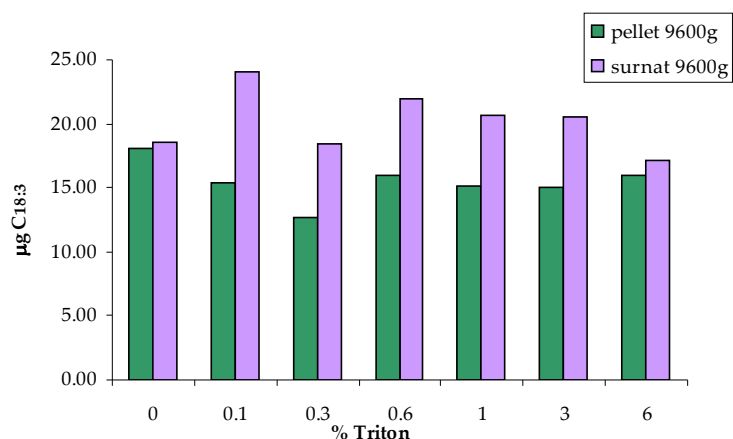


**Figure VI.21.** Relative amount of the C<sub>18:3</sub> detected in the supernatants and pellets derived after incubation of the membrane fraction P3 with different detergent concentrations ranging from 0% to 6% and subsequent centrifugation at 9600 g.

### VI. 3. 5. Substrate specificity of galactolipid-hydrolyzing enzyme

To determine the ability of the resulting enzymatic preparations to metabolize the different classes of complex lipids, active fractions, which were incubated with MGDG, was also incubated with the other class of complex lipids isolated from *P. oceanica* (DGDG and SQDG) and the commercial L- $\alpha$ -phosphatidyl-d,l-glyceroldioleoyl and L- $\alpha$ -phosphatidyl-d,l-glyceroldioleoyl/tristearine as phospholipids (PL) and tryglycerides (TG), respectively. On the contrary of *Chattonella marina* (Terasaki & Itabashi, 2002) and *Gracilaria Vermiculophylla* (Ilijas et al., 2008) in which hydrolyzing activity was observed both on MGDG and PL the hydrolyzing activity, which was reported, exhibited a specific activity only on the monogalactosyldiacylglycerols (MGDG) and digalactosyldiacylglycerols (DGDG) (Figure VI.22).

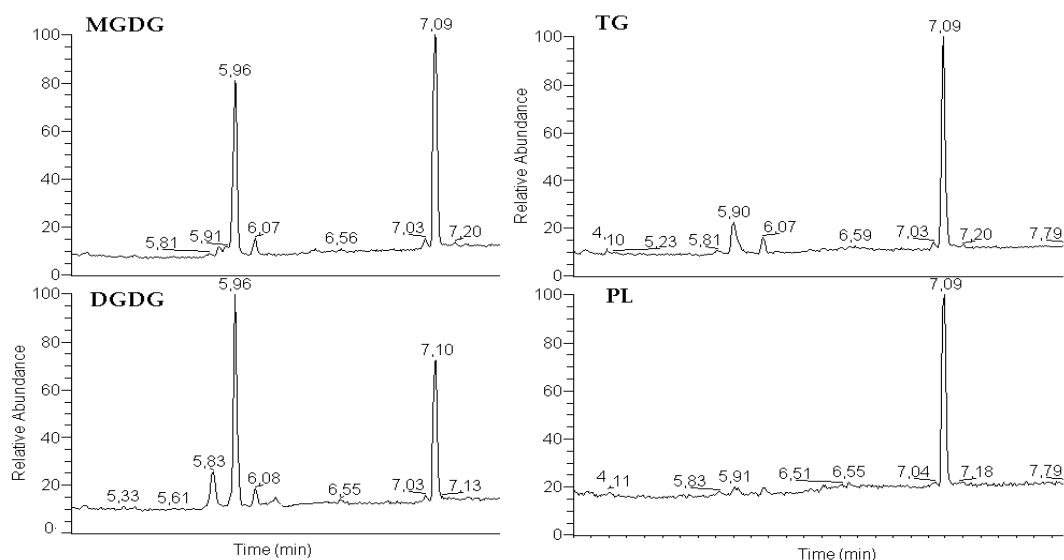


**Figure VI.22.** GC profile of  $C_{18:3}$  from *P. oceanica* after incubation of monogalactosyldiacylglycerols (MGDG), digalactosyldiacylglycerols (DGDG), tryglycerides (TG) and phospholipids (PL).

#### VI. 4. Discussion

The work presented in this chapter represents the preliminary study for the purification of a galactolipid-hydrolyzing enzyme from the marine diatom *Thalassiosira rotula*. Mobilisation of galactolipids by a lipase enzyme has been shown to be the initial step for downstream oxylipin synthesis upon cell wounding. A previous work on the same diatom (Cutignano et al., 2006) identified a protein band of about 42 kDa with hydrolytic activity. However, this activity was obtained by using an unspecific substrate (MUF-butyrate) to monitor the lipase activity. This did not exclude that other lipids, such as galacto- and phospo-lipids, were hydrolyzed alike. The isolation plan chosen during this research was supported on a home-made assay based on the hydrolysis of natural glycolipids isolated from *P. oceanica* by protein extracts and fractions from *T. rotula*. The three purification procedures described above started with an ion exchange chromatography, but the operative conditions, such as pH and ionic strength, were modified in order to optimize the protein separation. Concentration of NaCl around 300-400 mM gave the best results with a highly active peak eluted in a rather short time window. Comparison of the different purification schemes, also reveals that good and reproducible separation of the hydrolytic activity was obtained with amount of injected protein that did not exceed 2 mg (see Figure VI.6). Interestingly, the results of the elution by gel filtration (Figure VI.3) showed an activity

pattern with the hydrolytic properties restricted to very few chromatographic fractions. This seems to be noteworthy for future developments, although it has to be noted that the protein mixture remained complex. On SDS-PAGE, the number of bands in the range of 35-42 kDa clearly indicates that the putative galactolipase co-migrates with other proteins (see for example: Figure VI.10). Therefore, it was not surprising that peptide mass fingerprinting showed erratic results with homologous sequences corresponding, for example, to ferredoxin-NADP-reductase or GLP-binding protein. Although this part of the research work did not lead to conclusive results with the isolation of a single protein responsible for the galactolipid-hydrolyzing activity, the studies allow making conclusions for future purification steps. In particular, the identification of the hydrolyzing activity is in the cell pellets (P3 and P4) after differential centrifugation (see scheme VI.1) suggests that the enzyme is bound to the membranes and has to be solubilized. Attempts with Triton X-100 showed that the hydrolyzing activity remains stable over a large range of detergent concentrations. Comparison between the amount of protein and activity suggests that the best concentration of the detergent is approximately 0.1% (v/v). Extraction with Tween-20 did not result in activity (data not shown), highlighting the importance of using different extraction protocols with various detergents for future purifications.

## Chapter VII

### Conclusions

Diatoms account for almost 40% of primary productivity due to plankton communities, thus sustaining the entire life food chain in the oceans, seas and lakes of the world. Their photosynthetic rates in natural assemblages are always higher than those of other algae. It is also well known that diatoms have the capability to outcompete other algae. Since '70s, (Venrick et al., 1977) a relevant number of studies have shown that diatoms have an intrinsic ability to withstand stress factors as compared with other algae.

Except perhaps during algal blooms, the number of different species of phytoplankton found in natural waters is high with usually some tens of species coexisting. This condition was termed by Hutchinson in 1961 "*the paradox of the plankton*". Nevertheless, diatoms, together with dinoflagellates and coccolithophores, each with plastids derived from red algae by secondary endosymbiosis, have come to dominate the oceans' flora over the past 250 million years. The reasons of this ecological success have been discussed for years, but have remained rather obscure. Obviously, there have been many studies about the forces responsible for this domination. Diatoms are better able to utilize low levels of nitrogenous nutrients and can take advantage from a mixed photosynthetic metabolism that uses both phosphoenolpyruvate carboxylase of the C-4 pathway and ribulosediphosphate carboxylase via the Calvin C-3 pathway. In the last years, a number of researches have also underlined the ability of these microalgae to interact actively with the other components of the plankton communities. These reports have been questioning the basic assumption about the beneficial role of diatoms in plankton communities. These microalgae are not regarded just as "food" for the marine grazers, but, as summarized in the diatom-copepod paradox (Ban et al., 1997), worldwide studies have taken into account the negative effects that many diatom species have against natural zooplankton grazers, the copepods. The pioneering work of Miralto et al. (1999) revealed for the first time that chemicals, namely the polyunsaturated aldehydes, are involved in these interactions. This

research thesis is in this mainstream and has been devoted to study the biochemical basis of chemically-mediated relations of marine diatoms.

Most of the species studied show the capability to produce oxylipins through enzymatic oxidation of polyunsaturated fatty acids stored in complex lipids of cell and chloroplastic membranes. To address the analysis of these molecules part of the research work has aimed to establish a novel protocol for the characterization and quantification of these elusive and unstable compounds, collectively named phyco-oxylipins, that include three major chemical classes: hydroxy fatty acids, epoxy alcohols and oxo- or keto- fatty acids. The methodology is based on a combination of LC-DAD-ESI-MS/MS and GC-MS/MS techniques and has been designed for the study of oxylipins in marine samples. In particular, it allows high throughput profiling of newly isolated strains and complex mixtures of marine phytoplankton collections. Particularly significant is the application of MS/MS analysis to the epoxy alcohols. These molecules that are encountered in almost all samples give a predictable fragmentation pattern (Figures II.4, II.5, V.5, V.6, V.7) that is very useful to assign the position of the hydroxy and epoxy groups, thus determining the original attack of the lipoxygenase (Cutignano et al., 2009). This makes the LC-MS/MS analysis by itself capable to indicate the lipoxygenase pathways present in unknown species. On these basis, the technique has been used in this thesis for i) rapid screening of biological samples to identify both genetic alteration and enzymatic regulation ii) sensitive quantification to understand eco-physiological studies resulting in difference of the oxylipin signature iii) simple evaluation to follow the taxonomy of cryptic and pseudo-cryptic species.

A very clear example of this analytic technique is represented by the study on the chemical fingerprinting of different species from the genera *Pseudo-nitzschia*, *Chaetoceros*, *Thalassiosira* and *Skeletonema*. The oxylipin profiles of these diatoms, even of those belonging to cryptic species, are highly species-specific and, accordingly, suggest that the lipoxygenase products can be used as chemical markers for taxonomy, phylogeny and characterization of diatoms in phytoplankton. In particular, this part of the research work has underlined that oxylipin profiling may serve as analytical tool at a level of complexity higher than was previously realized and may provide the key for

interpreting apparently meaningless patterns in the distribution, biology, and succession of marine phytoplankton species. It is worth noting that as many as nine different lipoxygenase activities have been inferred during this PhD study through the analysis of the end products of these pathways.

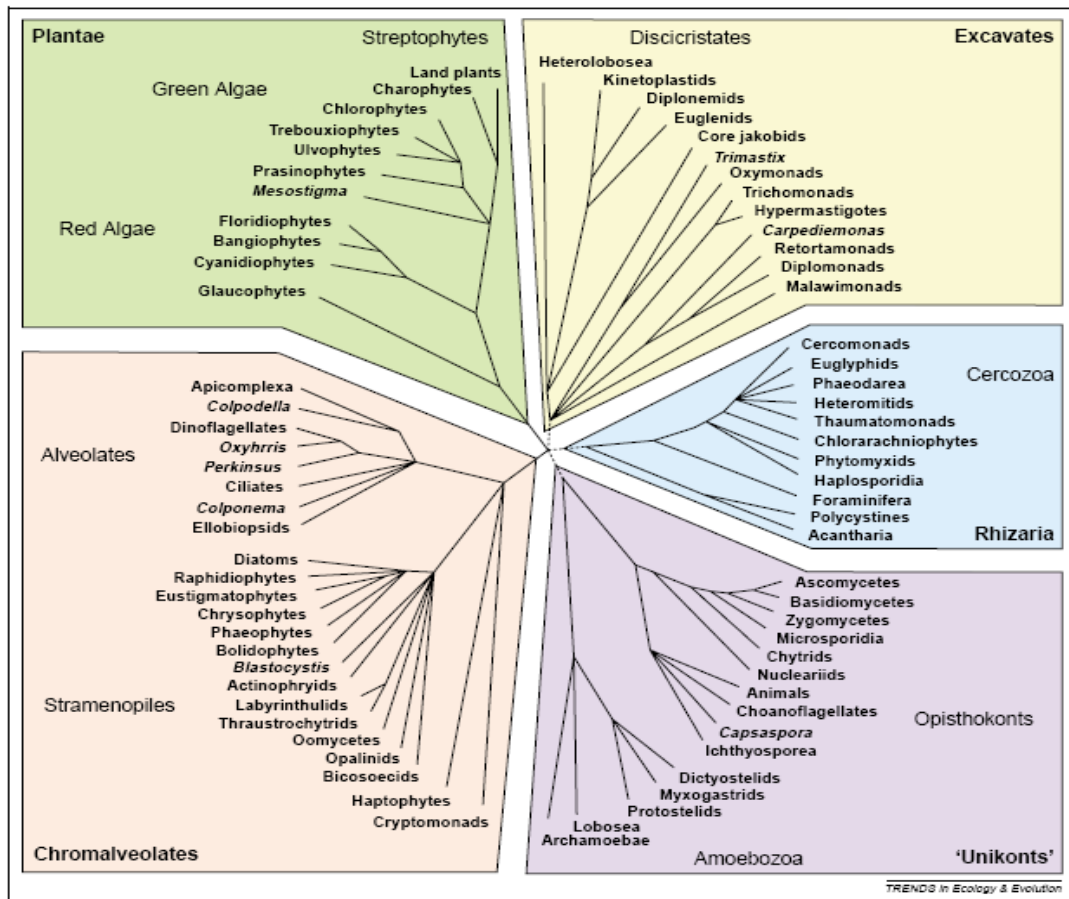


Figure VII.1. Tree of Eukaryotes as described by Keeling et al. (2005).

As suggested by the “Tree of Eukaryotes” reported in Figure VII.1, diatoms belong to the most firmly established protist assemblage that shows phylogenetic characters intermediate between plants and animals. It is therefore not surprising that the chemistry and biochemistry of diatom oxylipins reveal traits that are common to both lineages. In fact, the modular array of molecular signals similar to the oxylipins described in this thesis has physiological or ecological importance in mammalian and plant systems (Chang et al., 1996; Kühn, 1996; Blée, 1998; Reynaud et al., 1999; Kühn et al., 2002; Nigam et al., 2007). Various compounds, such as the polyunsaturated aldehydes arising from activation of LOX pathways, have already been suggested to

function in defence reactions and in physiological regulation in diatoms (Miralto et al., 1999; Pohnert, 2000; Pohnert & Boland, 2002; Ianora et al., 2004; Vardi et al., 2006; Brownlee, 2008). The studies carried out on the synthesis and effects of oxylipins in *Skeletonema marinoi* and two species of *Chaetoceros*, namely *C. socialis* and *C. affinis*, establish a clear correlation between the enzymatic oxidation of diatom PUFAs and consequent teratogenic effects in copepods. In analogy with higher plants, damage of diatom cells leads to synthesis of LOX products that sustain the negative impact of diatom diets on copepod reproductive capacity through the direct involvement of fatty acid hydroperoxides (FAHs) and other oxylipins in specific steps of defence signalling and through the indirect boost of the oxidative stress with synthesis of lethal radical chemicals (e.g. hROS). Such a dichotomic mechanism is in agreement with the observations on the absence of a correlation between diatom toxicity on copepods and presence of aldehydic compounds (Wichard et al., 2005b; Jones & Flynn, 2005), because the negative impact of the microalgae is probably not due to a single class of molecules, as previously believed, but rather to an overall activity that is dependent, at least during the early steps, on the LOX-mediated oxidation of polyunsaturated fatty acids. This process resembles the one described in plants, but it also shows very specific facets in diatoms. In particular, there are two characteristics that have to be underlined. Many diatoms use both C<sub>16</sub> and C<sub>20</sub> polyunsaturated fatty acids. The latter ones, called EPA, are the only substrate to feed the lipoxygenase pathways in genera like *Chaetoceros* or *Pseudo-nitzschia*. Since C<sub>20</sub> fatty acids are typically metabolized in mammalian tissues, this aspect is a further confirmation of the genetic heterogeneity of this lineage of microalgae. The second very interesting aspect that emerges from this study concerns the role of chloroplastic galactolipids. As visible at the electronic microscope, most of the cytoplasm of a diatom cell is occupied by one or more chloroplasts. Therefore, the lipid component that can derive from these organelles is not little and this finds a direct verification in the percentage of oxylipins derived by hexadeca-6Z,9Z,12Z-trienoic (HTrA) acid and hexadeca-6Z,9Z,12Z,15-tetraenoic acid (HTA) that typically are only bound to galactolipids of the thylakoid membranes. At the moment is not clear if the lipoxygenase-mediated oxidation precedes or follows the release of the fatty acids from the complex lipids. However, the galactolipase activity,

that has been already proven to play a key role in the synthesis of polyunsaturated aldehydes of diatoms (d'Ippolito et al., 2004; Cutignano et al., 2006), is suggested to regulate the entire pathway. It is interesting to note that recently galcatolipids and galactolipase(s) have also been attracting an increasing interest for the synthesis of defensive oxylipins in plants. At the moment no molecular data or biochemical information are available about galactolipase, thus the preliminary attempts carried out during the synthesis represent an important starting point for the purification of this class of enzymes.

The control of the lipoxygenase pathway and the factors which trigger the synthesis of oxylipins under physiological conditions have been the focus of the last part of this PhD research. In addition to the role of galactolipase, another facet on the regulation of the lipoxygenase pathways in diatoms was added by the study on the modulation of the oxylipin pattern during algal growth. The studies based on the pennate diatom *P. delicatissima* proved that the synthesis of these compounds is dependent on the number of cells in a population. Such effect reminds on the cell density dependent change of the metabolism (quorum sensing) observed in culture of growing bacteria and fungi. Furthermore, a remarkable quantitative and qualitative change of specific oxylipins, namely 15-oxoacid, was found immediately before the demise of a simulated bloom (Figures IV.4 and IV.5). Such a regulation of the biosynthetic mechanism may correspond to a signalling system that leads to or somehow mediates bloom growth and termination. In this respect, the oxylipins are suggested to have two possible roles: they may act as intracellular signals in order to synchronize the diatom population in response to an environmental signal of death (for example, the absence of specific nutrients) or as inter-specific mediators and carry the signal of "death" from one cell to another. These two functions, that can also co-exist, represent fascinating questions at the moment.

## Abbreviations

<b>DAD,</b>	diode array detector
<b>EI,</b>	electron impact
<b>ESI,</b>	electrospray ionization
<b>FPLC,</b>	fast protein liquid chromatography
<b>GC-EI MS,</b>	gas chromatography – electron impact mass spectrometry
<b>GC-MS,</b>	gas chromatography - mass spectrometry
<b>HPLC,</b>	high performance liquid chromatography
<b>LC-DAD-MS,</b>	liquid chromatography-diode array detector-mass spectrometry
<b>LC-MS,</b>	liquid chromatography - mass spectrometry
<b>MALDI – ToF,</b>	matrix assisted laser desorption/ionization – time of flight
<b>MS,</b>	mass spectrometry
<b>nESI,</b>	nano-electrospray ionization
<b>NMR,</b>	nuclear magnetic resonance
<b>Q – ToF</b>	quadrupole - time of flight
<b>rDNA,</b>	recombinant DNA
<b>RP-HPLC,</b>	reverse phase high performance liquid chromatography
<b>SDS-PAGE,</b>	sodium dodecyl sulphate polyacrylamide gel electrophoresis
<b>SP-HPLC,</b>	straight phase high performance liquid chromatography
<b>TIC,</b>	total ion current
<b>TLC,</b>	thin layer chromatography
<b>UV,</b>	ultraviolet
<b>ACN,</b>	acetonitrile
<b>APS,</b>	ammonium persulfate
<b>ASP,</b>	amnesic shellfish poisoning
<b>BSA,</b>	bovine serum albumin
<b>CHCl<sub>3</sub>,</b>	chloroform
<b>DGDG,</b>	digalactosyldiacylglycerols
<b>EPA,</b>	eicosa-5Z,8Z,11Z,14Z,17Z-pentaenoic acid

<b>Et<sub>2</sub>O,</b>	diethyl ether
<b>FAHs,</b>	fatty acid hydroperoxides
<b>FSW,</b>	filtered seawater
<b>HEPE,</b>	hydroxy-eicosapentaenoic acid
<b>HEpETE,</b>	α-hydroxy epoxy-eicosapentaenoic acid
<b>HHME,</b>	hydroxy-hexadecenoic acid methyl ester
<b>HPL,</b>	hydroperoxide lyase
<b>HPF,</b>	2-[6-(4'-hydroxy)-phenoxy-3H-xanthen-3-on-9-yl]-benzoic acid
<b>hROS,</b>	highly reactive oxygen species
<b>HTA,</b>	hexadeca-6Z,9Z,12Z,15-tetraenoic acid
<b>HTrA,</b>	hexadeca-6Z,9Z,12Z-trienoic acid
<b>ITS,</b>	internal transcribed spacers
<b>LMW,</b>	low molecular weight
<b>LOX,</b>	lipoxygenase
<b>LSU,</b>	large ribosomal subunit
<b>MeOH,</b>	methanol
<b>MGDG,</b>	monogalactosyldiacylglycerols
<b>PBS,</b>	phosphate buffered saline
<b>PCR,</b>	polymerase chain reaction
<b>PHOXYs,</b>	phyco-oxylipins
<b>PL,</b>	phospholipids
<b>PUAs,</b>	polyunsaturated aldehydes
<b>PUFAs,</b>	polyunsaturated free fatty acids
<b>rbcL,</b>	large subunit of rubisco
<b>SD,</b>	standard deviation
<b>SDS,</b>	sodium dodecyl sulphate
<b>SQDG,</b>	sulphoquinovosyldiacylglycerols
<b>TEMED,</b>	tetramethylethylenediamine
<b>TFA,</b>	trifluoroacetic acid
<b>TG,</b>	triglycerides
<b>THF,</b>	tetrahydrofuran

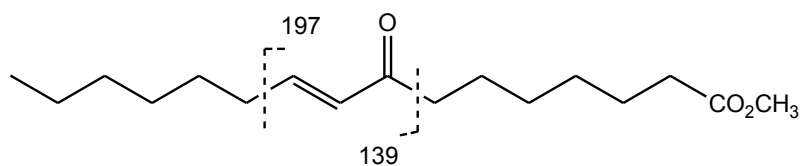
<b>TMP,</b>	trimethylphospite
<b>TUNEL,</b>	terminal-deoxynucleotidyl-transferase-mediated-dUTP nick end labelling
<b>5-HEPE,</b>	5-hydroxy-eicosa-6 <i>E</i> ,8 <i>Z</i> ,11 <i>Z</i> ,14 <i>Z</i> ,17 <i>Z</i> -pentaenoic acid
<b>6-KHTE,</b>	6-ketohexadeca-7 <i>E</i> ,9 <i>Z</i> ,12 <i>Z</i> ,15-tetraenoic acid
<b>6-KHTrE,</b>	6-ketohexadeca-7 <i>E</i> ,9 <i>Z</i> ,12 <i>Z</i> -trienoic acid
<b>6-HHTE,</b>	6-hydroxy-hexadeca-7 <i>E</i> ,9 <i>Z</i> ,12 <i>Z</i> ,15-tetraenoic acid
<b>6-HHTrE,</b>	6-hydroxy-hexadeca-7 <i>E</i> ,9 <i>Z</i> ,12 <i>Z</i> -trienoic acid
<b>7,5-HEpETE,</b>	7-hydroxy-5,6-epoxy-eicosa-8 <i>Z</i> ,11 <i>Z</i> ,14 <i>Z</i> ,17 <i>Z</i> -tetraenoic acid
<b>8-KHME,</b>	8-keto-hexadec-9 <i>E</i> -enoic methyl ester
<b>8-KOME,</b>	8-keto-octadec-9 <i>Z</i> -enoic acid methyl ester
<b>8-HEPE,</b>	8-hydroxy-eicosa-5 <i>Z</i> ,9 <i>E</i> ,11 <i>Z</i> ,14 <i>Z</i> ,17 <i>Z</i> -tetraenoic acid
<b>8-HOME,</b>	8-hydroxy-octadec-9 <i>Z</i> -enoic acid methyl ester
<b>9-KHME,</b>	9-keto-7 <i>E</i> -hexadecenoic acid methyl ester
<b>9-HEPE,</b>	9-hydroxy-eicosa-5 <i>Z</i> ,7 <i>E</i> ,11 <i>Z</i> ,14 <i>Z</i> ,17 <i>Z</i> -pentaenoic acid
<b>9-HHME,</b>	9-hydroxy-7 <i>E</i> -hexadecenoic acid methyl ester
<b>9-HHTE,</b>	9-hydroxy-hexadeca-6 <i>Z</i> -10 <i>E</i> -12 <i>Z</i> ,15-tetraenoic acid
<b>9-HHTrE,</b>	9-hydroxy-hexadeca-6 <i>Z</i> -10 <i>E</i> -12 <i>Z</i> -trienoic acid
<b>9-HODE,</b>	9-hydroxy-octadeca-10 <i>E</i> ,12 <i>Z</i> -dienoic acid
<b>10,8-HEpETE,</b>	10-hydroxy-8,9-epoxy-eicosa-5 <i>Z</i> ,11 <i>Z</i> ,14 <i>Z</i> ,17 <i>Z</i> -tetraenoic acid
<b>11-KHME,</b>	11-keto-hexadec-9 <i>E</i> -enoic methyl ester
<b>11-HEPE,</b>	11-hydroxy-eicosa-5 <i>Z</i> ,8 <i>Z</i> ,12 <i>E</i> ,14 <i>Z</i> ,17 <i>Z</i> -pentaenoic acid
<b>11,9-HEpHDE,</b>	11-hydroxy-9,10-epoxy-hexadeca-6 <i>Z</i> ,12 <i>Z</i> -dienoic acid
<b>11-HOME,</b>	11-hydroxy-octadec-9 <i>Z</i> -enoic acid methyl ester
<b>12-HEPE,</b>	12-hydroxy-eicosa-5 <i>Z</i> ,8 <i>Z</i> ,10 <i>E</i> ,14 <i>Z</i> ,17 <i>Z</i> - pentaenoic acid
<b>13,14-HEpETE,</b>	13-hydroxy-14,15-epoxy-eicosa-5 <i>Z</i> ,8 <i>Z</i> ,11 <i>Z</i> ,17 <i>Z</i> -tetraenoic acid
<b>13-HODE,</b>	13-hydroxy-octadeca-9 <i>Z</i> ,11 <i>E</i> -dienoic acid
<b>13-HOTrE,</b>	13-hydroxy-octadeca-6 <i>Z</i> ,9 <i>Z</i> ,11 <i>E</i> -trienoic acid
<b>14-HEPE,</b>	14-hydroxy-eicosa-5 <i>Z</i> ,8 <i>Z</i> ,11 <i>Z</i> ,15 <i>E</i> ,17 <i>Z</i> -pentaenoic acid
<b>15-HEPE,</b>	15-hydroxy-eicosa-5 <i>Z</i> ,8 <i>Z</i> ,11 <i>Z</i> ,13 <i>E</i> ,17 <i>Z</i> -pentaenoic acid

<b>15-HpEPE,</b>	15-hydroperoxy-eicosa-5Z,8Z,11Z,13E,17Z-pentaenoic acid
<b>15-HpETE,</b>	15S-hydroperoxy-eicosa-5Z,8Z,11Z,13E-tetraenoic acid
<b>15-oxoacid,</b>	15-oxo-5Z,9E,11E,13E-pentadecatetraenoic acid
<b>16,14-HEpETE,</b>	16-hydroxy-14,15-epoxy-eicosa-5Z,8Z,11Z,17Z-tetraenoic acid

## Appendix

Figure A.1

8-keto-hexadec-9E-enoic methyl ester (8-KHME)



- R<sub>f</sub> (Petroleum ether/diethyl ether 7:3)= 0.58;
- <sup>1</sup>H-NMR (400 MHz, C<sub>6</sub>D<sub>6</sub>): 6.67 (dt, J= 15.7, 6.4 Hz, 1H), 6.01 (bd, J= 15.7 Hz, 1H), 3.37 (s, 3H; OCH<sub>3</sub>), 2.27 (t, J= 7.4, 2H), 2.09 (t, J= 7.4 Hz, 2H; H<sub>22</sub>), 1.82 (m, 2H), 1.62-1.51 (m, 4H), 1.30-1.11 (m, 14H), 0.89 (t, J= 6.5, 3H; H<sub>316</sub>);
- UV max (MeOH) 220 nm (4604);
- MS (EI) *m/z* 305.2 (M+Na<sup>+</sup>);
- GC-EI MS spectrum *m/z* 283 (M+H<sup>+</sup>) shows fragments at *m/z* 139 and 197.

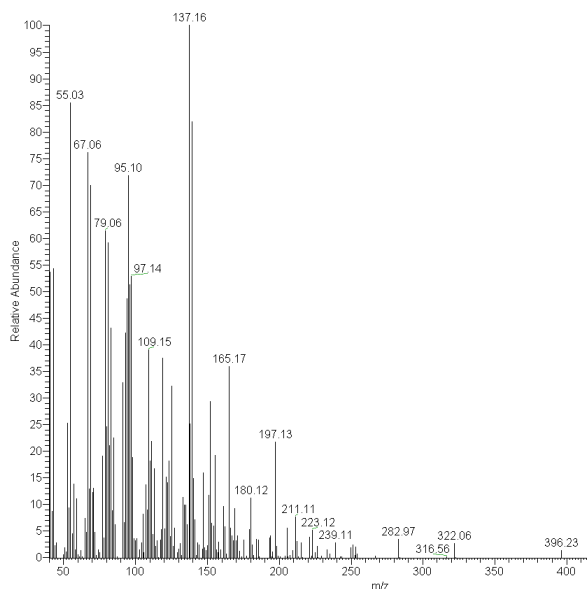
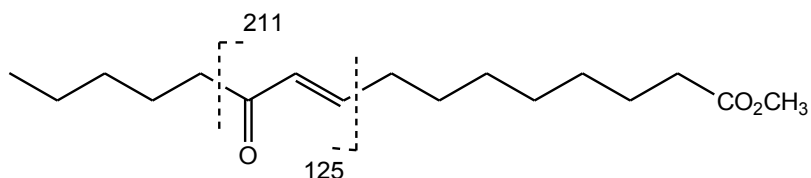


Figure A.2

11-keto-hexadec-9E-enoic methyl ester (11-KHME)



- R<sub>f</sub> (Petroleum ether/diethyl ether 7:3)= 0.56;
- <sup>1</sup>H-NMR (400 MHz, C<sub>6</sub>D<sub>6</sub>) 6.67 (dt, J= 15.7, 6.4 Hz, 1H), 6.01 (bd, J= 15.7 Hz, 1H), 3.38 (s, 3H; OCH<sub>3</sub>), 2.28 (t, J= 7.4, 2H), 2.10 (t, J= 7.4 Hz, 2H; H<sub>22</sub>), 1.81 (m, 2H), 1.63-1.50 (m, 4H), 1.30-1.10 (m, 14H), 0.89 (t, J= 6.5, 3H; H<sub>31</sub>6);
- UV max (MeOH) 220 nm (4442);
- MS (EI) *m/z* 305.2 (M+Na<sup>+</sup>);
- GC-EI MS spectrum *m/z* 283 (M+H<sup>+</sup>) shows fragments at *m/z* 211 and 125.

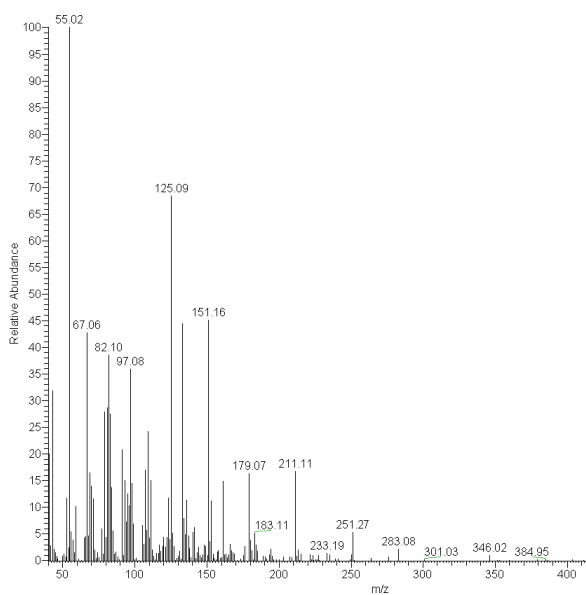
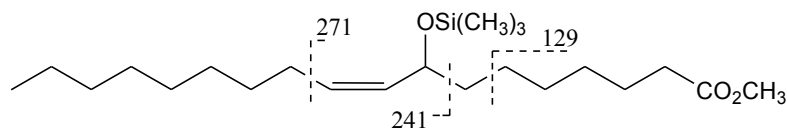


Figure A.3

8-hydroxy-octadec-9Z-enoic acid methyl ester (8-HOME)



- R<sub>f</sub> (Petroleum ether/diethyl ether 7:3)= 0.30;
- <sup>1</sup>H-NMR (400 MHz, C<sub>6</sub>D<sub>6</sub>) 5.50 (dd, J= 15.9, 6.0 Hz, 1H; H9), 5.44 (dt, J= 15.9, 5.5 Hz, 1H; H10), 3.94 (m, 1H; H8), 3.39 (s, 3H; OCH<sub>3</sub>), 2.10 (t, J= 7.1, 2H;H2), 1.95 (m, 2H; H11), 1.66-1.49 (m, 6H), 1.32-1.11 (m, 16H), 0.90 (t, J= 6.6, 3H; H318);
- UV max (MeOH) 210 nm (453), 217 nm (330);
- MS (EI) *m/z* 335.3 (M+Na<sup>+</sup>);
- GC-EI MS spectrum of the trimethylsilyl derivative of 8-HOME *m/z* 384 (M<sup>+</sup>) shows fragments at *m/z* 271, 241 and 129.

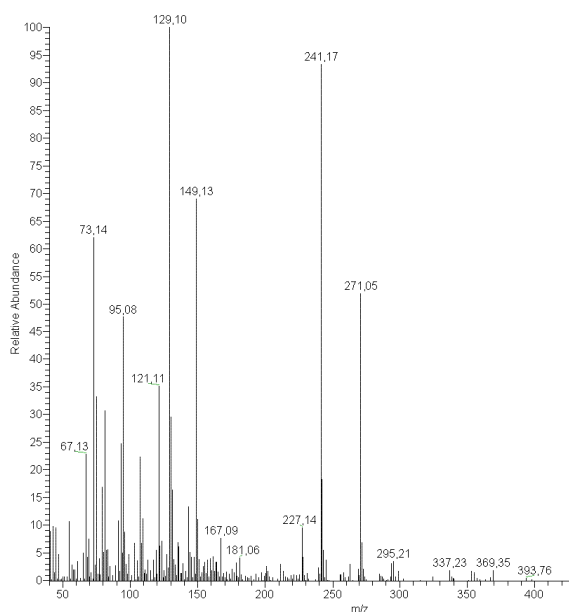
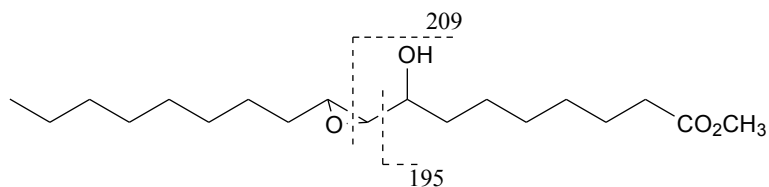


Figure A.4

8-hydroxy-9,10-epoxy-octadecanoic acid methyl ester



- R<sub>f</sub> (Petroleum ether/diethyl ether 7:3)= 0.06;
- <sup>1</sup>H-NMR (400 MHz, C<sub>6</sub>D<sub>6</sub>) 3.36 (s, 3H; OCH<sub>3</sub>), 3.29 (m, 1H; H<sub>8</sub>), 2.73 (m, 1H), 2.54 (m, 1H), 2.09 (t, J= 7.5, 2H;H<sub>2</sub>), 1.73-1.20 (m, 24H), 0.90 (t, J= 6.2, 3H; H<sub>318</sub>);
- MS (EI) *m/z* 351.2 (M+Na<sup>+</sup>);
- ESI<sup>+</sup> MS/MS spectrum shows fragments at *m/z* 209 and 195.

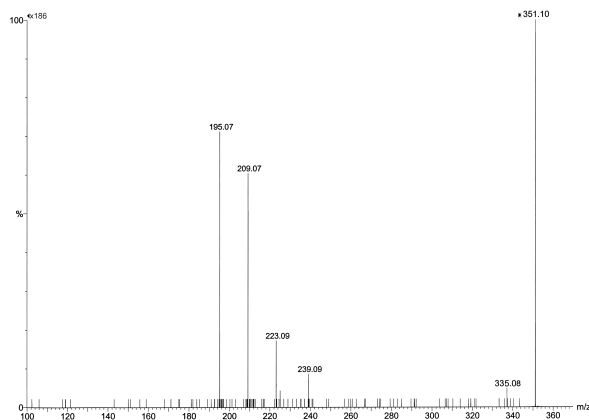
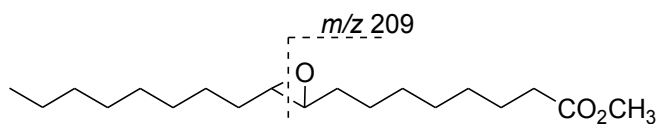


Figure A.5

9,10-epoxy-octadecanoic acid methyl ester



- Rf (Petroleum ether/diethyl ether 7:3) 0.55;
- $^1\text{H-NMR}$  (400 MHz,  $\text{CDCl}_3$ ) 3.41 (s, 3H;  $\text{OCH}_3$ ), 2.62 (m, 2H; H9, H-10) 2.07 (t, J=7.1, 2H;  $\text{H}_2$ ), 1.41 (m, 2H), 1.32-1.06 (m, 24 H), 0.67 (t, J= 6.6, 3H;  $\text{H}_3$ -18);
- MS (EI)  $m/z$  335 ( $\text{M}+\text{Na}^+$ );
- $\text{ESI}^+$  MS/MS spectrum shows fragment at  $m/z$  209.

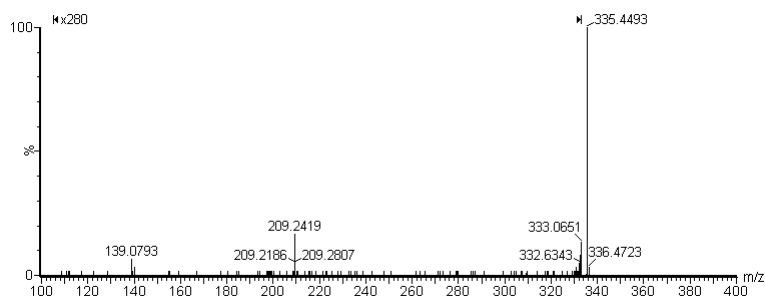
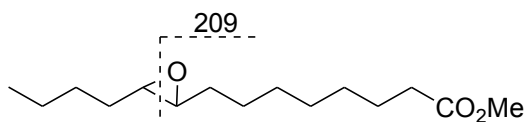


Figure A.6

9,10-epoxy-tetradecanoic acid methyl ester



- Rf (Petroleum ether/diethyl ether 7:3) 0.58;
- $^1\text{H-NMR}$  (400 MHz,  $\text{CDCl}_3$ ) 3.42 (s, 3H;  $\text{OCH}_3$ ), 2.62 (m, 2H; H9, H10) 2.08 (t, J=7.1, 2H; H-2), 1.40 (m, 2H), 1.32-1.06 (m, 16 H), 0.67 (t, J= 6.6, 3H; H<sub>3</sub>-14);
- MS (EI)  $m/z$  279 ( $\text{M}+\text{Na}^+$ );
- ESI<sup>+</sup> MS/MS spectrum shows fragment at  $m/z$  209.

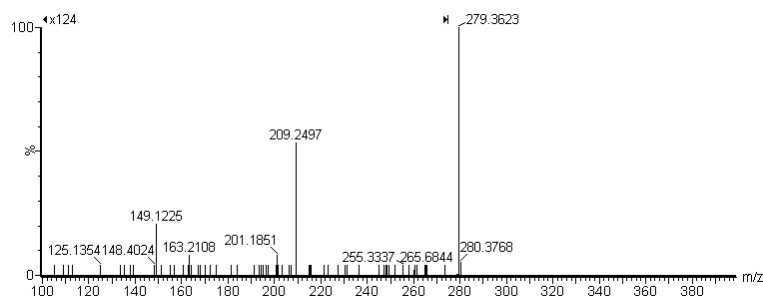
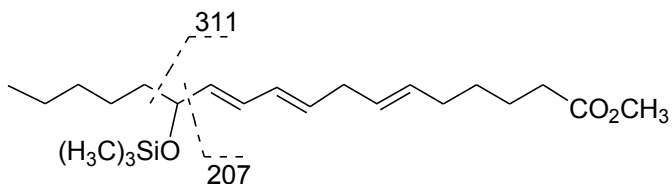
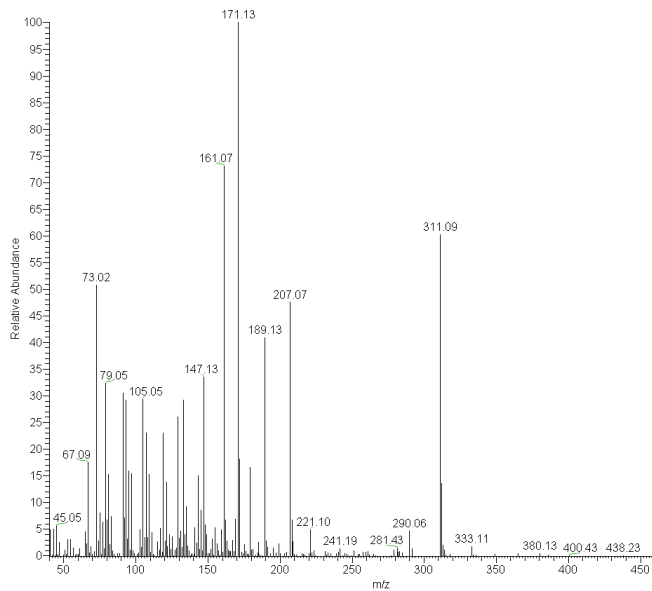


Figure A.7

13-hydroxy-octadeca-6Z,9Z,11E-trienoic acid methyl ester (13-HOTrE)

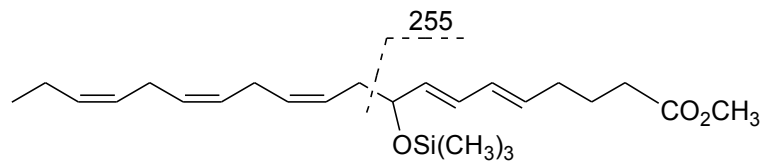


GC-EI MS spectrum  $m/z$  380 ( $M^+$ ) shows fragments at  $m/z$  311 and 207.



**Figure A.8**

9-hydroxy-eicosa-5Z,7E,11Z,14Z,17Z-pentaenoic acid methyl ester (9-HEPE)



GC-EI MS spectrum  $m/z$  404 ( $\text{M}^+$ ) shows fragment at  $m/z$  255.

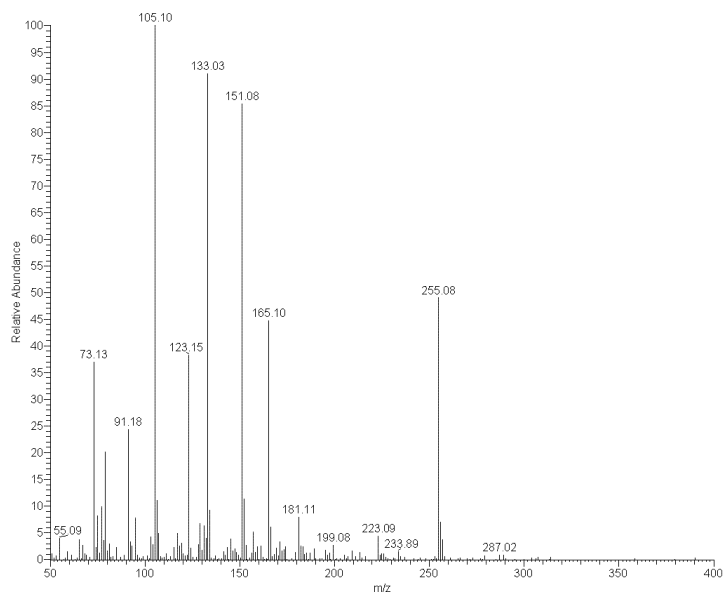
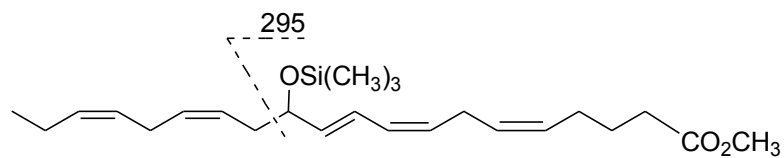


Figure A.9

12-hydroxy-eicosa-5Z,8Z,10E,14Z,17Z- pentaenoic acid methyl ester (12-HEPE)



GC-EI MS spectrum  $m/z$  404 ( $\text{M}^+$ ) shows fragment at  $m/z$  295.

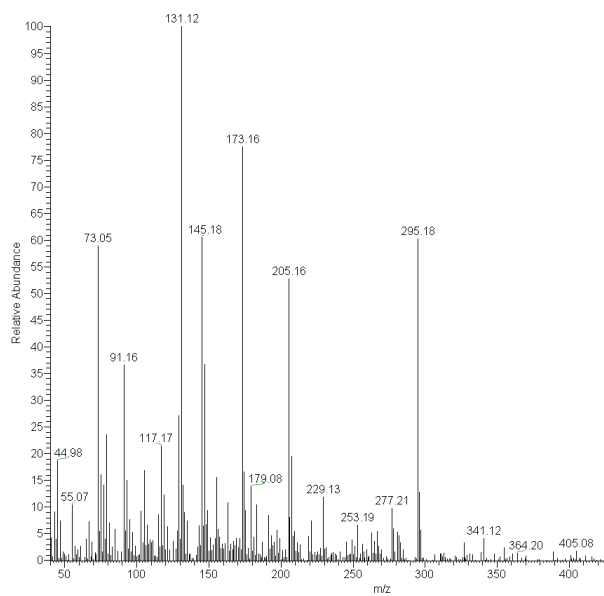
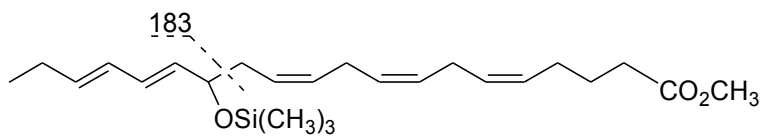


Figure A.10

14-hydroxy-eicosa-5Z,8Z,11Z,15E,17Z- pentaenoic acid methyl ester (14-HEPE)



GC-EI MS spectrum  $m/z$  404 ( $M^+$ ) shows fragment at  $m/z$  183.

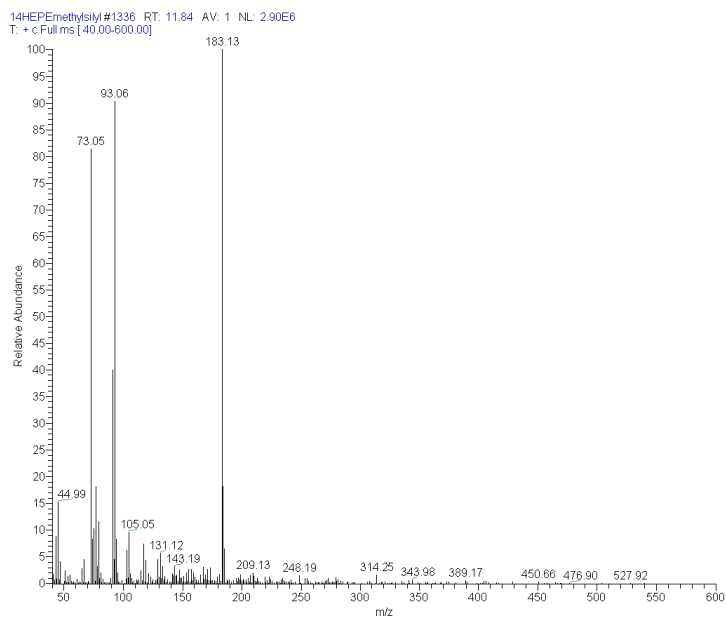
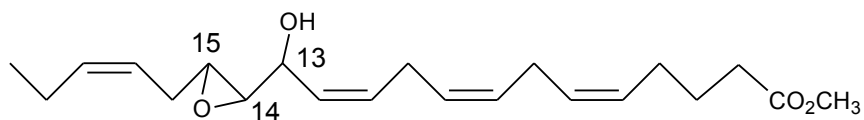
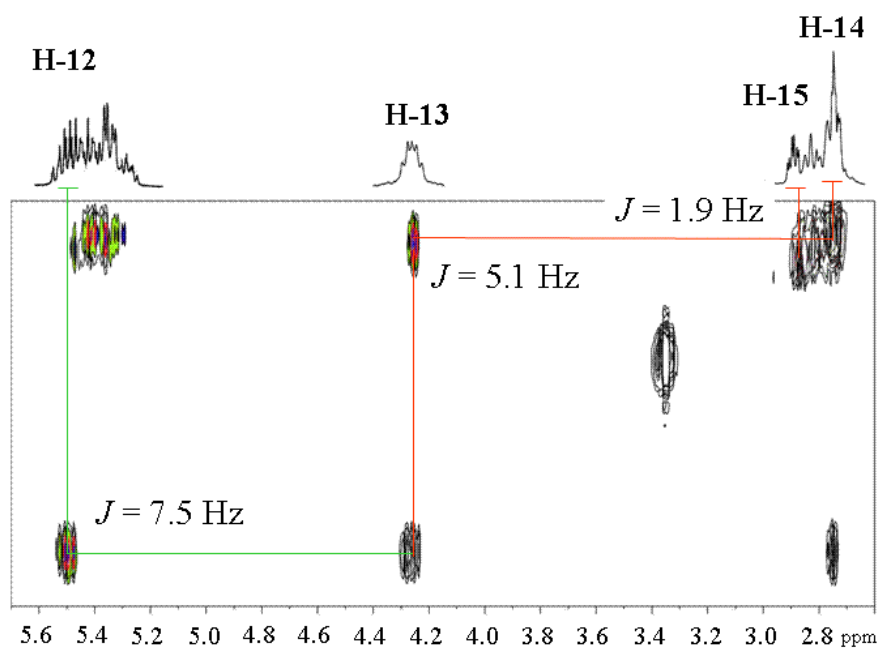
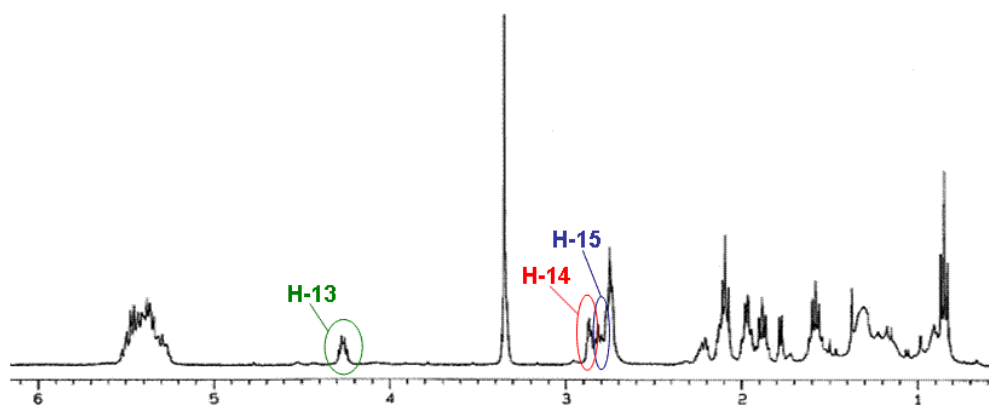


Figure A.11

13-hydroxy-14,15-epoxy-eicosa-5Z,8Z,11Z,17Z-tetraenoic acid methyl ester



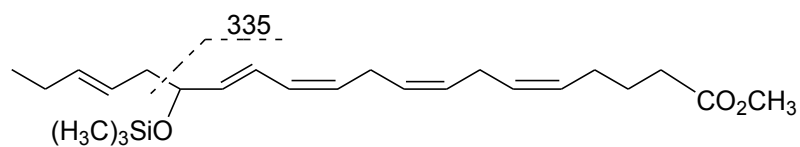
$^1\text{H-NMR}$  (400 MHz,  $\text{C}_6\text{D}_6$ )  $\delta$  4.26, 2.71 and 2.86 for H-13, H-14 and H-15;  $J_{\text{H14/H15}} = 1.9$  Hz and  $J_{\text{H13/H14}} = 5.1$  Hz





**Figure A.13**

15-hydroxy-eicosa-5Z,8Z,11Z,13E,17Z-pentaenoic acid methyl ester (15-HEPE)



GC-EI MS spectrum of trimethyl-silyl of 15-HEPE isolated from *Pseudo-nitzschia delicatissima* clade 1  $m/z$  404 ( $\text{M}^+$ ) shows fragment at  $m/z$  335.

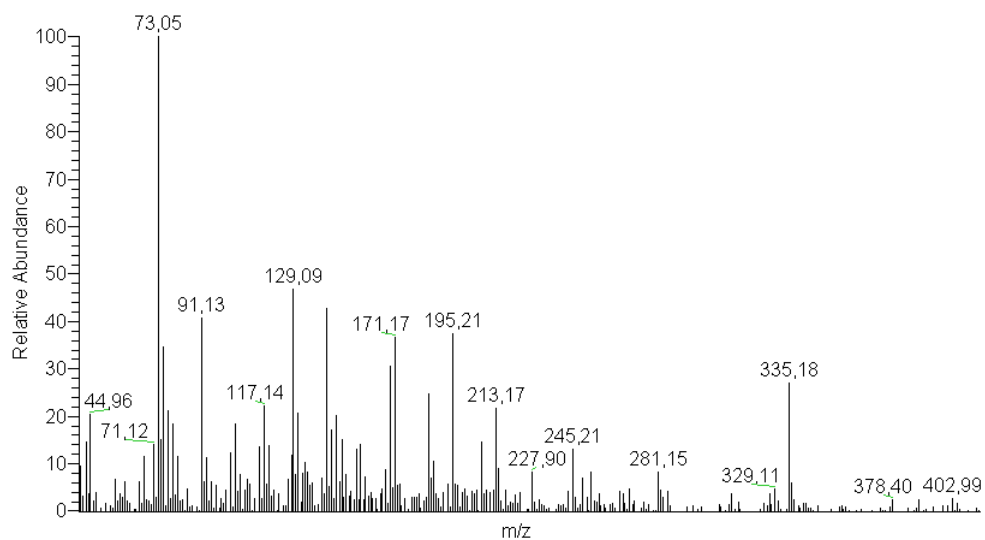
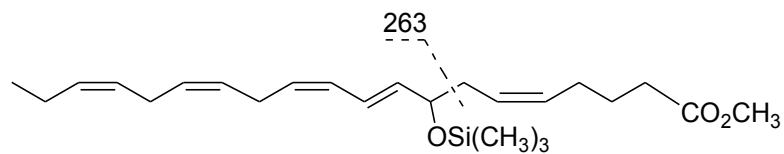


Figure A.14

8-hydroxy-eicosa-5Z,9E,11Z,14Z,17Z-tetraenoic acid methyl ester (8-HEPE)



GC-EI MS spectrum of trimethyl-silyl of 8-HEPE isolated from *Pseudo-nitzschia pseudodelicatissima*  $m/z$  404 ( $M^+$ ) shows fragment at  $m/z$  263.

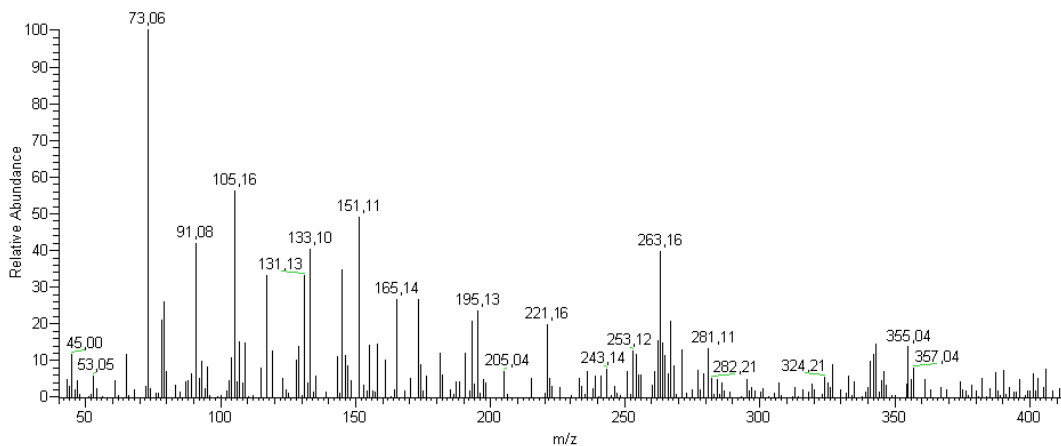
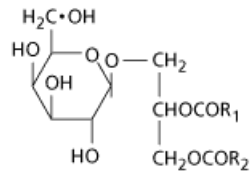


Figure A.15

monogalactosyldiacylglycerols (MGDG)



R1=R2= C18:3 ω6

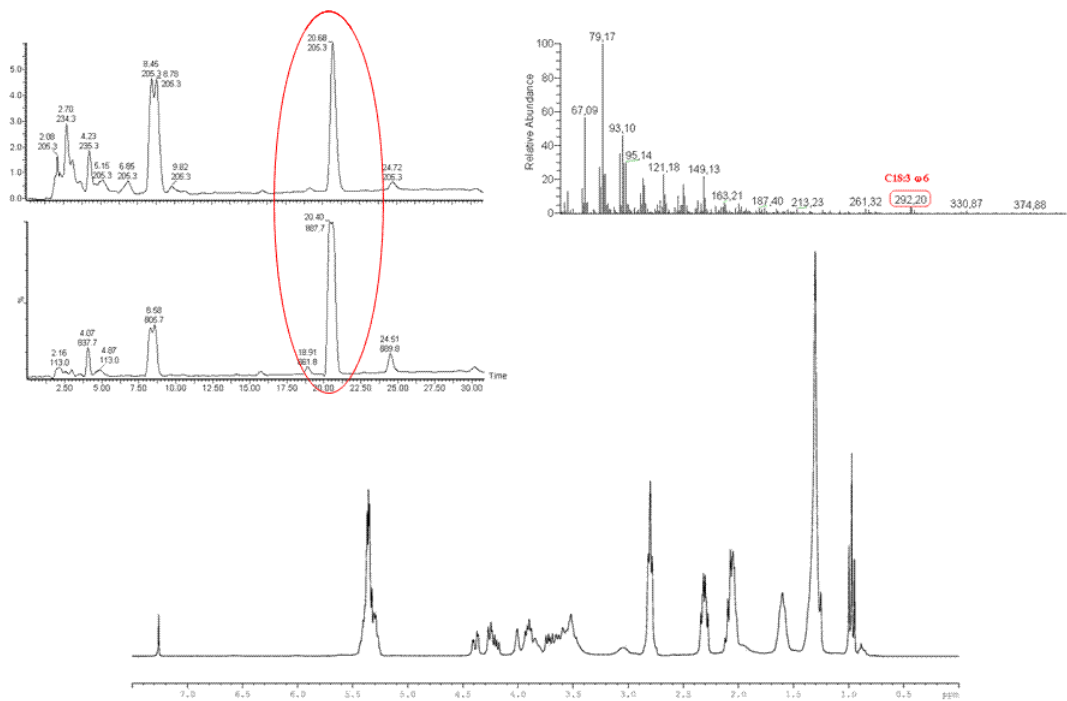
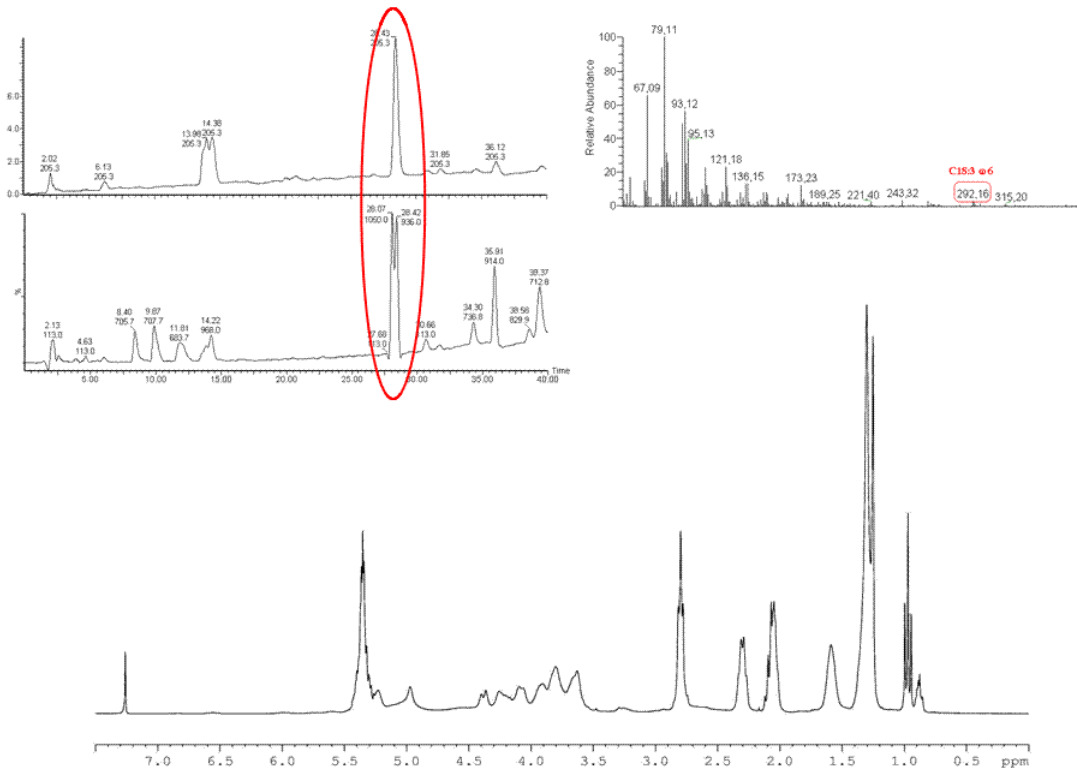
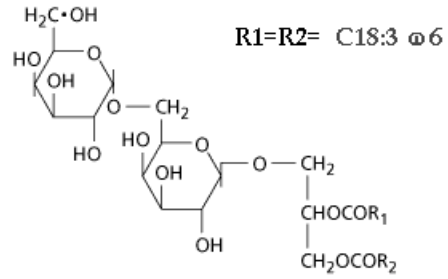


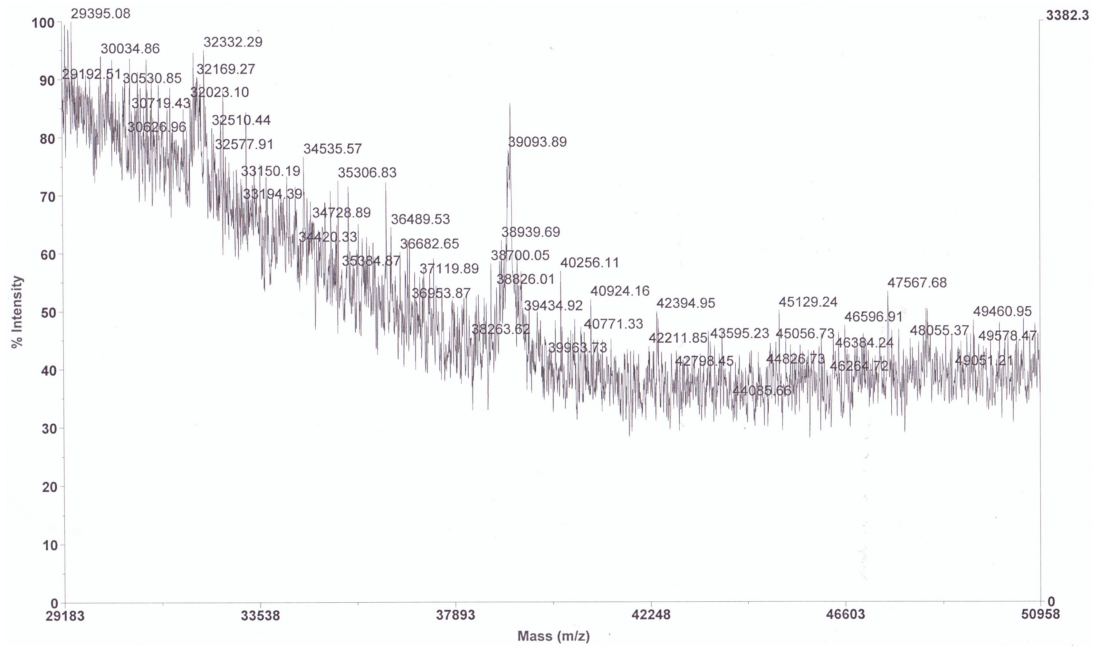
Figure A.16

digalactosyldiacylglycerols (DGDG)



**Figure A.17**

The MALDI-ToF analysis of the not-hydrolyzed protein provided a signal at molecular mass of 39 kDa.



The peptide mass fingerprinting of the tryptic digest.

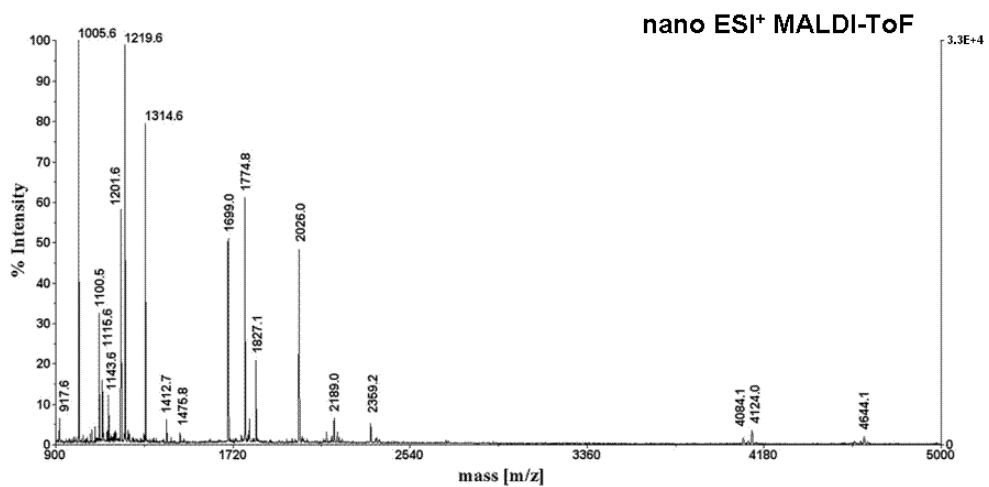
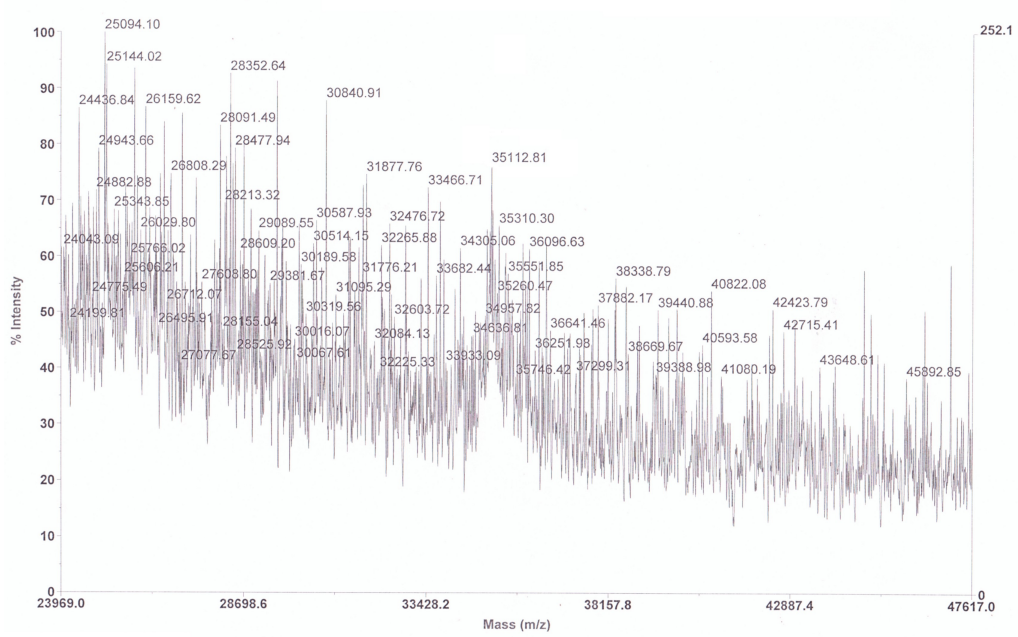


**Figure A.18**

The MALDI-ToF analysis of the not-hydrolyzed protein provided a signal at molecular mass of 35.1 kDa.



## References

- Agrawal AA. 2000.** Mechanisms, ecological consequences and agricultural implications of tri-trophic interactions. *Current Opinion in Plant Biology*. 3: 329-335.
- Amato A, Kooistra WHCF, Leviaidi Ghiron JH, Mann DG, Pröschold T, Montresor M. 2007.** Reproductive isolation among sympatric cryptic species in marine diatoms. *Protist*. 158: 193-207.
- Anderson DM, Kulis DM, Sullivan JJ, Lee C. 1990.** Dynamics and physiology of saxitoxin production by the dinoflagellates *Alexandrium* spp. *Marine Biology*. 104: 511-524.
- Anthon GE, Barrett DM. 2001.** Colorimetric method for the determination of Lipoyxygenase activity. *Journal of Agricultural and Food Chemistry*. 49: 32-37.
- Ban S, Burns C, Castel J, Chaudron Y, Christou E, Escribano R, Fonda Umani S, Gasparini S, Guerrero Ruiz F, Hoffmeyer M, Ianora A, Kang HK, Laabir M, Lacoste A, Miralto A, Ning X, Poulet S, Rodríguez V, Runge J, Shi J, Starr M, Uye SI, Wang J. 1997.** The paradox of diatom – copepod interactions. *Marine Ecology Progress Series*. 157: 287-293.
- Barofsky A, Pohnert G. 2007.** Biosynthesis of polyunsaturated short chain aldehydes in the diatoms *Thalassiosira rotula*. *Organic Letters*. 9: 1017–1020.
- Bates SS, Bird CJ, de Freitas ASW, Foxall R, Gilgan MW, Hanic LA, Johnson GR, McCulloch AW, Odense P, Pocklington R, Quilliam MA, Sim PG, Smith JC, Subba Rao DV, Todd ECD, Walter JA, Wright JLC, 1989.** Pennate diatom *Nitzschia pungens* as the primary source of domoic acid, a toxin in shellfish from eastern Prince Edward Island. *Canadian Journal of Fisheries and Aquatic Sciences*. 46: 1203–1215.

- Bates SS, Garrison DL, Horner RA, 1998.** Bloom dynamics and physiology of domoic-acid-producing *Pseudo-nitzschia* species. In: Anderson DM, Cembella AD, Hallegraeff GM. (Eds.). *Physiological Ecology of Harmful Algal Blooms*. Springer-Verlag, Heidelberg, pp. 267–292.
- Behnke A, Friedl T, Chepurinov VA, Mann DG. 2004.** Reproductive compatibility and rDNA sequence analyses in the *Sellaphora pupula* species complex (Bacillariophyta). *Journal of Phycology*. 40: 193-208.
- Blée E. 1998.** Phyto-oxylipins and plant defense reactions. *Progress in Lipid Research*. 37: 33–72.
- Blée E. 2002.** Impact of phyto-oxylipins in plant defence. *Trends in Plant Science*. 7: 315-321.
- Berman-Frank I, Bidle K, Haramaty L, Falkowski PG. 2004.** The demise of the marine cyanobacterium, *Trichodesmium* spp., via an autocatalyzed cell death pathway. *Oceanography*. 49: 997–1005.
- Bernart MW, Whatley GG, Gerwick WH. 1993.** Unprecedented oxylipins from the marine green-alga *Acrosiphonia Coalita*. *Journal of Natural Products*. 56: 245–259.
- Beszteri B, Ács É, Medlin LK. 2005.** Ribosomal DNA sequence variation among sympatric strains of the *Cyclotella meneghiniana* complex (Bacillariophyceae) reveals cryptic diversity. *Protist*. 156: 317-333.
- Bidle K, Falkowski PG. 2004.** Cell death in planktonic, photosynthetic microorganisms. *Nature Reviews Microbiology*. 2: 643–655.
- Brash AR. 1999.** Lipoxygenase: Occurrence, functions, catalysis, and acquisition of substrate. *Journal of Biological Chemistry*. 274: 23679-23682.

**Brash AR, Boeglin WE, Chang MS, Shieh BH. 1996.** Purification and molecular cloning of an 8R-lipoxygenase from the coral *Plexaura homomalla* reveal the related primary structures of R- and S-lipoxygenases. *Journal of Biological Chemistry*. 271: 20949-20957.

**Brown SH, Zarnowski R, Sharpee WC, Keller NP. 2008.** Morphological transitions governed by density dependence and lipoxygenase activity in *Aspergillus flavus* *Applied. Environmental Microbiology*. 74: 5674–5685.

**Brownlee C. 2008.** Diatom signaling: deadly messages. *Current Biology*. 18: 518–519.

**Cacas JL, Vaillau F, Davoine C, Ennar N, Agnel JP, Tronchet M, Ponchet M, Blein JP, Roby D, Triantphylides C, Montillet JL. 2005.** The combined action of 9 lipoxygenase and galactolipase is sufficient to bring about programmed cell death during tobacco hypersensitive response. *Plant Cell and Environment*. 28: 1367-1378.

**Carotenuto Y, Ianora A, Buttino I, Romano G, Miralto A. 2002.** Is postembryonic development in the copepod *Temora stylifera* negatively affected by diatom diets? *Journal of Experimental Marine Biology and Ecology*. 276: 49-66.

**Ceballos S, Ianora A. 2003.** Different diatoms induce contrasting effects on the reproductive success of the copepod *Temora stylifera*. *Journal of Experimental Marine Biology and Ecology*. 294: 189-202.

**Cembella A, John U. 2006.** Molecular physiology of toxin production and growth regulation in harmful algae. In: Granéli E, Turner JT, eds. *Ecology of harmful algae*. Springer Verlag, Berlin Heidelberg, *Ecological Studies* vol. 189: 215–227.

**Chang MS, Boeglin WE, Guengerich FP, Brash AR. 1996.** Cytochrome P450-dependent transformations of 15R- and 15S-hydroperoxyeicosatetraenoic acids: stereoselective formation of epoxy alcohol products. *Biochemistry*. 35: 464-471.

**Cristea M, Oliw EH. 2006.** A G316A mutation of manganese lipoxygenase augments hydroperoxide isomerase activity. *Journal of Biological Chemistry*. 281: 17612–17623.

**Croft KPC, Jüttner F, Slusarenko AJ. 1993.** Volatile products of the lipoxygenase pathway evolved from *Phaseolus vulgaris* (L.) Leaves inoculated with *Pseudomonas syringae* pv *phaseolicola*. *Plant Physiology*. 101: 13-24.

**Cutignano A, d'Ippolito G, Romano G, Lamari N, Cimino G, Febbraio F, Nucci R, Fontana A. 2006.** Chloroplastic glycolipids fuel aldehyde biosynthesis in the marine diatom *Thalassiosira rotula*. *ChemBioChem*. 7: 450-456.

**Cutignano A, Lamari N, d'Ippolito G, Manzo E, Fontana A. 2009.** Oxylin analysis in marine diatoms. *Journal of Phycology*, submitted.

**Dhondt S, Geoffroy P, Stelmach BA, Legrand M, Heitz T. 2000.** Soluble phospholipase A2 activity is induced before oxylin accumulation in tobacco mosaic virus-infected tobacco leaves and is contributed by patatin-like enzymes. *Plant Journal*. 23: 431–440.

**d'Ippolito G, Romano G, Iadicicco O, Miralto A, Ianora A, Cimino G, Fontana A. 2002a.** New birth-control aldehydes from the marine diatom *Skeletonema costatum*: characterization and biogenesis. *Tetrahedron Letters*. 43: 6133-6136.

**d'Ippolito G, Iadicicco O, Romano G, Fontana A. 2002b.** Detection of short chain aldehydes in marine organisms: the diatom *Thalassiosira rotula*. *Tetrahedron Letters*. 43: 6137-6140.

**d'Ippolito G, Romano G, Caruso T, Spinella A, Cimino G, Fontana A. 2003.** Production of octadienal in the marine diatom *Skeletonema costatum*. *Organic Letters*. 5: 885-887.

**d'Ippolito G, Cutignano A, Tucci S, Romano G, Miralto A, Cimino G, Fontana A. 2004.** The Role of Complex Lipids in the Synthesis of Bioactive Aldehydes of the Marine Diatom *Skeletonema costatum*. *Biochimica et Biophysica Acta*. 1686: 100-107.

**d'Ippolito G, Cutignano A, Briante R, Febbraio F, Cimino G, Fontana A. 2005.** New C<sub>16</sub> fatty-acid-based oxylipin pathway in the marine diatom *Thalassiosira rotula*. *Organic and Biomolecular Chemistry*. 3: 4065-4070.

**d'Ippolito G, Cutignano A, Tucci S, Romano G, Cimino G, Fontana A. 2006.** Biosynthetic intermediates and stereochemical aspects of aldehyde biosynthesis in the marine diatom *Thalassiosira rotula*. *Phytochemistry*. 67: 314-322.

**d'Ippolito G, Lamari N, Montresor M, Romano G, Cutignano A, Gerech A, Cimino G, Fontana A. 2009.** 15S-Lipoxygenase metabolism in the marine diatom *Pseudonitzschia delicatissima*. *New Phytologist*. 183:1064-1071.

**Dunn WB, Ellis DI. 2005.** Metabolomics: current analytical platforms and methodologies. *Trends in Analytical Chemistry*. 24: 285-294.

**Dutz, J, Koski, M, Jónasdóttir SH. 2008.** Copepod reproduction is unaffected by diatom aldehydes or lipid composition. *Limnology and Oceanography*. 53: 225-235.

**Evershed RP. 1992.** Mass spectrometry of lipids. In: Hamilton RJ, Hamilton S, eds. *Lipid Analysis: A practical approach*. Oxford, UK: Oxford University Press, 263-308.

**Falkowski PG, Barber RT, Smetacek V. 1998.** Biogeochemical controls and feedbacks on ocean primary production. *Science*. 281: 200-206.

**Falkowski PG, Raven JA. 2007.** Aquatic Photosynthesis. Second Edition. Princeton University Press.

**Field CB, Behrenfeld MJ, Randerson JT, Falkowski P. 1998.** Primary production of the Biosphere: Integrating terrestrial and oceanic components. *Science*. 281: 237-240.

**Fontana A, d'Ippolito G, Cutignano A, Miralto A, Ianora A, Romano G, Cimino G. 2007a.** Chemistry of oxylipin pathway in marine diatoms. *Pure and Applied Chemistry*. 79: 481-490.

**Fontana A, d'Ippolito G, Cutignano A, Romano G, Lamari N, Massa Gallucci A, Cimino G, Miralto A, Ianora A. 2007b.** LOX- induced lipid peroxidation mechanism responsible for the detrimental effect of marine diatoms on zooplankton grazers. *ChemBioChem*. 8: 1810-1818.

**Fox SR, Akpinar A, Prabhune AA, Friend J, Ratledge C. 2000.** The biosynthesis of oxylipins of linoleic and arachidonic acids by the sewage fungus *Leptomitus lacteus*, including the identification of 8R-hydroxy-9Z, 12Z-octadecadienoic acid. *Lipids*. 35: 23-30.

**Gallagher JC. 1980.** Population genetics of *Skelotonema costatum* (Bacillariophyceae) in Narragansett Bay. *Journal of Phycology*. 16: 464-474.

**Gerard L, Bannenberg G, Aliberti J, Hong S, Sher A, Serhan C. 2004.** Exogenous pathogen and plant 15-lipoxygenase initiate endogenous lipoxin A4 biosynthesis. *Journal of Experimental Medicine*. 199: 515–523.

**Gerwick WH, Moghaddam MF, Hamberg M. 1991.** Oxylipin metabolism in the red alga *Gracilariopsis lemaneiformis*: Mechanism of formation of vicinal dihydroxy fatty acids. *Archives of biochemistry and biophysics*. 290: 436-444.

**Giovannoni S, Rappé M. 2000.** Evolution, diversity, and molecular ecology of marine prokaryotes. In: *Microbial ecology of the Oceans*. Kirchmann DL (ed.) pp. 47-83. Wiley-Liss, New York.

- Göbel C, Feussner I, Hamberg M, Rosahl S. 2002.** Oxylipin profiling in pathogen-infected potato leaves. *Biochimica et Biophysica Acta*. 1584: 55–64.
- Guillard RRL. 1983.** Culture of phytoplankton for feeding marine invertebrates. In: *Culture of Marine Invertebrates – Selected readings*. Berg Jr. CJ (ed.) pp. 108-132. Hutchinson Ross Publishing Co. Stroudsburg, PA.
- Hampson DR, Manolo JL, 1998.** The activation of glutamate receptors by kainic acid and domoic acid. *Natural Toxins*. 6: 153-158.
- Hasle GR. 1965.** *Nitzschia* and *Fragilariopsis* species studied in the light and electron microscopes. II. The group *Pseudo-nitzschia*. *Skr Nor Vidensk-Akad Oslo I Mat-Naturvidensk KI*. 18: 1-45.
- Hasle GR. 2002.** Are most of the domoic acid-producing species of the diatom genus *Pseudo-nitzschia* cosmopolites? *Harmful Algae*. 1: 137-146.
- Hasle GR, Lange CB, Syvertsen EE. 1996.** A review of *Pseudo-nitzschia*, with special reference to the Skagerrak, North Atlantic, and adjacent waters. *Helgoländer Meeresuntersuchungen*. 50: 131-175.
- Hasle GR, Syvertsen EE. 1997.** Marine diatoms. In: *Identifying marine phytoplankton* (ed. Tomas CR) pp. 5-385. Academic Press, San Diego
- Hay ME. 1996.** Marine chemical ecology: What's known and what's next? *Journal of Experimental Marine Biology and Ecology*. 200: 103-134.
- Hay ME, Fenical W. 1996.** Chemical ecology and marine biodiversity: insights and products from the sea. *Oceanography*. 9: 10-20.

**Hombeck M, Boland W. 1998.** Biosynthesis of the algal pheromone fucoserratene by the freshwater diatom *Asterionella formosa* (Bacillariophyceae). *Tetrahedron*. 54: 11033-11042.

**Hombeck M, Pohnert G, Boland W. 1999.** Biosynthesis of dictyopterene A: stereoselectivity of a lipoxygenase/hydroperoxide lyase from *Gomphonema parvulum* (Bacillariophyceae). *Journal of the Chemical Society Chemical Communications*. 3: 243–244.

**Hughes RK, Yousafzai FK, Ashton R, Chechetkin IR, Fairhurst SA, Hamberg M, Casey R. 2008.** Evidence for communality in the primary determinants of CYP74 catalysis and of structural similarities between CYP74 and classical mammalian P450 enzymes. *Proteins*. 72: 1199–1211.

**Hutchinson GE. 1978.** An introduction to population ecology. Yale University Press, New Haven.

**Hwa Lee S, Williams MV, DuBois RN, Blair IA. 2003.** Targeted lipidomics using electron capture atmospheric pressure chemical ionization mass spectrometry. *Rapid Communications in Mass Spectrometry*. 17: 2168-2176.

**Ianora A, Poulet SA. 1993.** Egg viability in the copepod *Temora stylifera*. *Limnology and Oceanography*. 38: 1615-1626.

**Ianora A, Poulet SA, Miralto A, Grottoli R. 1996.** The diatom *Thalassiosira rotula* affects reproductive success in the copepod *Acartia clausi*. *Marine Biology*. 125: 279-286.

**Ianora A, Miralto A, Buttino I, Romano G, Poulet SA. 1999.** First evidence of some dinoflagellates reducing male copepod fertilization capacity. *Limnology and Oceanography*. 44: 147-153.

**Ianora A, Miralto A, Poulet S, Carotenuto Y, Buttino I, Romano G, Casotti R, Pohnert G, Wichard T, Colucci-D'Amato L, Terrazzano G, Smetacek V. 2004.** Aldehyde suppression of copepod recruitment in blooms of a ubiquitous planktonic diatom. *Nature*. 429: 403-407.

**Ianora A, Boersma M, Casotti R, Fontana A, Harder J, Hoffmann F, Pavia H, Potin P, Poulet SA, Toth G. 2006.** New trends in Marine Chemical Ecology. *Estuaries and Coasts*. 29: 531-551.

**Illijas M, Terasaki M, Nakamura R, Iijima N, Hara A, Fusetani N, Itabashi Y. 2008.** Purification and characterization of glycerolipid acyl-hydrolase from the red alga *Gracilaria vermiculophylla*. *Fisheries Science*. 74: 670-676.

**Irigoien X, Head RN, Harris RP, Cummings D, Harbour D, Meyer-Harms B. 2000.** Feeding selectivity and egg production of *Calanus helgolandicus* in the English Channel. *Limnology and Oceanography*. 45: 44-54.

**Ishiguro S, Kawai-Oda A, Ueda J, Nishida I, Okada K. 2001.** The defective in anther dehiscence gene encodes a novel phospholipase A1 catalyzing the initial step of jasmonic acid biosynthesis, which synchronizes pollen maturation, anther dehiscence, and flower opening in *Arabidopsis*. *Plant Cell*. 13: 2191-2209.

**Jones RH, Flynn KJ. 2005.** Nutritional status and diet composition affect the value of diatoms as copepod prey. *Science*. 307: 1457-1459.

**Keeling PJ, Burger G, Durnford DG, Lang BF, Lee RW, Pearlmann RE, Roger AJ, Gray MW. 2005.** The Tree of Eucaryotes. *Trends in Ecology and Evolution*. 20: 670-676.

**Kleppel GS. 1993.** On the diets of calanoid copepods. *Marine Ecology Progress Series*. 99: 183-195.

**Knight VI, Wang H, Lincoln JE, Lulai EC, Gilchrist DG, Bostock RM. 2001.** Hydroperoxides and fatty acids induce programmed cell death in tomato protoplasts. *Physiological and Molecular Plant Pathology*. 59: 277-286.

**Kooistra WHCF, De Stefano M, Medlin LK, Mann DG. 2003.** The phylogenetic position of *Toxarium*, a pennate-like lineage within centric diatoms (Bacillariophyceae). *Journal of Phycology*. 39: 185-189.

**Kooistra WHCF, Sarno D, Balzano S, Gu H, Andersen RA, Zingone A. 2008.** Global diversity and biogeography of *Skeletonema* species (Bacillariophyceae). *Protist*. 159: 177-193.

**Kühn H. 1996.** Biosynthesis, metabolization and biological importance of the primary 15-lipoxygenase metabolites 15-hydro(pero)xy- 5Z,8Z,11Z,13E-eicosatetraenoic acids and 13 hydro(pero)xy-9Z,12Eoctadecadienoic acid. *Progress in Lipid Research*. 3: 203–226.

**Kühn H, Walther M, Kuban, RJ. 2002.** Mammalian arachidonate 15-lipoxygenases. Structure, function, and biological implications. *Prostaglandins and Other Lipid Mediators*. 68–69: 263–290.

**Landsberg JH. 2002.** The effects of harmful algal blooms on the aquatic organisms. *Reviews in Fisheries Science*. 10: 113-390.

**Lee DS, Nioche P, Hamberg M, Raman CS. 2008.** Structural insights into the evolutionary paths of oxylipin biosynthetic enzymes. *Nature*. 455: 363–368.

**Leftley JW, Keller DK, Selvin RC, Claus W, Guillard RRL. 1987.** Media for the culture of oceanic ultraphytoplankton. *Journal of Phycology*. 23: 633-638.

**Lenaers G, Maroteaux L, Michot B, Herzog M. 1989.** Dinoflagellates in evolution. A molecular phylogenetic analysis of large subunit ribosomal RNA. *Journal of Molecular Evolution*. 29: 40-51.

**Lundholm N, Moestrup Ø, Hasle GR, Hoef-Emden K. 2003.** A study of the *Pseudo-nitzschia pseudodelicatissima/cuspidata* complex (Bacillariophyceae): what is *P. pseudodelicatissima*? *Journal of Phycology*. 39: 797-813.

**Lundholm N, Moestrup Ø, Kotaki Y, Hoef-Emden K, Scholin C, Miller P. 2006.** Inter- and intraspecific variation of the *Pseudo-nitzschia delicatissima* complex (Bacillariophyceae) illustrated by rRNA probes, morphological data and phylogenetic analyses. *Journal of Phycology*. 42: 464-481.

**Maccarone M, Van Zadelhoff G, Veldink GA, Vliegenthart JFG, Finazzi-Agrò A. 2000.** Early activation of lipoxygenase in lentil (*Lens culinaris*) root protoplasts by oxidative stress induces programmed cell death. *European Journal of Biochemistry*. 267: 5078-5084.

**Mann DG. 1999.** The species concept in diatoms. *Phycologia*. 38: 437-495.

**Matsui K, Kurishita S, Hisamitsu A, Kajiwara T. 2000.** A lipid-hydrolysing activity involved in hexenal formation. *Biochemical Society Transactions*. 28: 857-860.

**Miralto A, Barone G, Romano G, Poulet SA, Ianora A, Russo GL, Buttino I, Mazzarella G, Laabir M, Cabrini M, Giacobbe MG. 1999.** The insidious effect of diatoms on copepod reproduction. *Nature*. 402: 173-176.

**Montillet JL, Cacas JL, Garnier L, Montané MH, Douki T, Bessoule JJ, Polkowska-Kowalczyk L, Maciejewska U, Agnel JP, Vial A, Triantaphylidès C. 2004.** The upstream oxylipin profile of *Arabidopsis thaliana*: a tool to scan for oxidative stresses. *Plant Journal* 40: 439-451.

- Mos L. 2001.** Domoic acid: a fascinating marine toxin. *Environmental Toxicology and Pharmacology*. 9: 79-85.
- Mueller MJ, Mène-Saffrane L, Grun C, Karg K, Farmer EE. 2006.** Oxylin analysis methods. *Plant Journal*. 45: 472-489.
- Nevitt GA, Veit RR, Kareiva P. 1995.** Dimethyl sulphide as foraging cue for Antarctic *Procellariiform* seabirds. *Nature*. 376: 680-682.
- Niessen WMA. 2003.** Progress in liquid chromatography-mass spectrometry instrumentation and its impact on high-throughput screening. *Journal of Chromatography B*. 1000: 413-416.
- Nigam S, Zafiriou MP, Deva R, Ciccoli R, Roux-Van der Merwe R. 2007.** Structure, biochemistry and biology of hepoxilins: an update. *FEBS Journal*. 274: 3503–3512.
- Noordermeer MA, Veldink GA, Vliegthart JF. 2001.** Fatty acid hydroperoxide lyase: a plant cytochrome P450 enzyme involved in wound healing and pest resistance. *ChemBioChem*. 2: 494-504.
- Noverr MC, John R, Erb-Downward JR, Huffnagle GB. 2008.** Production of eicosanoids and other oxylin by pathogenic eukaryotic microbes. *Clinical Microbiology Reviews*. 16: 517–533.
- Orsini L, Sarno D, Procaccini G, Poletti R, Dahlmann J, Montresor M. 2002.** Toxic *Pseudo-nitzschia multistriata* (Bacillariophyceae) from the Gulf of Naples: morphology, toxin analysis and phylogenetic relationships with other *Pseudonitzschia* species. *European Journal of Phycology*. 37: 247-257.

**Orsini L, Procaccini G, Sarno D, Montresor M. 2004.** Multiple rDNA ITS-types within the diatom *Pseudo-nitzschia delicatissima* (Bacillariophyceae) and their relative abundances across a spring bloom in the Gulf of Naples. *Marine Ecology Progress Series*. 271 :87-98.

**Paffenhöfer GA. 1970.** Cultivation of *Calanus helgolandicus* under controlled conditions. *Helgoländer Wissenschaftliche Meeresuntersuchungen*. 20: 346-359.

**Paffenhöfer GA, Ianora A, Miralto A, Turner JT, Kleppel GS, Ribera d'Alcala M, Casotti R, Caldwell GS, Pohnert G, Fontana A, Müller-Navarra D, Jonasdottir S, Armbrust V, Båmstedt U, Ban S, Bentley MG, Boersma M, Bundy M, Buttino I, Calbet A, Carlotti F, Carotenuto Y, d'Ippolito G, Frost B, Guisande C, Lampert W, Lee RF, Mazza S, Mazzocchi MG, Nejstgaard JC, Poulet SA, Romano G, Smetacek V, Uye S, Wakeham S, Watson S, Wichard T. 2005.** Colloquium on Diatom-Copepod interactions. *Marine Ecology Progress Series*. 286: 293-305.

**Pan Y, Bates SS, Cemballa AD. 1998.** Environmental stress and domoic acid production by *Pseudo-nitzschia*: a physiological perspective. *Natural Toxins*. 6: 127-135.

**Paré PW, Tumilson JH. 1999.** Plant volatiles as a defense against insect herbivores. *Plant Physiology*. 121: 325-331.

**Peers KE, Coxon DT. 1983.** Controlled synthesis of monohydroperoxides by  $\alpha$ -tocopherol inhibited autoxidation of polyunsaturated lipids. *Chemistry and Physics of Lipids*. 32: 49-56.

**Pérez Gilabert M, García Carmona F. 2002.** Chromatographic analysis of lipoxygenase products. *Analitica Chimica Acta*. 465: 319-335.

**Pohnert G. 2000.** Wound-activated chemical defense in unicellular planktonic algae. *Angewandte Chemie International Edition*. 39: 4352-4354.

- Pohnert G. 2002.** Phospholipase A<sub>2</sub> activity triggers the wound-activated chemical defense in the diatom *Thalassiosira rotula*. *Plant Physiology*. 129: 1-9.
- Pohnert G. 2004.** Chemical defense strategies of marine organisms. *Topics in Current Chemistry*. 239: 179-219.
- Pohnert G, Boland W. 2002.** The oxylipin chemistry of attraction and defense in brown algae and diatoms. *Natural Product Reports*. 19: 108-122.
- Pohnert G, Lumineau O, Cueff A, Adolph S, Cordevant C, Lange M, Poulet S. 2002.** Are volatile unsaturated aldehydes from diatoms the main line of chemical defence against copepods? *Marine Ecology Progress Series*. 245: 33-45.
- Poulet SA, Ianora A, Miralto A, Meijer L. 1994.** Do diatoms arrest embryonic development in copepods? *Marine Ecology Progress Series*. 111: 79-97.
- Pratt DM. 1966.** Competition between *Skelatonema costatum* and *Olisthodiscus luteus* in Narragansett Bay and in culture. *Limnology and Oceanography*. 11: 447-455.
- Quijano-Scheggia S.I., GarcE., Lundholm N., Moestrup O., Andree K. & Camp J. 2009.** Morphology, physiology, molecular phylogeny and sexual compatibility of the cryptic *Pseudo-nitzschia delicatissima* complex (Bacillariophyta), including the description of *P. arenysensis* sp. nov. *Phycologia* 48: 492-509.
- Ren JG, Xia HL, Just T, Dai YR. 2001.** Hydroxyl radical induced apoptosis in human tumor cells is associated with telomere shortening but not telomerase inhibition and caspase activation. *FEBS Letters*. 488: 123-132.
- Reynaud D, Ali M, Demin P, Pace-Asciak CR. 1999.** Formation of 14,15-hepoxilins of the A3 and B3 series through a 15-lipoxygenase and hydroperoxide isomerase present in garlic roots. *Journal of Biological Chemistry*. 274: 28213–28218.

**Rhodes LL, White D, Syhre M, Atkinson M, 1996.** *Pseudo-nitzschia* species isolated from New Zealand coastal waters: domoic acid production in vitro and links with shellfish toxicity. In: Yasumoto T, Oshima Y, Fukuyo Y. (Eds.). *Harmful and Toxic Algal Blooms*. Intergov. Oceanogr. Comm. UNESCO, Paris, pp. 155–158.

**Ribalet F, Wichard T, Pohnert G, Ianora A, Miralto A, Casotti R. 2007.** Age and nutrient limitation enhance polyunsaturated aldehyde production in marine diatoms. *Phytochemistry*. 68: 2059 – 2067.

**Rijstenbil JW. 2002.** Assessment of oxidative stress in planktonic diatom *Thalassiosira pseudonana* in response to UVA and UVB radiation. *Journal of Plankton Research*. 24: 1277-1288.

**Rijstenbil JW. 2003.** Effects of UVB radiation and salt stress on growth, pigments and antioxidative defence of the marine diatom *Cylindrotheca closterium*. *Marine Ecology Progress Series*. 254: 37-48.

**Rijstenbil JW. 2005.** UV- and salinity-induced oxidative effects in the marine diatom *Cylindrotheca closterium* during simulated emersion. *Marine Biology*. 147: 1063-1073.

**Romano G, Russo GL, Buttino I, Ianora A, Miralto A. 2003.** A marine diatom-derived aldehyde induces apoptosis in copepod and sea urchin embryos. *The Journal of Experimental Biology*. 206: 3487-3494.

**Rorrer GL, Yoo HD, Huang B, Hayden C, Gerwick WH. 1997.** Production of 15-lipoxygenase metabolites by gametophyte cell suspension cultures of the marine brown alga *Laminaria saccharina*. *Phytochemistry*. 46: 871–877.

**Salvador JAR, Sà e Melo ML, Campos Neves AS. 1997.** Copper-catalysed allylic oxidation of  $\Delta^5$ -steroids by *t*-butyl hydroperoxide. *Tetrahedron Letters*. 38: 119-122.

**Sarno D, Kooistra WCHF, Medlin LK, Percopo I, Zigone A. 2005.** Diversity in the genus *Skelotonema* (Bacillariophyceae). II. An assessment of the taxonomy of *S. costatum*-like species, with the description of four new species. *Journal of Phycology*. 41: 151-176.

**Scholin CA, Villac MC, Buck KR, Krupp JM, Powers DA, Fryxell GA, Chavez FP. 1994.** Ribosomal DNA sequences discriminate among toxic and non-toxic *Pseudonitzschia* species. *Natural Toxins*. 2: 152-165.

**Schulze B, Lauchli R, Mekem Sonwa M, Schmidt A, Boland W. 2006.** Profiling of structurally labile oxylipins in plants by in situ derivatization with pentafluorobenzyl hydroxylamine. *Analytical Biochemistry*. 348: 269-283.

**Setsukinai K, Urano Y, Kakinuma K, Majima HJ, Nagano T. 2003.** Development of novel fluorescence probes that can reliably detect reactive oxygen species and distinguish specific species. *Journal of Biological Chemistry*. 278: 3170-3175.

**Smetacek V. 1999.** Diatom and the carbon cycle. *Protist*. 150: 25-32.

**Smetacek V. 2001.** A watery arms race. *Nature*. 411: 745.

**Steinke M, Malin G, Gibb SW, Burkill PH. 2002.** Vertical and temporal variability of DMSP lyase activity in a coccolithophorid bloom in the northern North Sea. *Deep Sea Research Part II: Topical Studies in Oceanography*. 49: 3001-3016.

**Subba Rao DV, Pan Y, Smith SJ. 1995.** Allelopathy between *Rhizosolenia alata* (Brightwell) and the toxigenic *Pseudonitzschia pungens* f. *multiseriata* (Halse). In Lassus P, Arzul G, Erard E, Gentien P, Marcaillou C (eds.). *Harmful marine algal blooms*. Lavoisier Intercept. Ltd., pp. 681-686.

- Tang DG, La E, Kern J, Kehrer JP. 2002.** Fatty acid oxidation and signaling in apoptosis. *Biological Chemistry*. 383: 425-442.
- Terasaki M, Itabashi Y. 2002.** Free fatty acid level and galactolipase activity in a red tide flagellate *Chattonella marina* (Rapidophyceae). *Journal of Oleo Science*. 51: 213-218.
- Tsitsigiannis DI, Keller NP. 2007.** Oxylipins as developmental and host-fungal communication signals. *Trends in Microbiology*. 15: 111-118.
- Todd ECD, 1993.** Domoic acid and Amnesic Shellfish Poisoning — a review. *Journal of Food Protection*. 56: 69-83.
- Tilman D. 2004.** Niche tradeoffs, neutrality, and community structure: a stochastic theory of resource competition, invasion, and community assembly. *Proceedings of the National Academy of Science of the United States of America*. 101: 10854-10861.
- Turner JT, Ianora A, Miralto A, Laabir M, Esposito F. 2001.** Decoupling of copepod grazing rates, fecundity and egg-hatching success on mixed and alternating diatom and dinoflagellate diets. *Marine Ecology Progress Series*. 220: 187-199.
- Utermohl H. 1958.** Zur Vervollkommnung der quantitativen Phytoplanktonmethodik. *Mitteilungen - Internationale Vereinigung für Theoretische und Angewandte Limnology*. 9: 1-38.
- Van Breusegam F, Dat JF. 2006.** Reactive oxygen species in plant cell death. *Plant Physiology*. 141: 384-390.
- Van Den Hoek C, Mann DG, Johns HM. 1997.** *Algae. An Introduction to Phycology*. Cambridge University Press, Cambridge, UK.

- Vanormelingen P, Chepurinov VA, Mann DG, Sabbe K, Vyverman W. 2008.** Genetic divergence and reproductive barriers among morphologically heterogeneous sympatric clones of *Eunotia bilunaris sensu lato* (Bacillariophyta). *Protist*. 159: 73-90.
- Vardi A, Formiggini F, Casotti R, De Martino A, Ribalet F, Miralto A, Bowler C. 2006.** A stress surveillance system based on calcium and nitric oxide in marine diatoms. *PLoS Biology*. 4: 411-419.
- Venrick EL, Beers JR, Heinbokel JF. 1977.** Possible consequences of containing microplankton for physiological rate measurements. *Journal of Experimental Marine Biology and Ecology*. 26: 55-76.
- Vos M, Vet LEM, Wackers FL, Middelburg JJ, Van der Putten WH, Mooij WM, Heip CHR, Van Donk E. 2006.** Infochemicals structure marine, terrestrial and freshwater food webs: Implications for ecological informatics. *Ecological Informatics*. 1: 23-32.
- Wang X. 2001.** Plant Phospholipases. *Annual Review of Plant Physiology and Plant Molecular Biology*. 52: 211-231.
- Wasternack C, Feussner I. 2008.** Multifunctional enzymes in oxylipin metabolism. *ChemBioChem*. 9: 2373–2375.
- Wendel T, Jüttner F. 1996.** Lipoxygenase-mediated formation of hydrocarbons and unsaturated aldehydes in freshwater diatoms. *Phytochemistry*. 41: 1445-1449.
- Wheelan P, Zirrolli JA, Murphy RC. 1995.** Analysis of hydroxy fatty acids as pentafluorobenzyl ester, trimethylsilyl ether derivatives by electron ionization gas chromatography/mass spectrometry. *Journal of the American Society for Mass Spectrometry*. 6: 40-51.

- White TJ, Bruns T, Lee S, Taylor J. 1990.** Amplification and direct sequencing of the fungal ribosomal RNA genes for phylogenetic. In: Innis MA, Gelfand DH, Sninsky JJ, White TJ (eds). *PCR Protocols*. Academic Press, New York, pp. 315-322.
- Wichard T, Pohnert G. 2006.** Formation of halogenated medium chain hydrocarbons by a lipoxygenase/hydroperoxide halolyase-mediated transformation in planktonic microalgae. *Journal of the American Chemical Society*. 128: 7114–7115.
- Wichard T, Poulet S, Pohnert G. 2005a.** Determination and quantification of  $\alpha,\beta,\gamma,\delta$ -unsaturated aldehydes as pentafluorobenzyl-oxime derivatives in diatom cultures and natural phytoplankton populations: application in marine field studies. *Journal of Chromatography B*. 814: 155-161.
- Wichard T, Poulet SA, Halsband-Lenk C, Albaina A, Harris R, Liu D, Pohnert G. 2005b.** Survey of the chemical defence potential of diatoms: Screening of fifty one species for  $\alpha,\beta,\gamma,\delta$ -unsaturated aldehydes. *Journal of Chemical Ecology*. 31 (4): 949-958.
- Wichard T, Poulet SA, Boulesteix AL, Ledoux JB, Lebreton B, Marchetti J, Pohnert G. 2008.** Influence of diatoms on copepod reproduction. II. Uncorrelated effects of diatom-derived  $\alpha,\beta,\gamma,\delta$ -unsaturated aldehydes and polyunsaturated fatty acids on *Calanus helgolandicus* in the field. *Progress in Oceanography*. 77: 30-44.
- Wiseman H, Halliwell B. 1996.** Damage to DNA by reactive oxygen and nitrogen species: role in inflammatory disease and progression to cancer. *Biochemical Journal*. 313: 17-29.
- Wolfe GV. 2000.** The chemical defense ecology of marine unicellular plankton constraints, mechanisms, and impacts. *The Biological Bulletin (Woods Hole)*. 198: 225-244.
- Wolfe GV, Steinke M, Kirst GO. 1997.** Grazing-activated chemical defence in a unicellular marine alga. *Nature*. 387: 894-897.

**Wolfe-Simon F, Starovoytov V, Reinfelder JR, Schofield O, Falkowski PG. 2006.** Localization and role of manganese superoxide dismutase in a marine diatom. *Plant Physiology*. 142: 1701-1709.

**Zurzolo C, Bowler C. 2001.** Exploring bioinorganic pattern formation in diatoms. A story of polarized trafficking. *Plant Physiology*. 127: 1339-1345.